TRACKING EGRESS OF DOUBLY ENCAPSULATED CELLS

RUSHI PANCHAL

Thesis is submitted to the Faculty of Engineering in partial fulfillment of requirements for the degree of

Master of Applied Science

in

Biomedical Engineering

Ottawa Carleton Institute for Biomedical Engineering
University of Ottawa
Ottawa, Ontario

ABSTRACT

Droplet-based microfluidics can be used to enhance stem cell-based therapy by creating cell-laden hydrogel encapsulations to increase engraftment and retention while providing protection from immune responses caused by the host environment. Current research involves gaining better control over therapeutic mechanisms and one focus is to understand the mechanisms behind cell egress. Control over egress is vital to determining how long cells remain in proximity to the therapeutic target. We propose a microfluidic platform capable of encapsulating cells in two subsequent steps in order to create a double emulsion structure around the cell. In this project, hydrogel-in-hydrogel microdroplets are successfully manufactured without the presence of an intermediate oil layer and are used to observe model *NIH 3T3* cell egress. In studying cell egress from singly or doubly encapsulated microcapsules, we are able to better understand the mechanisms that drive egress. Specifically, we hypothesize that cells egress when close to the edge of the microcapsule. In a double emulsion, cells are naturally located away from the edge and closer to the center. Results show that double emulsion microdroplets significantly reduce cell egress but do not eliminate it.

STATEMENT OF ORIGINALITY

The content presented in this body of work is original and the product of work done under the supervision of Dr. Michel Godin at the University of Ottawa in Ottawa, Ontario.

As partial requirement for the degree of Master of Science (Biomedical Engineering) at the University of Ottawa, research on the creation of double emulsion microdroplets using a microfluidic platform to understand cell egress has been presented at the Ottawa Carleton Institute of Biomedical Engineering symposium:

Rushi Panchal and Michel Godin, USING DROPLET-BASED MICROFLUIDICS TO CREATE HYDROGEL-IN-HYDROGEL DOUBLE EMULSIONS FOR THE PURPOSE OF STUDYING CELL EGRESS. Ottawa Carleton Institute for Biomedical Engineering, 20-March 2018.

Posters on the same topic were also presented at the following:

1) MDII and NSERC CREATE BEST Poster Day. Ottawa, Ontario 14-September 2018.
2) Annual SCORR Scientific Research Day. Ottawa, Ontario. 22-March 2018.
3) 10th Annual Graduate Student Poster Competition. Ottawa, Ontario. 27-March 2018.
4) The 2nd Annual Eastern Ontario Canadian Biomaterials Society Symposium. Ottawa, Ontario. 11-May 2018.

Talks on the same topic were also presented at the following:

1) The 2nd Annual Eastern Ontario Canadian Biomaterials Society Symposium. Ottawa, Ontario. 11-May 2018.

STATEMENT OF CONTRIBUTIONS

Text present in this document is an original body of work written by the author. Figures and tables presented were designed and created by the author unless stated otherwise in the caption. All data acquisition and analysis was performed by the author. Single emulsions microfluidic devices were adapted by Ainara Benavente-Babace, PhD and originally designed by Nicolas Cataford, MASc. Double emulsion microfluidic devices were created by the author. Fabrication of devices was done by the author. Programs developed in LabVIEW intended for temperature and pressure control was developed by Michel Godin, PhD and adapted by Ainara Benavente, PhD. Cells were cultured by the author.

ACKNOWLEDGEMENTS

I would like to thank my supervisor, Dr. Michel Godin, for his support throughout my time at the University of Ottawa. He provided a positive working environment which encouraged critical thinking, discussion, collaboration and the pursuit of knowledge. I consider myself lucky to have had the opportunity to work in his lab and I am grateful for his positive impact on my academic and professional career.

Dr. Ainara Benavente-Babace provided continued support during my time in the Godin Lab. Her contribution to my project cannot be understated as she spent countless hours teaching, challenging and encouraging me about all things microfluidics.

While Dr. Godin and Dr. Benavente-Babace were the members of our group involved in my project - the support, advice and encouragement of all Godin Lab members is of note. Thank you to Dr. Ali Najafi Sohi, Eric Beamish, Enas Azhari, Adefemi Adeyami, Karan Dhingra, Nicholas Soucy, and Kaitlyn Kean.

I'd like to especially thank my mother, Chhaya Panchal, for her unconditional love and support through all my endeavors. Her support and guidance means the world to me. I've been lucky to have an amazing family and I'd like to thank them here as well– કાંતિભાઈ પંચાલ, રમિલાબેન પંચાલ, Kalpesh Panchal, Vaishali Panchal, and the best brother and sister – Jay and Adya Panchal.

LIST OF FIGURES

LIST OF TABLES

TABLE OF CONTENTS

INTRODUCTION

Background

Advances and innovations in technologies often aim to miniaturize tools, improve cost efficiency, and ease of use while maintaining or improving output quality. The medical field is not exempt from this. Tools including bioreactors, implants, sensors, and imaging modalities have decreased in size over time [1].

One such field is microfluidics, which uses chips containing channels on the order of microns to provide an easy to use and low-cost platform to carry out biological and chemical processes. Microfluidics can be considered both a science and a subtype of technology. The science of microfluidics deals with pico-liter sized samples [2]. While the volumes may seem limiting in the information they are able to provide, the forthcoming section on the applications of microfluidics will demonstrate that, on the contrary, it is a beneficial feature that can be exploited for many purposes.

Intuition derived from working with fluids on the macro-scale may not align with the fluid mechanics that govern a microfluidic system. For example, fluids traveling in macro-channels are affected by both viscous and inertial forces[3]. Viscous forces are caused by shear stresses on particles within a fluid moving against one another [4]. Resistance can be supplied from adjacent fluid particles, the surfaces of the channels or features within the channels. Inertial forces, on the other hand, are forces that exist due to a resistance to change in momentum [3]. In micro-channels, the flow regimes are far more influenced by viscous forces and leave the inertial forces negligible [4]. Behaviors of viscous-heavy flows can be studied through the Reynolds Number and Stokes flow, which will be discussed in the upcoming sections. Principles of surface tension can be studied to understand how fluids create droplets. An insight in the aforementioned fundamental principles aids in understanding

device geometries, strengths and weaknesses of microfluidic systems, and most importantly, the applications for which they are suitable. Prior to detailing relevant microfluidic fundamentals, some applications will be provided to explain how microfluidic technologies fit into the world of medicine and biochemical devices.

To serve as a point of reference and orient the reader, the goal of this project is to use a droplet-based microfluidic system to create hydrogel-in-hydrogel double emulsion microdroplets. Work done in the Godin lab explores the benefits of encapsulating stem cells within agarose hydrogel microdroplets with the aim of enhancing stem cell therapy. This project aims to understand how cells behave within the confines of a microdroplet – specifically in terms of egress.

Benefits and Applications of Microfluidics

Understanding and exploiting the science within a microfluidic flow regime has led to the creation of many technologies that propel and supplement the fields of chemistry, biology and medicine. Small form factored microchips give way to parallelize operations for high throughput and provide a modular platform with a diverse range of applications. Both features lead to a technology that can save time and money while creating an uncompromised output.

Progress in soft-lithography techniques has also aided the field of microfluidics by allowing for the fabrication and reproduction of designed devices in a short period of time (within a day). The small form factor also creates a platform with low sample consumption rates and the close proximity of different molecules in the channels can shorten reaction times for certain biochemical assays [5]. Microfluidic devices provide a platform for the study of individual cells by trapping them within droplets that closely mimic their native environment – an interesting contrast to liquid cell cultures in flasks [5]. Devices have been fabricated to perform biochemical analysis work such as polymerase chain reactions (PCR), or to study the kinetics of enzyme assays with the goal of shortening reaction

times and reducing the volume of sample used [6], [7]. For example, the mixing, reacting and separating of samples in certain immunoassays can all be done on a single chip. Cytometric alternatives to Fluorescent Activated Cell Sorting (FACS) systems have also been developed along with biosensors, three-dimensional cell cultures, and more [8], [9]. As a technology, microfluidic devices comfortably find a home within the worlds of biology, chemistry and medicine, however, a review of all microfluidic systems is beyond the scope of this work and can be found in some of the cited works [2], [4], [5], [9], [10].

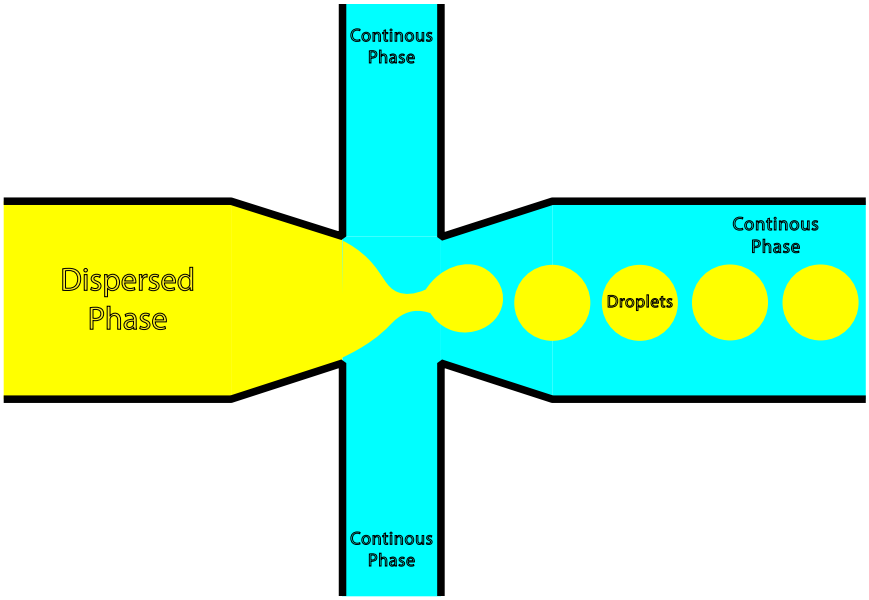

Figure 1. Schematic of a microfluidic device creating droplets using a flow focusing geometry, discussed in the coming sections. The yellow represents material, referred to as the dispersed phase, that will turn into a droplet, while the blue represents an immiscible fluid, referred to as the continuous phase, which 'cleaves' the droplets into spheres without mixing. Objects, such as cells and polystyrene beads, mixed in with the dispersed phase are incorporated into the droplets.

Single Emulsions

One specific use of microfluidic technology is to produce microdroplets, as seen in Figure 1. Droplet-based microfluidics, just like the field of microfluidics at large, has found a home within many biochemical applications. Though low sample consumption is a benefit to most microfluidic

applications, droplet-based devices have the advantage of creating microcompartments separated by immiscible phases allowing each droplet to act as an individual unit. Depending on the type of channel configurations, droplet-sized bioreactors can be used to carry out replicate experiments or a variety of experiments – allowing for a flexible platform [11].

Work done by Emilie Mercey et al. demonstrates that using droplet-based microfluidic devices, nano- to picoliter sized droplets containing a specific digestive enzyme and its target protein can be created, processed by means of mixing, incubated, and then analyzed all on-chip [12]. The study was able to demonstrate the ability of microfluidics to carry out assays rapidly due to the low sample volumes. Detection of specific bovine biomarkers was possible with sample volumes of less than 1 nanoliter using fully integrated microfluidic devices [13]. By incorporating different solutions, spacers between the droplets made of immiscible fluids prevented mixing of samples and contaminants. Additionally, isolated droplets were able to provide statistical power as each droplet could be counted as an individual experiment/data-point.

Within the scope of drug delivery systems, versatility of microfluidic devices can be exemplified through a study which created monodisperse droplets that solidified through the exposure of UV light and then later released the contents over time as the polymerization process began to reverse [14]. Finally, in the field of biological sciences, droplet-based microfluidics have been used to study a population of nematodes, Caenorhabditis elegans, a species often studied in the field of developmental neurobiology [15]. Researchers were interested in imaging their first larval stage, referred to as L1, however the species is highly mobile which made them particularly difficult to handle and manipulate while taking quality images. Using droplet-based microfluidics in conjunction with a hydrogel that gels and melts at specific temperatures, researchers were able to encapsulate the nematodes inside of a

droplet, solidify the droplet, and then image the otherwise hard to image sample [15]. Further work with droplet-based microfluidics can be found in reviews cited in this work [16], [17].

One specific use of microfluidic devices is to encapsulate cell populations. Droplets can be used to isolate single cells and the process has found applications within biochemical and medical research. Encapsulation of single cells using microfluidic devices has been used to isolate cells and study their secreted metabolites, as described in the manuscript by Yin & Marshall [18]. Their work takes isolated cells and provides each sample with various concentrations of drugs using the laminar flows present in a microfluidic channel while studying the effects of each individual cell. Another study used microfluidic devices to encapsulate cells within an agarose hydrogel microdroplet to study their genomic and proteomic outputs by supplementing agarose with markers to indicate antibody secretion [19].

Double Emulsions

To create a double emulsion, the initial microdroplet must be encapsulated again, leading to a droplet-in-droplet sphere. Double emulsion microdroplets have been used for drug delivery systems, as well as in the make-up and food industries [20]. Common double emulsion configurations include alternating immiscible fluids such as water-in-oil-in-water (w/o/w) or oil-in-water-in-oil (o/w/o). Benefits of using a second emulsion is that the product is able to have previously incompatible features. Immiscibility of oil and water leads to isolated compartments that can prevent inter-compartmental transfer and contamination. In pharmaceuticals, the outer layer is used as a means to protect drugs from the biological environment, mask unpleasant flavors of certain drug ingredients and create coatings that dissolve at the presence of molecules found in specific target locations, leading to a targeted drug [21]. Markers or stains that could otherwise be toxic to cells can be incorporated into an outer layer, successfully separating the two components [22]. Using multiple channels controlled by valves, the outer emulsion can be tuned and the effects of a different surrounding

microenvironment can be studied with cells [23]. Similar to cell studies using single emulsions, double emulsions would be able to monitor the effects of different external environments on a single cell, as opposed to with a 2D petri dish. Uses of double emulsions, especially in terms of cell encapsulation, will be expanded upon in upcoming sections.

Microfluidics Theory

Behavior of fluids in a microchannel is largely governed by viscous flow – flow that is influenced by shear stresses applied to the particles of the fluid [24]. Such a flow regime leaves inertial effects negligible and the behaviors can thus be understood through the concepts of the Reynolds Number, *Re*, Stokes Flow and the capillary number, *Ca* [24].

Reynolds Number

Intuitively, the Reynolds number is the ratio of inertial forces to viscous forces. If inertial forces dominate a system, then the Reynolds number will be large; if viscous forces dominate a system, the Reynolds number will be small [25].

$$Re = \frac{F_{inertial}}{F_{viscous}}$$

Formally, the Reynolds number is a dimensionless value defined by the product of the density (ρ), speed (u), and travelled length (L) over the viscosity of the fluid (η) [25].

$$Re = \frac{\rho u L}{\eta}$$

Flow is considered laminar when the Re is less than 2300, in transition when the values are between 2300 and 4000, and turbulent when the number is greater than 4000, shown in

Table 1 [26]. Turbulent flow is identified through chaotic fluctuations in velocity, pressure, and density, and has the presence of random eddies and irregularities that lead to random spatio-temporal variations as shown in Figure 2 [27]. Mixing of flow streams takes place in turbulent flows. In a laminar flow regime, there are no fluctuations that arise from the time dependent and independent variables.

Lack of fluctuations leads to a smooth flow with no random or chaotic mixing in the system but rather through diffusion at the fluid-to-fluid interfaces in a multiphasic flow [28].

Flow regimes within droplet-based microfluidic devices are by and large laminar in nature. Multiphasic flows do not mix outside of surface diffusion and the movement of particles is fairly predictable.

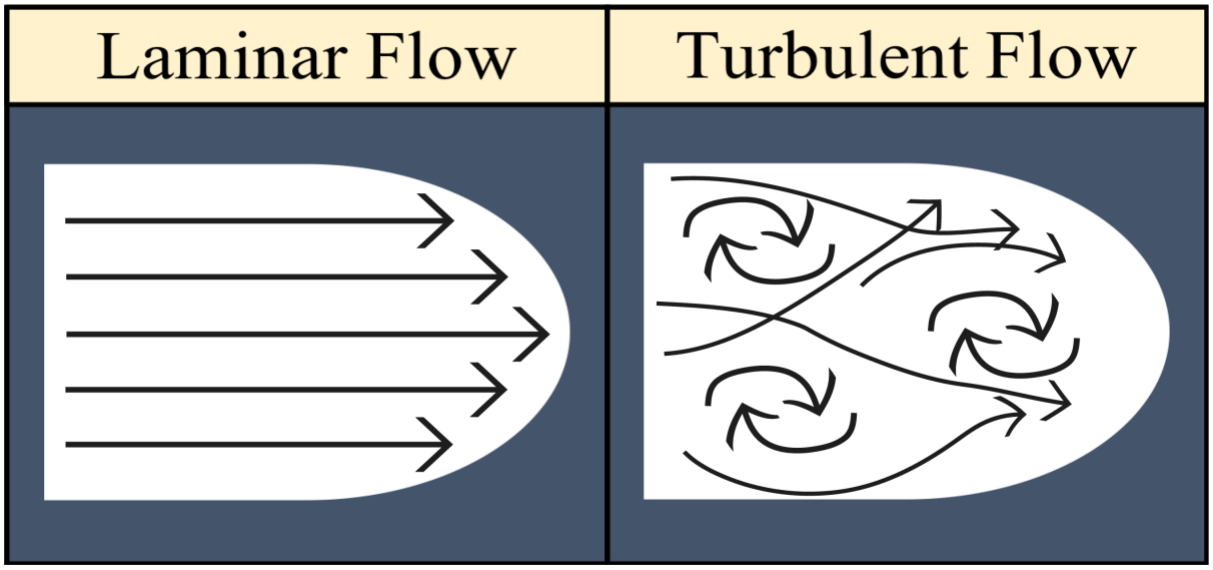

Figure 2. Laminar flow versus turbulent flow. Laminar Flow has smooth flow patterns with no chaotic mixing at any point. Should there be a multiphasic flow, mixing will only take place through diffusion at the fluid to fluid interfaces. Turbulent flow contains more chaotic flow patterns. Fluids often mix at random points and there are eddies which cause disturbance in the flow.

Table 1. Types of flow given a range of the Reynolds Number. Flow regimes are considered turbulent when the Re is

greater than 4000, transitional when the Re is between 2300 and 4000, and laminar when below 2300. In microfluidic systems, the Re is generally considered to be Re<<1.

Type of Flow	Reynolds Number (Re)
Laminar	< 2300
Transitional	2300 < Re < 4000
Turbulent	> 4000

Stokes Flow

As mentioned in the previous section, fluids are almost exclusively influenced by viscous forces rather than inertial forces at the microfluidic scale and thus attributed with a low Re [29]. Transitioning from turbulent to laminar flow is considered to be when the Reynolds number is less than 2300, however, flows in microfluidic channels are assumed to have Re << 1 [30]. With a significantly small Re, the flow within a microchannel operates under parameters described by the Stokes Flow equation, also referred to as the creeping flow. Stokes Flow is an interpretation of Newton's second law which states that the net force acting on an object is equal to the product of its mass and acceleration, with the terms swapped out for forces and accelerations present in a microfluidic channel. Change in pressure across an area, such as within a microfluidic channel, can be referred to as a pressure gradient. While pressure is described as force per unit area, a change in pressure in a gradient over a constant area suggests a change in force, which can only come about given an acceleration. This force moves

from the region of high pressure towards the region of lower pressure. The equation for Stokes flow looks as such:

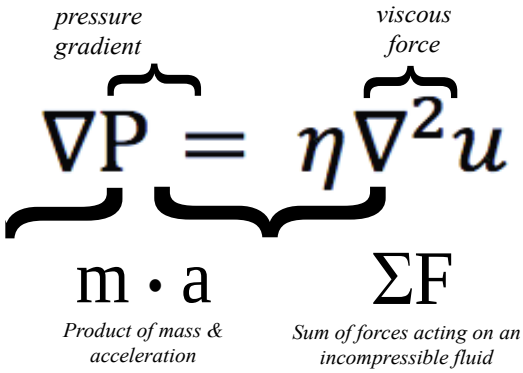

where ∇P is the pressure gradient, η is the viscosity, and u the velocity. On a macroscopic scale, Stokes Flow can be seen in highly viscous fluids such as honey or molasses, shown in Figure 3. Movement of these highly viscous fluids are so strongly impacted by the frictional forces that the inertial effects are almost wholly ignored, leading to a laminar flow. Such imagery can also accurately describe how fluid might move around obstacles in a microfluidic channel [31].

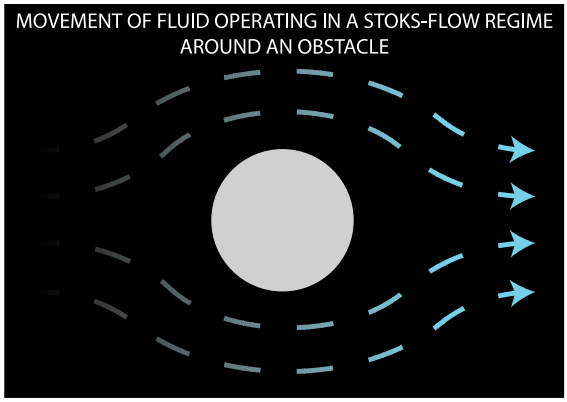

Figure 3. Visual representation of flow patterns around an object when operating in a flow-regime described by stokes flow, or creeping flow. Viscous fluids tend to wrap around an object and revert back to their initial positioning, much like the behavior of molasses or honey.

Droplet Formation

Microfluidic devices containing a biphasic flow can generate droplets using specific geometries. Biphasic flows consist of two immiscible fluids, one referred as the continuous phase and the other the dispersed phase. The continuous phase is the fluid that acts as a 'cleaving agent' in order to create

droplets and the dispersed phase is the substance which is shaped into the droplets [32]. Often times, as is the case for this project, the continuous phase is an oil that may be paired with a surfactant to prevent coalescence, and the dispersed phase is a liquid that is immiscible to the oil such as water and agarose hydrogel. Surfactants are amphiphilic in nature, meaning they have a polar and non-polar side, which allows them to reduce surface tension at the oil-droplet interface [33].

Formation of droplets in a microfluidic regime is based on the interfacial tension between the two fluids, the surface chemistry and the geometry of the device [34]. Co-flow, flow-focusing or T-junction geometries are most commonly used for droplet formation, and each geometry can be seen in Figure 4.

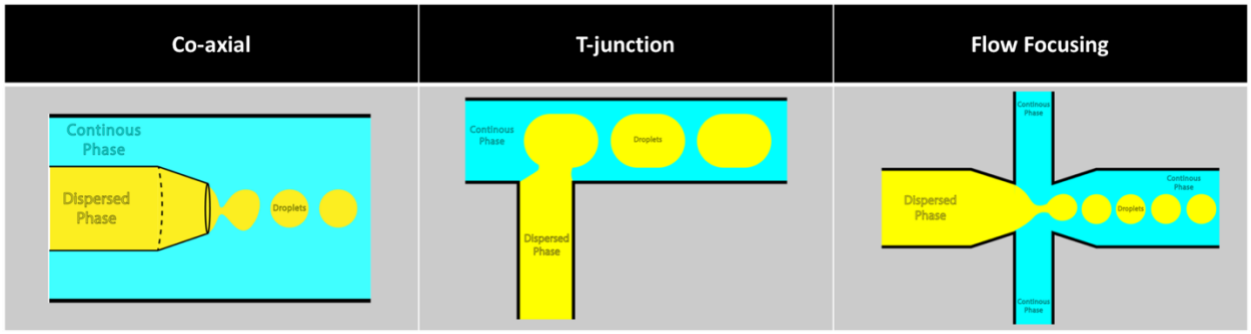

Figure 4. Common microdroplet production geometries.

Co-flow geometries contain two coaxial channels, with an inner channel generally made of a glass capillary tube and an outer channel made of polydimethylsiloxane (PDMS). If the outer flow and inner flow move in the same direction, the contents of the inner channel become droplets; if the flows move in opposite directions, the outer fluid material is cleaved into a droplet [20]. Co-flow geometries have been found useful in many industrial microfluidic applications that require the creation of especially small droplets, down to 10 μm in size. Additionally, because the channel orifices are not in contact with the walls, the devices are safe to use for a prolonged period of time without worry of

contamination. Disadvantages of co-flow geometries include difficulties in fabrication and a time-consuming preparation process [35].

T-junctions work by squeezing the dispersed phase against the continuous phase. Here, the size of the microdroplet formed is based on the ratio of the flows rates and the widths of the channels. Although surfactants help stabilize droplets, it has been found that droplets can be formed simply by properly balancing the flow rates [36]. Droplets formed using a T-junction geometry can be configured to act as a droplet or a plug based on the surface tension [37].

A flow focusing geometry operates on similar principles as the T-junction, however, it has two channels that intersect the dispersed phase at the encapsulation point, leading to a higher droplet throughput, and allowing for the production of tunable droplets without depending on the specific channel size [38], [39]. More so, the flow focusing geometry is better equipped to more easily change droplet sizes using pressure regulators [40]. Flow focusing geometry can create both droplets and jets depending on the flow stability. A stable flow will produce jets, which are elongated microdroplets, while unstable flows will immediately break up at the phase junction, leading to the production of droplets. Because inertial effects are negligible in microfluidic devices, the major factor of droplet production in a flow-focusing junction is the capillary number.

Capillary Number

The capillary number, *Ca*, is a dimensionless number that describes the effects of viscous forces and surface tensions acting at the interface of two fluids. Intuitively, the *Ca* can be thought of as the ratio of viscous forces to the surface tension.

$$Ca = \frac{viscous\ forces}{surface\ tension}$$

Surface tension effects at a flow focusing junction aim to create a shape with the lowest possible surface energy and effectively describe the formation of microdroplets. Polydispersity in the size of the formed droplets is based on the viscosities of the fluids in the continuous and dispersed flow regimes [41]. The size of the droplet is related only to the ratio of the flow rates in the dispersed and continuous phases, which can be demonstrated in our systems [34]. Using physical terms, Ca is then defined as:

$$Ca = \frac{\mu V}{\sigma}$$

where μ is the dynamic viscosity, V is the velocity and σ is the surface tension between the fluid interfaces. At the encapsulation point, one can assume a constant viscosity and velocity, thus the production of microdroplets are dependent on surface tension. When the surface tension is low, the molecules of the flowing material will have a tendency to break up from contact with the interjecting continuous flow, and thus lead to droplet formation. When the surface tension is high, the molecules will a tendency to stick together and fight against the forces of the incoming continuous phase. Low Ca implies an increased presence of surface tension forces, suggesting that droplets are unlikely to form. Bonds between the droplets favour 'staying together' while a high Ca puts focus on the viscous

forces and consequently encourages the break-up of streams into droplets. High and low Ca can be correlated to jetting and droplet regimes as shown in Figure 5.

To further promote the formation of droplets, surfactants are mixed in with the oil. Surfactants are amphiphilic substances, meaning they have a hydrophilic and hydrophobic side, that are responsible for reducing the surface tension and consequently promoting droplet formation [42].

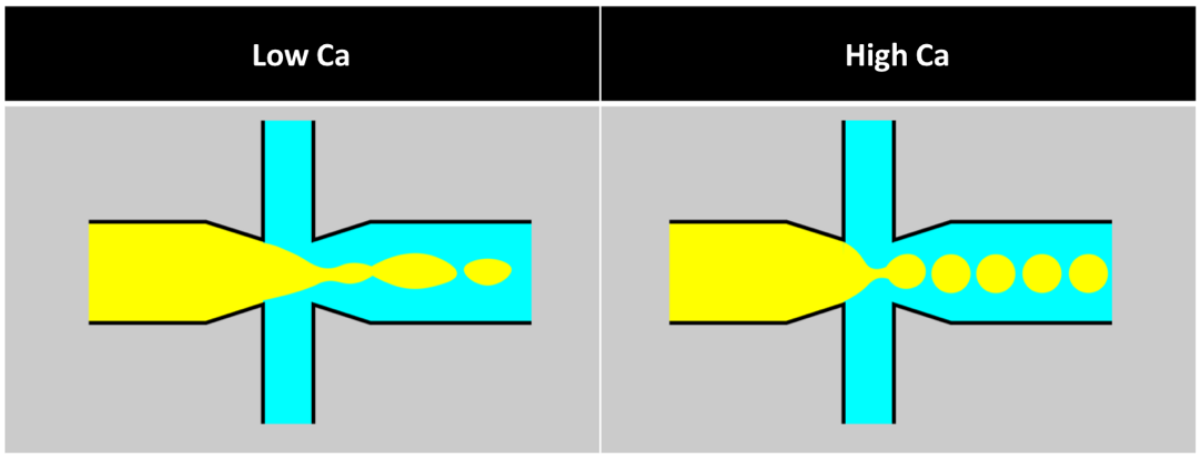

Figure 5. Droplet production in a system with low capillary number versus high capillary number. Surface tension forces dominate flow regimes with a low *Ca* and lead to a jetting regime while viscous forces dominate regimes with

Stem Cell Based Therapy

One specific application of droplet-based microfluidics is in the context of stem cell-based therapy, or cell therapy. In short, cell therapy aims to provide a therapeutic effect to damaged tissue via the presence of therapeutic cells such as stem cells, progenitor cells and others [43]. This method of therapy certainly has advantages as illustrated by its growing use, but it is not without limitation such as the need for continuous immunosuppression, potential for graft rejection and a lack of cell

retention [44]. Microfluidic devices that encapsulate the stem cells in a protective microdroplet can be used to offset some of the inherent limitations and increase the therapeutic outcome.

Cell therapy aims to forego the management approach of pharmaceuticals and instead treat the underlying cause to restore lost functionality by supplying the target location with functional stem cells that work through engraftment and paracrine signaling mechanisms [45], [46]. The principle for cell therapy is to use adult undifferentiated cells, which are cells that have yet to develop into a specialized cell line, and implant them at the target location [17]. Adult stem cells are obtained from postnatal subjects, pluripotent in nature and have been found to play a crucial role in maintaining tissues during regular cell regeneration cycles [47]. The adult undifferentiated cells offer three main advantages. Firstly, the stem cells can be harvested and cultured, which means that upon collection from a patient or donor, the cell line can be cultured in a lab and kept frozen to be re-cultured when needed. Secondly, stem cells are mobile within the body and can move to neighboring regions post-implantation. Finally, stem cells are able to carry out normal metabolic functions and act as native cells to the damaged tissue [48].

Various forms of stem cell therapy exist at both the research and clinical stage. Stem cell therapy has been used in many clinical applications. For example, a study on mice with regions of infarcted myocardium found that the presence of bone marrow derived stem cells provided a therapeutic effect by reducing the size of the damaged tissue while also regenerating myocardial functions [45]. Human Mesenchymal Stem Cells (hMSCs) are used in a variety of applications for therapeutic outcomes in cardiovascular diseases, in neurological system injuries, as well as damages to bones, tendons, cartilage and meniscus [49], [50]. Therapeutic outcomes are thought to be caused by the secretion of trophic factors, which are chemicals with anti-inflammatory and angiogenesis promoting effects that reduce the likelihood of apoptosis in cells [51]. Clinical trials are ongoing with cardiac stem cells for the use of ischemic heart failure treatments [52]. Although the exact mechanisms for stem cell therapy are not

fully understood for each application, it is widely accepted that a significant amount of benefits come from the presence of stem cells and allowing said cells to undergo their normal functions [53].

Cell therapies can be differentiated into two overall categories, autologous and allogenic, depending on where the cells are harvested from [54]. A schematic of autologous and allogenic method is shown in Figure 6. Autologous approaches involve taking adult stem cells from the patients, harvesting the cells, and reintroducing them at the target location; allogenic approaches take cells from a donor source [54]. There are many factors that go into selecting which approach is appropriate.

Autologous cells are convenient because the process forgoes the need for tests ensuring cell compatibility. Survival rates from autologous cell therapy treatments are greater than 95% in a majority of the studies and are not significantly affected by the age of the patient, which can be an issue in the allogenic approach [55]. Unfortunately, samples collected from the patient may not be of usable quality. Other ailments the patient may be experiencing in addition to the disease in question may harm the viability and usability of the stem cells. Outcome of the autologous approach is also dependent on previous treatments the patient has undergone [55]. It has been found that the relapse rate of the disease is greater in autologous stem cell therapy than the allogenic counterpart [55][10].

Stem cells taken from a donor ensure a lack of malignant cells that can otherwise be found in the patient. Cells harvested in a bank are generally well preserved and selected for the best phenotypical traits, therefore the quality is often better than stem cells collected for autologous therapies [53]. Cardiovascular, neurological, and orthopedic disease recurrences are also lower in allogenic approaches, and because of stem cell banks, cells are more readily available [53]. Much like its autologous counterparts, allogenic cell therapy approaches have their share of issues. First and most importantly, allogenic cell therapy involves using foreign cells in a biological system which has inherent immune risks, the most fatal being graft versus host disease (GVHD), an ailment in which the patient's immune system rejects the donor cells [55]–[57]. To prevent GVHD, the patient has to undergo pre-

treatment immune suppression which may not be suitable for older patients and consequently, allogenic methods are most generally reserved for younger patients in otherwise good health [55], [56].

Regardless of the type of cell therapy, there are still risks associated with the approach as well as points where improvement is needed. One point of focus is on the issue of cell retention. Of all the cells injected into a sample, only a small amount remains at the intended target location. A study published in Nature Communications found that in some cases there is less than 10% retention hours after injection [58]. As the effectiveness of cell therapy is thought to be based on the presence of stem cells at the target location, losing a significant number of cells is problematic. Although a work around to this issue could be solved by increasing the number of cells that are injected, a greater number of injected cells, especially when coming from a foreign host, can lead to a higher chance of GVHD [59]. Therapeutic effects of stem cell presence at the target location is limited by the metabolic output, which takes place when the cell has access to the appropriate nutrients (i.e. oxygen). It has been reported that in the standard cell-based therapy method, there is issue with a sufficient amount of oxygen reaching the cells [58], [60]. Another major issue is that, because the majority of cells are from a donor sample, GVHD may occur if the stem cells has not been purified [56].

Advances in microfluidic technologies and droplet formations have shown great potential in the aid of stem cell-based therapies. Stem cells used in the treatment of isolated tumors have benefited from the long-term protection provided by a hyaluronic acid (HA) hydrogel shell, enabling the release of beneficial proteins over time [61]. Embryonic stem cells (ESCs) used in heart cell replacement therapies were found to express beneficial biomarkers and proliferate at a higher rate when cultured

after being encapsulated in a hydrogel [62]. For further applications of cell encapsulation in cell therapy, a review is provided [63].

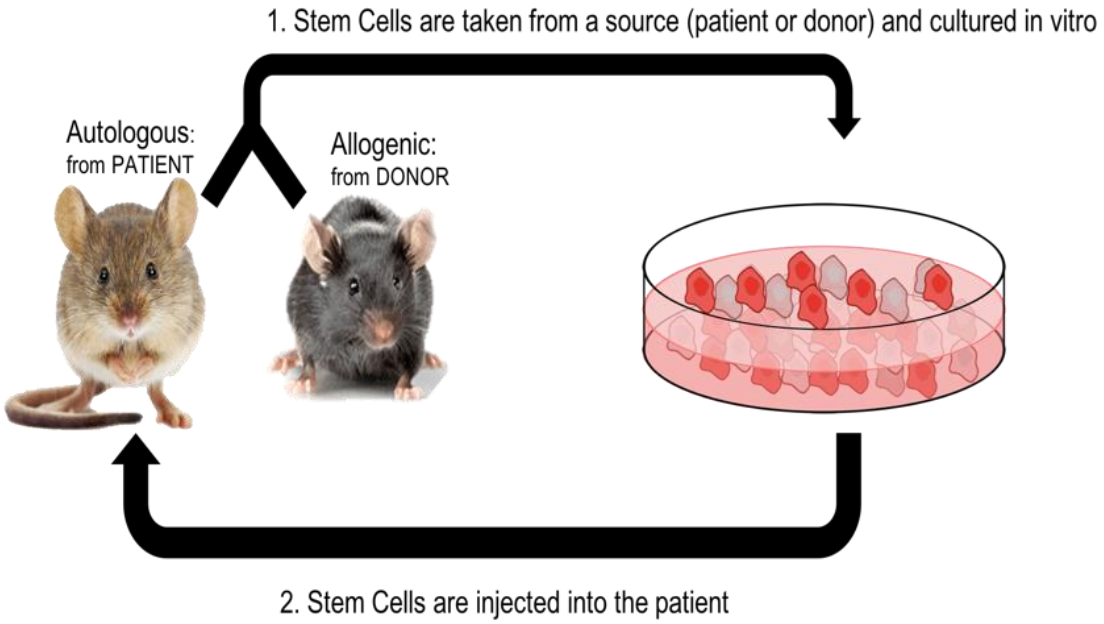

Figure 6. Schematic of autologous stem cell therapy versus allogenic stem cell therapy. Autologous methods culture cells from the patients before re-implanting them for therapeutic purposes whereas allogenic methods acquire cells from a donor. Donor cells are then cultured and implanted into the patient.

Cell Encapsulation

The process of cell encapsulation involves placing therapeutic cells within a microdroplet prior to delivery – and is done so to enhance the therapeutic efficacy by ensuring viability, promoting engraftment and enhancing retention [64]. Generally, the microdroplet is composed of a hydrogel polymeric matrix. Such matrices provide a semi-permeable structure from which waste products from the cell are able to leave and nutrients such as oxygen and cell signaling molecules are able to enter. Materials chosen for the polymer are also selected to be inert and biocompatible so as to not trigger

an immune response from the patient and prevent adverse effects to the cell [65]. A schematic of a cell encapsulation can be seen in Figure 7 while the benefits are shown in Figure 8.

Encapsulation can be done using two methods. Vortex-based encapsulation involves mixing cells, the hydrogel polymer and oil on a vortex machine [66]. While this method does indeed encapsulate therapeutic cells, the microdroplets created are highly polydisperse in size. Depending on the application, such as lung therapy where the channels are small, polydisperse samples need to be filtered for size. Doing so eliminates the larger droplets which are more likely to contain cells [22]. Creating polydisperse samples also reduces the ability to control the approximate cell distribution within the droplets. One might desire such control when cells are limited and need to be distributed.

The second method of cell encapsulation is through the use of microfluidic devices, which offers clear advantages to the vortex-based method. First, and arguably the most important, is that the microdroplets created are monodisperse in size – sometimes with a polydispersity range of between 1% to 3% [67]. This is significant as it allows studies to hold the volume of the microenvironment relatively constant between experiments while giving the operator the ability to change sizes rather quickly by changing pressure ratios. Secondly, controlling the environment of microfluidic devices

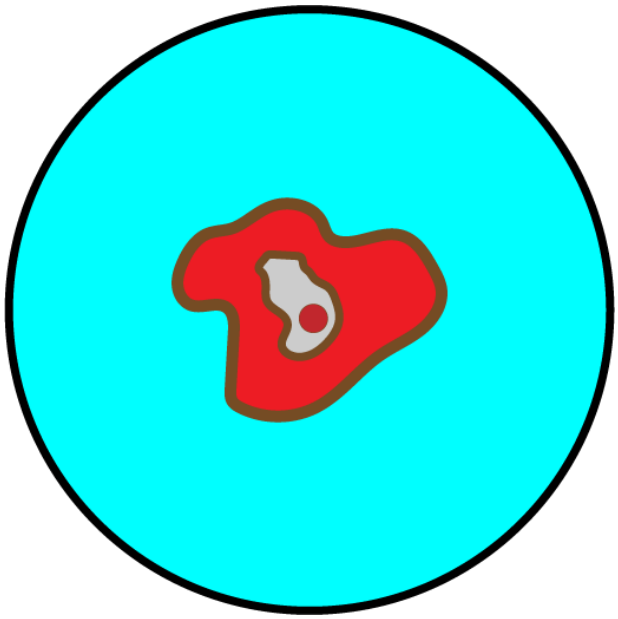

Figure 7. Example of an encapsulated cell. The blue surroundings represent a material used for encapsulation, generally a hydrogel material. For this project, a agarose hydrogel at various concentrations was used. Inside the microdroplet is a cell, here represented in red. Microdroplet sizes can vary depending on the application, as can the size of the cell depending on the cell line. Figure 7 is not to scale but simply a representation of an encapsulated cell. Furthermore, cell-laden microdroplets are not limited to simply one cell, but can have more than one cell.

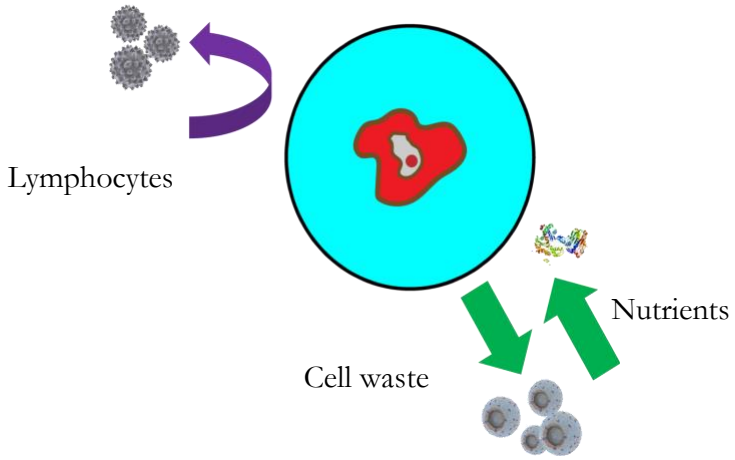

Figure 8. Schematic of the benefits of cell encapsulation on cells intended to be injected into a patient for therapeutic purposes. Cells are protected from immune responses caused by foreign cells due to the inert and non-bioactive nature of selected hydrogels. Additionally, the porous nature of the hydrogel allows for cell wastes and secretions to diffuse out while allow nutrients and cell signalling molecules in.

with regards to temperature is far quicker, on the timescales of 10^{-3} seconds to 1 seconds compared to bulk samples which can take as long as 104 seconds [68]. Devices are made to function specific so the opportunity for sample manipulation is extensive. For example, through minor modifications in the form of addition/subtraction or reorientation of microchannels, a polydimethylsiloxane (PDMS) based microfluidics chip can be quickly fabricated to incorporate hydrogels that work based on different gelation and melting principles such as agarose hydrogels, which work based on a temperature gelling regime, to say alginate, which requires the presence of calcium carbonate to begin gelling instead of temperature [69]. Finally, the number of cells that end up in the agarose microdroplets can be approximated and controlled using statistical models, in particular microfluidics cell encapsulation follows a Poisson distribution, a concept elaborated on in the methods section [70].

Agarose

Agarose is a fairly stable hydrogel that has been extensively studied for applications in the food industry, separation of DNA in gel-based electrophoresis, as well as for cell culturing purposes [71]–[74]. As a biomedical material, it has been FDA approved and used as a biocompatible, inert, and non-cytotoxic platform for work with cells, with the additional benefits of being soft as to stimulate a natural cell environment while being transparent, allowing for easy visualization of cells [74]. The

gelling kinetics of agarose hydrogels are temperature based, which make it possible to easily control on a microfluidic platform with heating and cooling elements. Ultra-low gelling point agarose transitions from solid to liquid at 37 °C and gels at around 15 °C [75], a range of temperatures well tolerated by therapeutic stem cells [76]. The porosity and rigidity of the hydrogel can also be controlled using agarose concentration. Porosity is ideal for allowing cells to undergo normal metabolism functions, allowing the metabolites to leave the encapsulation, and receive nutrients such as oxygen and cell signaling molecules from neighboring cells and native biology.

More so, each microcapsule can only hold a certain number of cells based on volume and thus the competition for nutrients in the microenvironment is far less than it would be under standard conditions where cells are injected together into the target location [77]. Rigidity of the agarose provides adherent cells a three-dimensional platform as opposed to the 2D platform of cell culture – more closely mimicking a natural biological environment. Cells within a microdroplet also benefit from the inert nature of agarose, as it helps prevent immune responses caused by the presence of foreign bodies within the patient's internal biology, leading to major benefits such as the reduction in the likelihood of GVHD. Finally, perhaps due to the sticky nature of hydrogel, encapsulated stem cells have a much higher rate of retention at target locations [78], [79].

Double Emulsion for Cell Encapsulation

Using microdroplets in conjunction with cell therapy provides an effective approach to enhancing treatment efficacy, however, not all is known about how cells behave post-encapsulation. Investigations into cell viability, presence or absence of specific extracellular matrix (ECM) proteins are on-going for therapeutic cells inside of microdroplets [80]. Understanding the mechanisms of cell egress is also subject to investigation as it has been found that for each injected sample, some cells exit the microdroplets [81]. It is still unclear as to what causes the cells to egress out. Knowledge of

cell behavior allows for clinicians to tune whether the therapeutic cells leave the microdroplet and move towards the target location, or if the therapeutic cells stay within microdroplet for their therapeutic effect. Certain therapies may require the direct contact between the therapeutic cell and the target tissue, while other times, the therapeutic outcome is dependent on the cell secretions that take place from within the protection of the microdroplet [82].

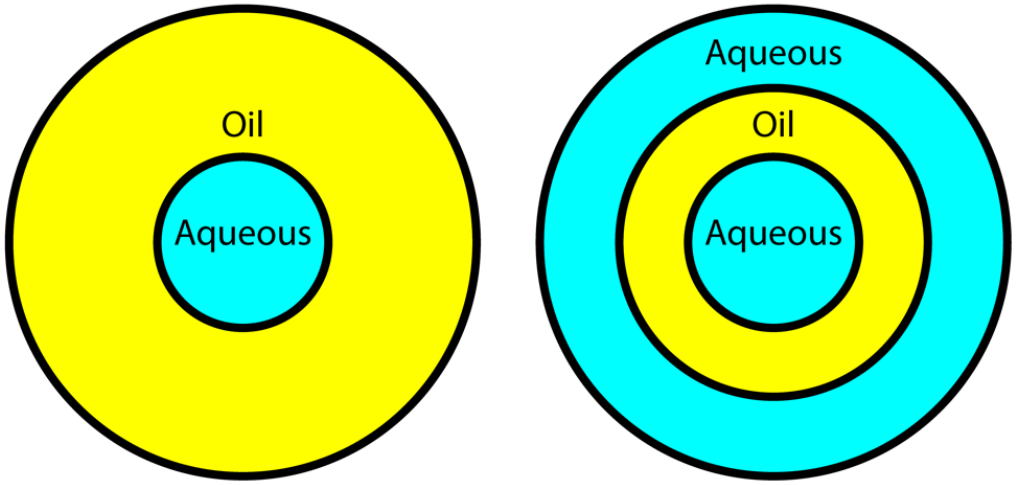

Figure 9. Schematic of a typical double emulsion containing an oil layer. The schematic on the left represents a typical water-in-oil (W/O) emulsion whereas the schematic on the right shows a water-in-oil-in-water (W/O/W) emulsion. Typical emulsions done on a single chip have a layer of oil.

It is hypothesized that it is more likely the cells at the edges of the cocoons that tend to leave, while the cells positioned away from the edges of the cocoons remain inside. To test this hypothesis, this project aims to create double emulsions in order to push the cells away from the edges of a microdroplet. The second emulsion will be made of an identical material and simply extend the pre-existing droplet. Concentration of the outer hydrogel shell will not change and there will be no barrier between the inner and outer shell.

Double emulsions, for cell encapsulation and otherwise, generally have an in-between oil layer which limits their application, as shown in Figure 9. Microfluidic devices with a T-junction geometry were used as far back in 2004 to create double emulsions [83]. Double emulsion microdroplets

produced by the group Okushima et al was done as a proof of concept and had the water-in-oil-in-water (W/O/W) and oil-in-water-in-oil (O/W/O) configuration [83]. A review of double emulsions presented by Wang et al. describes an ample amount of ways that double emulsions are created [21] and the information that follows will be adapted from said review in the subsequent paragraph.

Production of double emulsions initially started via a whole batch mixing method, much like for single emulsions. Droplets would be created in a two-stage process with an initial mixing followed by a gentler mixing stage to create the inner and outer emulsion respectively. The mixing approach suffered from a reduced occupancy load due to the shear stress causing cells to pop out.

To address the limitations of the mixing method, a membrane emulsification method was created which involved letting droplets pass through a membrane of a specific size and exploiting properties of surface tension to create droplets. Membrane emulsification created reasonably sized microdroplets and reduced the shear stresses placed on the droplet but was more difficult to control in terms of occupancy.

It was then that the droplet microfluidics was used to create double emulsions. The benefits of using microfluidics was that the designs intended for single emulsions could easily be translated to double emulsions. Co-axial, T-junction and flow focusing geometries all worked to create double emulsions and have been demonstrated. It brings with it the advantages of microfluidic systems as well such as highly monodisperse samples, scalability and control over both the inner and outer droplet volumes.

Outside of being a technological achievement, double emulsion microdroplets have found many applications. One such use of double emulsions was demonstrated by Martinez et al. in 2012 with an early use of double emulsion microdroplets for cell encapsulations [84]. Cell laden alginate hydrogel, which requires the presence of Ca^{2+} to cross link, was carried in a secondary oil shell to an off chip $CaCl_2$ solution, where the inner alginate shell had time to cross link before it exited the double emulsion

droplet. As a drug carrier, alginate double emulsions have been created in an O/W/O configuration whose phase properties are controlled via the presence of crosslinking molecules. This property has been used to allow drugs to be loaded after the capsules are created to protect drugs from the capsule preparation process [85][93]. Another use of double emulsions is to use the capsule as a bioreactor. Engineered bacteria encapsulated inside the inner droplet of a double emulsion system was monitored for gene activity and fluctuations in cell secretions as the outer shell was created with engineered fluorinated oil that allowed for nutrients to enter while keeping the cell secretions in place over time to be monitored [86].

The aforementioned examples all tend to exploit a significant characteristic of double emulsions – compartmentalization. Outer shells, especially when made of oil do an excellent job of keeping diffusive transport low. In fact, bioreactors, such as in the work mentioned in the previous paragraph [86], have to modify the oil used in order to allow for diffusivity of molecules such as oxygen. Double emulsions created in this project are unique compared to what is found in literature because they are hydrogel-in-hydrogel with a lack of oil layer in-between. While this eliminates the benefit of compartmentalization presented in the previous works, it offers a set of new advantages. Hydrogel-in-hydrogel microdroplets offer the same benefits to encapsulated cells as their single emulsion counterpart in terms of protection from immune responses, ability expel cell secretions, which can aide in paracrine responses, while receiving nutrients such as oxygen and larger molecules needed for viability. Function-based modularity is another useful feature of double emulsion droplets. As seen in the previous examples of double emulsion microdroplets, each shell can be designed based on a desired function. Outer shells might act as a means of protection for cells from things such as fluorescent dyes which are cytotoxic, or from shear forces that could damage the viability of cell lines or the molecular integrity of drugs. There are a plethora of examples in which hydrogels are modified

based on their usage and creating a hydrogel in hydrogel double emulsion opens up the possibility of using different types of hydrogels based on application [87].

Studies which explore tuning cell egress in single emulsions have recently been published in which agarose hydrogels are imbued with ECM proteins to change the behavior of cells [82]. While the work in the previously mentioned paper explores tuning egress using biocompatible chemicals, double emulsions provide a platform which does not change any of the hydrogel properties, outside of size.

Objective Statement

Work done towards the completion of this project is carried out in three steps. Firstly, a process of creating hydrogel-in-hydrogel double emulsion microdroplets is established and characterized. The double emulsion microdroplets will not contain an intermediate oil layer or shell and the characterization process will identify the level of polydispersity and throughput. Secondly, *NIH 3T3* cells are incorporated into the double emulsion microdroplets platform in order to test the impact on cell viability. Finally, the hypothesis on cell egress is tested using the developed system. Successful completion of this project will not only provide a means of controlling cell egress, it will also establish a proof of concept method to creating modular double emulsion platform which can incorporate multiple materials based on intended functionality.

METHODS

Device Fabrication

Microfluidics has often followed trends in microelectronics and fabrication techniques are no exception. Initially, to create microfluidic devices, one would use the method of photolithography and etching. Despite the precision of the techniques, they were found too expensive and unaccommodating for exploratory purposes. For these reasons, soft-lithography was developed. Soft-lithography offers a method to create replicable microfluidic devices using soft biocompatible polymers such as polydimethylsiloxane (PDMS) [88]. Previous work done in the lab had produced microfluidic devices capable of effectively and consistently creating droplets within the range of 40-50 micron in diameter. The devices were, however, not suitable for creating double emulsions given the height and width of the channels at the encapsulation point – points discussed in the results. Work on this project explored adapting the existing single emulsion microfluidic device geometries to suit the creation of hydrogel-in-hydrogel double emulsion microdroplets.

Design

Microfluidic devices are designed using computer-aided drawings (CAD). Designs for this project are created in AutoCAD ® software, an example of which is shown in Figure 10. Cell encapsulation devices can vary in finer details but all possess an inlet, an encapsulation point and an outlet. The inlet of a microfluidic device is the point at which the sample is introduced into the device. Due to potential impurities in the sample, the inlet is equipped with an array of posts which act as a filter to block large contaminants from moving through the device and causing a clog downstream. The encapsulation point is where the sample, referred to as the dispersed phase, meets the incoming immiscible fluid, referred to as the continuous phase, as illustrated in Figure 12. At this point, the two fluids meet and the continuous phase acts as a cleaving agent of sorts and creates microdroplets or '*cocoons*'. In this

project, the encapsulation point uses a flow focusing geometry to introduce the incoming continuous phase to the dispersed phase at a 90° angle. Following the encapsulation point, the samples move downstream to a serpentine geometry that lengthens the time it takes for the sample to reach the collection point. Geometrical features such as serpentines can be used to provide a platform to treat the samples within the device. For cell encapsulation with agarose hydrogel, the serpentine paired with the microfluidic platform (described later in this chapter) cools the cocoons in order promote gelation. Past the serpentine is the outlet where the cocoons are collected.

Once the CAD drawing is completed, the designs are printed onto a transparency, referred to as a photomask, and resemble the layout presented in Figure 11. The photomasks used for this project are purchased through CAD/Art Services and have a resolution of 10 μm - meaning that features

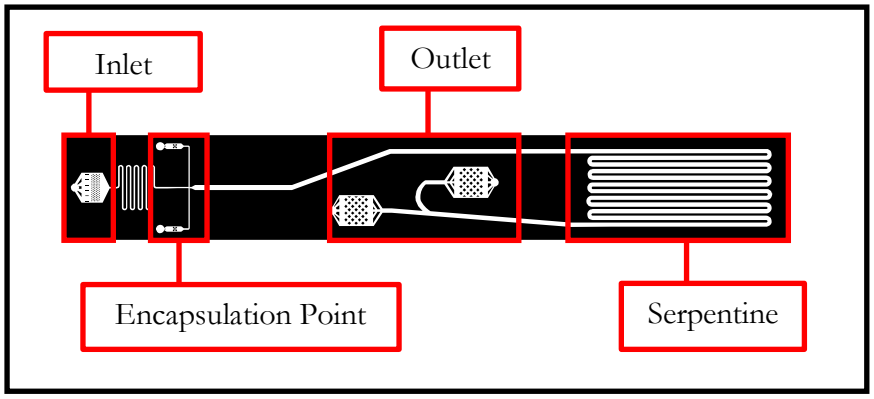

Figure 10. An example of a microfluidic cell encapsulation device used for the work done in this thesis project. Samples enter the device at the inlet, where they are passed through a filter. The filter acts to prevent clumps of microdroplets from moving through the device and causing clogs downstream. Once through the filter, sample moving through the device goes to a short serpentine, that adds resistance to the flow – slowing down the sample. Following the first serpentine, the sample moves through to the encapsulation point where an incoming continuous phase cleaves the samples into droplets. The newly created droplets move through the device to a secondary serpentine which is keeps samples in the device for longer so they have time to cool down and consequently, transition from a liquid to a solid phase. As described in forthcoming sections, the device is kept on a temperature gradient where the sample moves from a hot region to a cold region. This is done so that agarose, a hydrogel which solidifies based on temperature, remains liquid during encapsulation and solidifies after it is shaped into a droplet. Finally, the droplets are collected at the outlet point. There are two points of collection as a means of redundancy in the event that there is a clog.

smaller than 10 μm cannot be used in the design. Once the photomask is acquired, a master mold can be created.

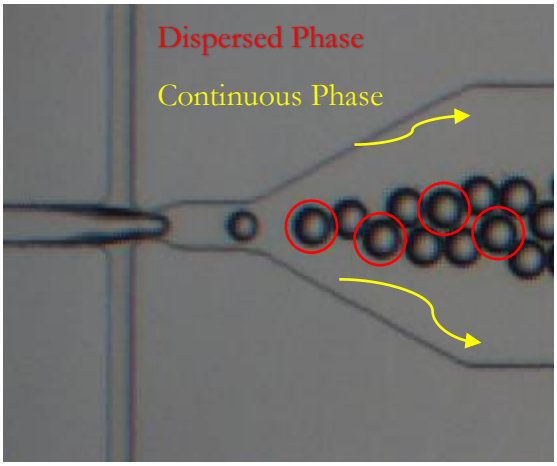

Figure 12. Image of a microfluidic encapsulation device at the encapsulation point. Here, the dispersed phase arrives at the encapsulation point and is cleaved into microdroplets while the continuous phase fills the surrounding space. The two materials are immiscible so they do not mix.

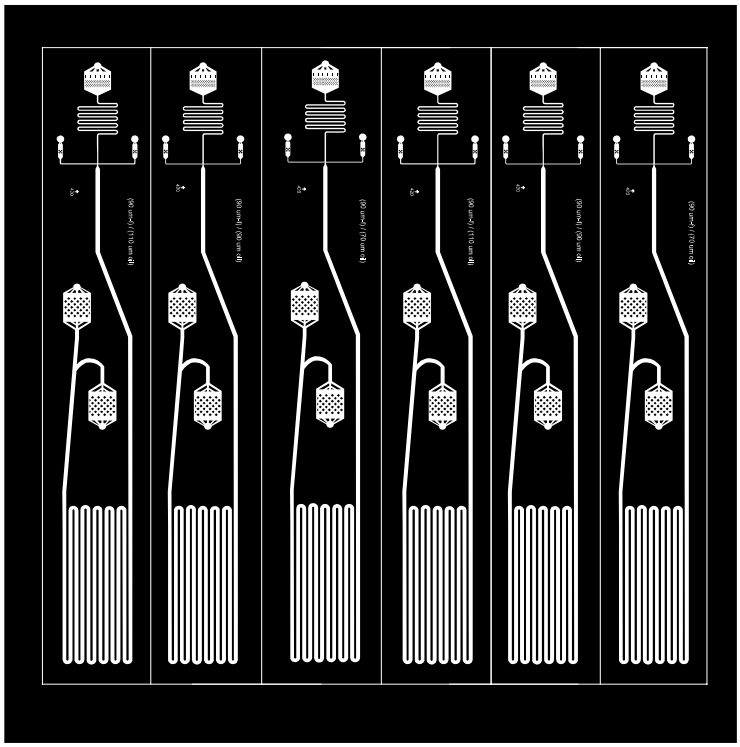

Figure 11. Photomask of microfluidic cell encapsulation devices. Microfluidic devices are designed using 2D CAD software. The design are printed onto a photomask which can then be used in a soft photolithography process to create a master mold, described in the following section.

Master Mold

A significant advantage of using soft lithography in microfluidic device fabrication is that once the master mold is created, it can be used repeatedly to create replicate devices. Due to the size of microfluidic device features, small contaminants can have big impacts, and therefore, it is necessary to create the master mold in a clean room which controls for temperature, humidity, pressure as well as dust and debris [88]. For this reason, all steps associated with creating a master mold are done within the confines of a clean room and the operator is equipped with a headcover, face mask, coverall, gloves and shoe covers.

The master mold itself is created on the surface of a clean silicon wafer with a nearly flat surface, as shown in Figure 13, and the entire process is described at a high level in Figure 14. Cleaning is done by rinsing the silicon wafer with acetone, then ethanol and finally isopropyl alcohol. Once the wafer has been cleaned with all three chemicals, the chemicals are blown off using clean N_2 air after which the wafer is dehydrated on a hot plate set to 115 °C for 2 minutes. After heating, the silicon wafer is oxidized via plasma treatment at 150 W for 5 minutes in order to increase the spreading of the negative photoresist, SU-8 in this case. Plasma treatment aides in wetting the surface and thus

Figure 13. Image of a silicon wafer onto which a SU-8 layer is deposited and polymerized. The photograph of the wafer has been edited to be black because the actual wafer is almost perfectly smooth and reflective, making it hard to photograph.

promotes adhesion of hydrophobic SU-8 photoresist on the silicon wafer [89]. SU-8 photoresist coats the silicon wafer and polymerizes when exposed to UV light [90].

Creating a thin film on the silicon wafer requires the use of a spin coater, which creates an even layer of photoresist atop the silicon wafer at a height determined by the user. Spinning the silicon wafer on the spin coater spreads the SU-8 wafer at a height inversely proportional to the spin speed. A protocol provided by MicroChem® is used for the creation of our master molds [91]. For the purposes of this study, devices intended for single emulsions were fabricated at a height of approximately 60 μm while devices intended for use in double emulsions were fabricated at a height of 160 μm. Here, the height of the photoresist set by the spin coating phase determines the height of the microfluidic devices. After spin coating, the SU-8 coated wafer is heated in a phase called the "pre-bake" where it is first heated to 65 °C and then to 95 °C. The pre-bake method evaporates the solvents present in the photoresist and allows the material to harden while the gradual increase in temperature prevents cracking [92]. The duration of the baking is dependent on the height of the film. After heating, the wafer must be cooled down to room temperature.

Next, the wafer must be exposed to UV light using a mask aligner. Prior to placing the wafer onto the mask aligner, the photomask is fixed onto a clear glass window on the machine that lets the UV light through. Placing the photomask in-between the UV light lamp and the wafer will allow only the features on the photoresist to be imprinted. Interaction between UV light and the negative photoresist causes a polymerization in the photoresist, leading to a solidified structure on the wafer. Exposure time is dependent on the height of the channels as well as the power of the UV lamp, and can be calculated using the SU-8 2000 data sheet provided by MicroChem [93]. After exposure, the wafer has to be heated again in the "post-bake" process at 65 °C and 95 °C for a time determined through the datasheet and again cooled to room temperature for approximately 5 minutes. Post-exposure bake is done to continue supplying energy to the photoactive reaction that takes place in the photoresist after

being exposed to UV light [92]. While the UV light starts the polymerization reaction, the post-exposure bake heating finishes it. Once the wafer has cooled, SU-8 developer is used to remove the unpolymerized deposits of photoresist in a process referred to as development. After the unwanted SU-8 photoresist has been washed away with the SU-8 developer, isopropyl alcohol is used to wash the wafer. The isopropyl alcohol must be air dried away using compressed N_2 air and then heat dried at 150 °C for 5 minutes before being cooled to room temperature again.

Finally, the wafer undergoes silanization in order to prevent PDMS from adhering to the master mold surface during the subsequent casting process. Silanization introduces the silanizing agent trichlorosilane to the surface of the master mold inside of a desiccator, which creates a vacuum, for 30 minutes as suggested by the Harvard Medical School protocol [94], [95]. Using the desiccator allows for faster evaporation of the trichlorosilane droplet and promotes vapor-based deposition that creates a monolayer on the silicon wafer [95]. Use of trichlorosilane prevents PDMS residue from sticking to the wafer after curing, lessening the likelihood of damaged or improperly cured devices.

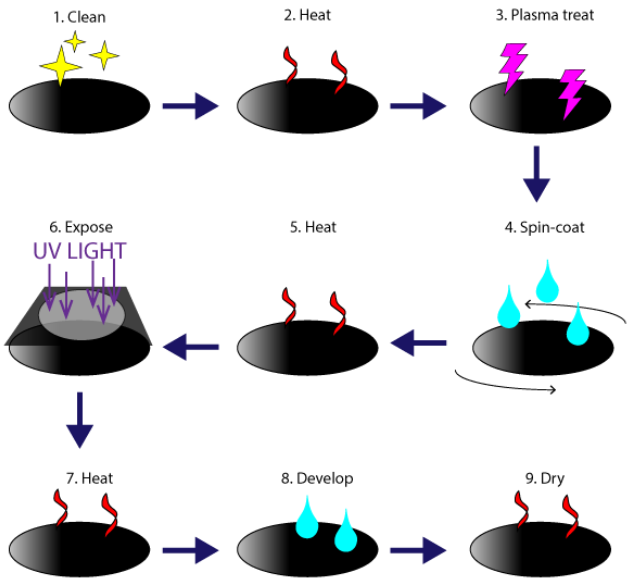

Figure 14. Overview of the soft-photolithography process. The black ellipse object represents the silicon wafer. Firstly, the wafer is cleaned and then heated. Next, using a plasma machine, the clean wafer is plasma treated. Upon plasma treating, SU-8 photoresist is added atop the wafer and it is placed in the spin-coater at a rotational speed set based on the desired height of the encapsulation device. After the spin coating process, the silicon wafer is heated and then exposed using a mask-aligner machine. A photomask is placed between the UV light and the wafer. UV light from the mask aligner will polymerize the features on the wafer and a final baking process is done to promote polymerization after exposure to UV light. SU-8 developer is used to wash the wafer in order to rinse away the photoresist that did not polymerize. Finally, the wafer is dried and ready to be used. Rationale behind the steps is described in text.

PDMS Casting

Microfluidic devices can be fabricated using many different types of polymers, however the most common materials are glass and polydimethylsiloxane (PDMS). Glass is compatible with biological samples as it is generally inert and can be formed using standard etching and soft lithography methods [96]. Unfortunately, glass microfluidic devices need to be fabricated using a wet etching method which is isotropic in nature and spreads in all directions and makes it difficult to control channel sizes dimensions and cannot create deep narrow groves, are more costly to work with than PDMS devices, require very specialized fabrication environments that require the use of dangerous chemicals such as hydrofluoric acid and the use of elastomeric materials for the incorporation of valves - which may not be easily available [97], [98]. Microfluidic chips used in the Godin Lab, and specifically for this project, are made with PDMS because of low material cost, the transparent properties which allow active monitoring of on-chip happenings with an optical microscope, biocompatibility, low surface energy which allows easy peeling from molds and elasticity that creates a natural seal with solid tubing [88], [99]. In terms of fabrication, PDMS is also easily bonded to a glass microscope slide by oxidizing the surface using a plasma treatment [100].

The master mold created in the previous step gives the operator a platform onto which liquid PDMS can be poured and cured in order to create the body of a microfluidic device. PDMS can be purchased as a kit from Sigma Aldrich consisting of a base and curing agent. Both chemicals are mixed at a 10:1 ratio of PDMS polymer to curing agent. The mixed product must then be degassed to remove the air bubbles formed in the mixing step by being put in a vacuum chamber. It is imperative that the mixture be free of air bubbles as negligence at this step can lead to unusable devices later in the process. The PDMS mixture can then be poured onto the master molds. If more bubbles arise in the pouring process, the master mold with PDMS must again be put into the vacuum chamber, otherwise, it can go in an oven set to 70 °C and cured for at least 2 hours. Cured PDMS can be cut into pieces small

enough to fit onto a standard glass microscope slide (75 mm x 25 mm). Once the pieces of PDMS are cut, the final step before bonding is to create the holes at the inlet, oil channels and outlets using a biopsy punch compatible with the outer diameter of tubing used. For this project, a bioposy punch of 0.75 mm is used

Bonding

The final step in creating a PDMS-based microfluidic device is bonding the cured PDMS piece to a glass microscope. Glass microscope slides must be cleaned thoroughly as improper cleaning can lead to poor bonding. To clean the microscope slides for bonding, they must be sonicated with acetone, then ethanol and finally isopropyl alcohol for 10 minutes each. Upon completion, the slides can be dried using clean N_2 air and stored in a dust free environment until they're ready to be used for bonding.

In order to bond PDMS to glass microscope slides, clean PDMS pieces and microscope slides are plasma treated at ~30-50 W for 0.8 seconds. Plasma treatments is done with the feature side facing up. Doing so creates an active SiO group on the exposed surface of the PDMS and an oxidized surface of glass. Plasma activated faces of the PDMS piece is brought into contact with the activated side of the glass slide. Contact between the two materials leads to a permanent Si-O-Si covalent bond [101].

After bonding the PDMS to a glass microscope slide, the device has to be placed in an oven set to 70 °C to alter the PDMS channel chemistry from hydrophilic to hydrophobic and complete bonding. A hydrophobic microfluidic device will prevent the aqueous phase from wetting the channels and promote the formation of microdroplets.

Cell Culturing

In order to understand cell behavior within the microdroplets, a *NIH 3T3* cell line was chosen as a model. cells are robust adherent fibroblasts derived from mice and can be seen in Figure 15. Culturing protocols followed were given by the cell line distributors [102].

Initial Culturing

NIH 3T3 cells are delivered frozen so they can be kept in -80 °C conditions until ready for usage. To start the first cell line, the cells must undergo a quick thaw to 37 °C. Once the cells are thawed, the contents are transferred into a sterile centrifuge tube with 9.0 mL of growth medium. The cell solution is then centrifuged at 125xg for 5-7 minutes. The centrifuged cells can then be seeded into a culture flask containing cell media at a pH of 7-7.6 and incubated in an incubator set to 37 °C with a 5% CO_2 air atmosphere. The cells must undergo at least two subcultures after the thawing process to be usable for experimental purposes.

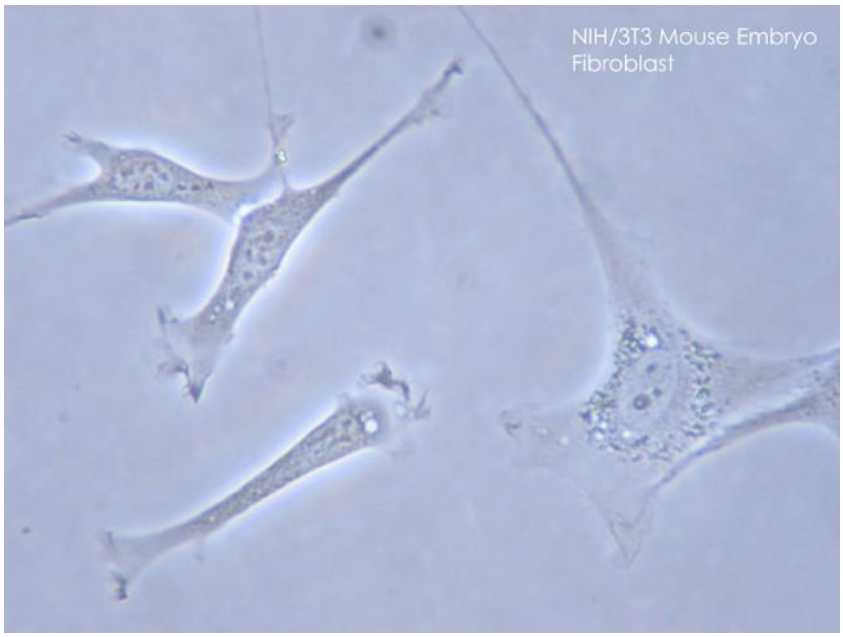

Figure 15. Mouse Embryo Fibroblasts. Used courtesy of Wikimedia commons.

Sub-culturing

To continue the cell line, cells are sub-cultured when the petri dish is at 80% confluency, meaning that the adherent cells cover 80% of the petri dish floor. Sub-culturing is done by aspirating the media present and washing the culture dish with phosphate-buffered saline (PBS). PBS is aspirated out and replaced with 3 mL of Trypsin-EDTA solution and then incubated for ~5 minutes. Incubation with trypsin cues the adherent cells to release from the base of the petri dish. It is important to monitor the incubation time as prolonged exposure to trypsin can be cytotoxic. After incubation, the cell-trypsin solution is diluted with 6 mL of cell media to deactivate the effects of trypsin and a hemocytometer is used to count the number of cells present. Apart from the cells used in counting, the remainder of the solution is centrifuged down and resuspended in 1 mL of cell culture media before being seeded into a culture dish of 10-12 mL of fresh cell media. Information on the passage number, number of cells and date are noted.

Cell Maintenance

Sub-culturing of cells is important when the cell culture dish reaches 80% confluency, however, it is important to refresh the cell media every 3 days. This is done by aspirating all the media in the culture dish and replacing it with 12 mL of fresh media.

Agarose Preparation

Cell encapsulation is carried out using Type IX Ultra Low Gelling Temperature Agarose provided by Sigma Aldrich as the dispersed phase. The preparation process is fairly simple and adapted from the datasheet provided by the manufacturers [75]. For the purposes of cell encapsulation, it is easiest to make stock agarose samples at a higher concentration so it can be diluted down with a component such as cells or polystyrene beads. Therefore, a stock agarose sample is prepared at 2.7% w/v in sterile PBS. The appropriate amount of agarose is mixed in with PBS and heated in a microwave until just

before it reaches a boil. Prepared agarose stocks can be stored at 4 °C until ready to be used, at which point it can be heated up past the melting point of 65 °C.

Cell Encapsulation

Single Emulsion

Cell encapsulation can be broken down into five essential components as described in Figure 17a. Temperature to control the state of agarose (38 °C for liquid phase and 4 °C for solid phase) and pressure, provided by compressed gas fed to a pressure regulator meant to move substances from the inlet to the outlet of the microfluidic device, during encapsulation are controlled through a custom LABVIEW program [103]. Additionally, the microscope is equipped with the BlackFly camera from FLIR for live visual feedback of the encapsulation process. SPINVIEW imaging software by Spinnaker is used to image and film the encapsulation process while monitoring average cocoon diameter.

It is important that the size of the cocoons fall into the desired range and using images taken from the microscope along with FIJI, a NIH software, we can check the sizes while the encapsulation process is taking place [104]. An image taken from the cocooning process is shown in Figure 17b.

Two pressure regulators pressurize the sample and oil/surfactant vials. Materials within the vials are sent to the microfluidic device through polyetheretherketone (PEEK) tubing with an outer diameter of 1/32" and an inner diameter of 0.007". Pressure regulators are turned on and off via LabVIEW and the amount of pressure is controlled via a valve on the regulators. Pressurizing the sample and oil channels creates a pressure gradient in the device which pushes the cocoons downstream towards the outlets where they leave the device through another set of PEEK tubing into the collection vial. One tube goes from the sample to the inlet, two from the oil vial to the two oil channels and two tubes run from the outlet to the sample collection vial. Due to two channel

continuous phase design of flow focusing geometry-based devices, two PEEK tubes are required for the oil channel. Two tubes are also used for the outlet in order to accept samples from the two outlets. As shown in Figure 10, it can be observed that the channel splits into two. This is done to prevent total sample loss in the event of clogging – the second channel acts as a backup.

Sample from the inlet and oil from the oil channels travel to meet at the encapsulation point. Here, the oil and span mixture acts as a cleaving agent and creates the spherical microdroplets. Oil/span and the agarose/cell sample are immiscible, so they do not mix. Once the spheres have been created, the oil acts as the surrounding medium of transport for the microdroplets. Occupancy of the microdroplets can be estimated using the Poisson Distribution and is dependent on the concentration of cells in the sample and the size of the droplets. Encapsulated microspheres, both cell-laden and empty, travel downstream through the serpentine, where the microspheres are exposed to 4 °C that promote on-chip gelling. Functionally, the serpentine section of the microfluidic device holds the microspheres on-chip for approximately 50 seconds of its total encapsulation time, increasing the time they're exposed to cool temperatures and consequently, increasing the time they have to gel. Following the serpentine segment of the microfluidic device, the microdroplets travel to the outlets where they are collected into a centrifuge tube containing 0.5 mL of cell media on ice. Collecting the sample on

ice further promotes gelling of the microdroplets, while the cell media provides a nutrient rich environment for the cells. An overview of the cell encapsulation process is described in Figure 17.

As a proof of concept, single and double emulsion agarose microdroplets were also created containing 11.8 μm polystyrene beads as a way to emulate the future cell encapsulations. Unlike cells, polystyrene beads have a higher tolerance for temperatures, with polystyrene possessing a melting point of ~240 °C and are far more monodisperse in their sizes [105]. Highly viscous samples tend to create clogging in the devices and prior work done with cell encapsulation has found that 7.5 x 10^6 $\frac{cells}{mL}$ is an ideal concentration. Single emulsions created in this project use polystyrene beads at 7.5 x 10^6 $\frac{cells}{mL}$. Cells were tested at 7.5 x 10^6 $\frac{cells}{mL}$ as well as 10 x 10^6 $\frac{cells}{mL}$ in order to increase the number

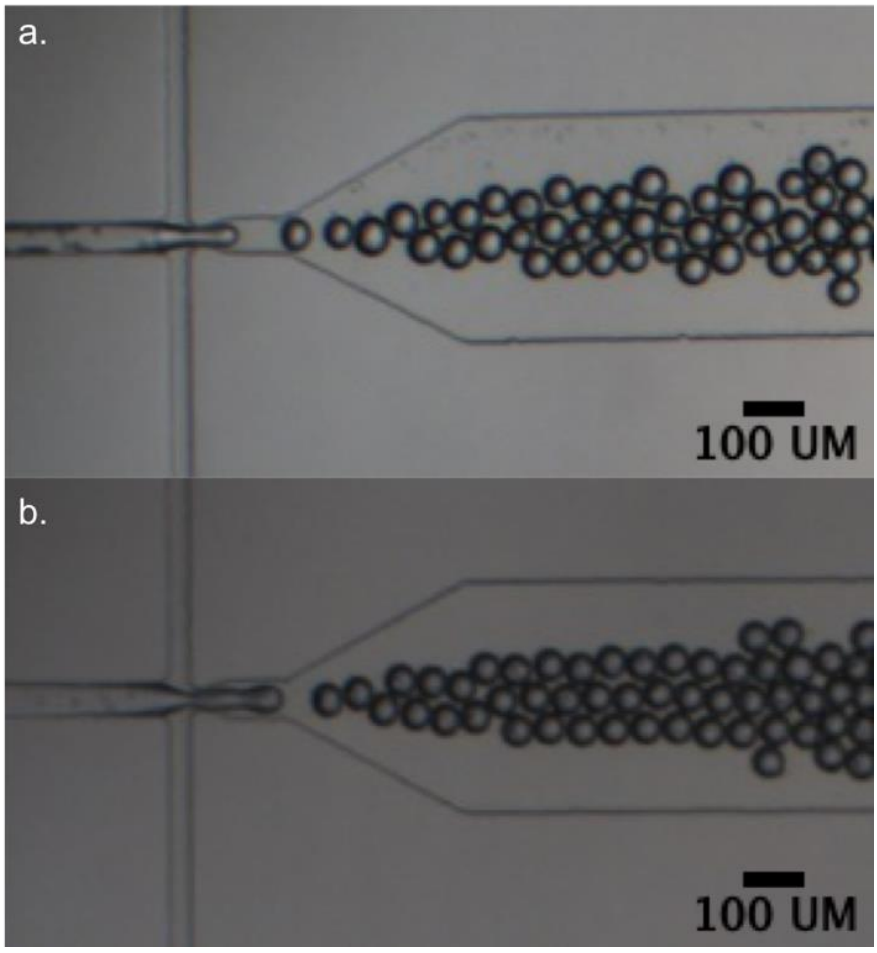

Figure 16. Cell encapsulation of single emulsions with polystyrene beads and cells. 16a depicts single cell encapsulation with polystyrene beads. 16b shows single cell encapsulation with *NIH 3T3* cells.

of cell laden microspheres. Figure 16a and Figure 16b illustrates the process of creating a single emulsion microdroplets with both polystyrene beads and cells.

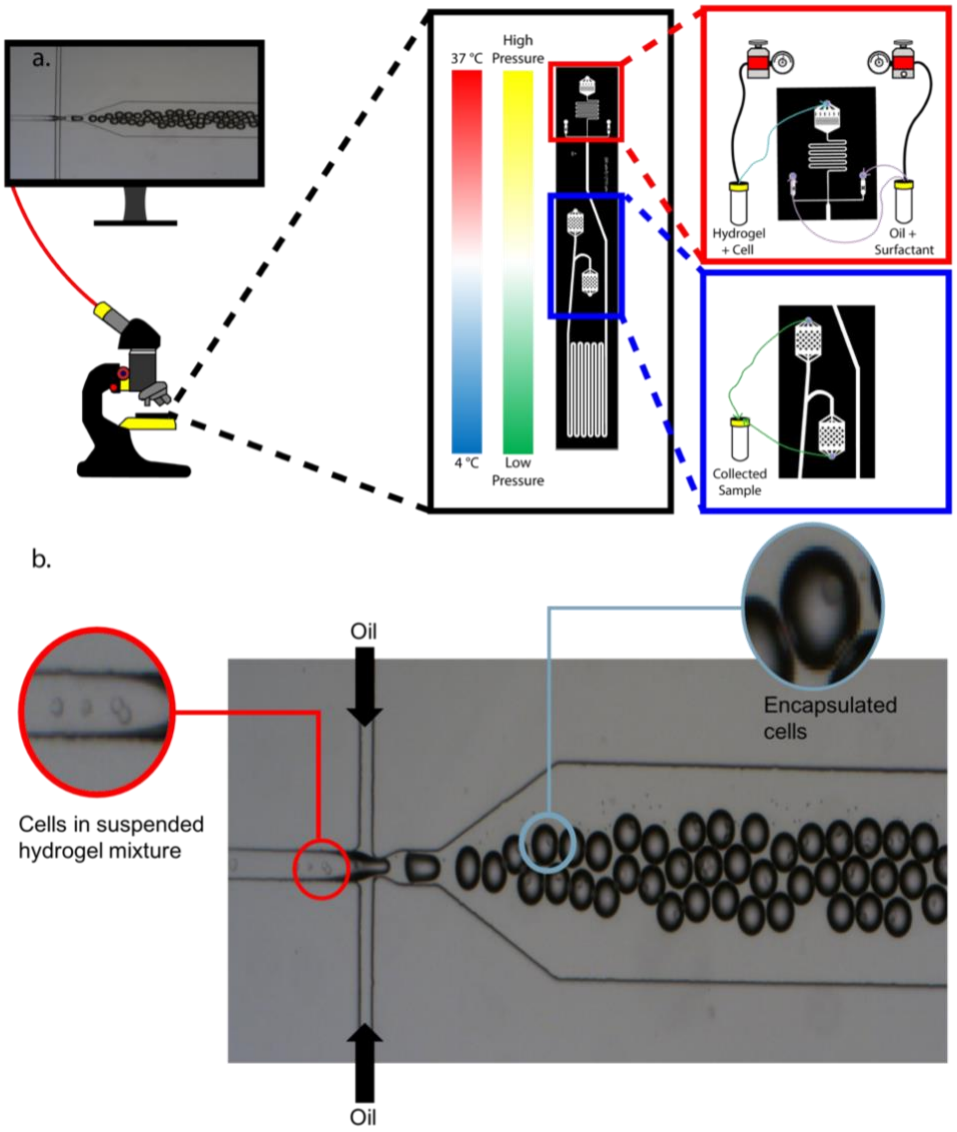

Figure 17. Overview of cell encapsulation. 17a describes the birds eye view of cell encapsulation. A microscope connected with a camera is used to monitor the cell encapsulation process which takes place on a pressure and temperature gradient. As the sample moves from the inlet to the outlet, the temperature goes from hot to cold – hot to maintain the hydrogel in liquid phase and cold to gel the formed droplets. In terms of pressure, the device uses a zone of high pressure to push the sample from the inlet to the outlet, which has lower pressure. The pressure gradient is set using pressure regulators that pressurize the inlet and oil channels. 17b zooms in on the cell encapsulation process. The cells suspended in a hydrogel mixture enter the encapsulation phase where they are met with immiscible oil and surfactant mixture. The hydrogel and cell sample are cleaved to create droplets, some of which are cell laden, while others are empty. Encapsulation occupancy rates are dependent on the Poisson distribution.

Sample Purification

Initially, the sample collection tube contains the initial media, microspheres and the immiscible oil used to cleave the microdroplets. In order to use the microdroplets for therapeutic purposes or double emulsions, the sample must be purified by removing the oil. The sample is centrifuged at 0.3xG for 3 minutes, the supernatant is removed, and this process is repeated. After the second oil removal step, the sample is transferred into a new centrifuge tube while avoiding the residual oil and new Dulbecco's modified eagle medium (DMEM) is added until the sample volume is 1 mL.

Quantification

With the purified sample, output of the microfluidic device can be quantified with throughput, total cell count, and cell viability using a hemocytometer and a trypan blue stain. It is necessary to incubate the trypan blue infused sample for 3-5 minutes in an incubator so as to give the dye enough time to be taken up by cells. After incubation, the number of empty cocoons, occupied cocoons, number of live cells and dead cells are counted. Single emulsions placed in a hemocytometer quadrant can be seen in Figure 18. The total number of microdroplets were measured using a hemocytometer using the following formula [106]:

$$total\ microdroplets = \frac{total\ microdroplets\ in\ four\ quadrants}{4} \times Dilution\ Factor \times 10{,}000$$

Once the total number of microdroplets have been calculated, divide the value by the time duration of the encapsulation process, in minutes, and then again 60 to get the throughput in droplets per second, or in other words, Hz. Cell viability is simply the number of live cells divided by the number of total cells.

Figure 18. Microdroplet samples on a hemocytometer for microdroplet and cell counting. Figure 18 represents a quadrant of the hemocytometer slide. Four quadrants are counted and averaged, multiplied by the dilution factor and then again multiplied by 10,000 to get the total number of cells. Additionally, the sample has been mixed with a trypan blue stain, which is a dye taken up by dead cells. When taken up, the dye looks dark blue. Live cells look like a glowing white.

Double Emulsion

The process of creating double emulsions is nearly identical to that of creating single cell encapsulations in every way except for the geometry of the microfluidic device used, as described in Figure 19. To accommodate for the larger incoming cocoons, the encapsulation nozzle has been enlarged, and because a larger amount of agarose mixture is entering the encapsulation point, the oil channels have, too, been widened. Increasing the width of the oil channels allows for a lower resistance in the oil channels and therefore increases the amount of the oil that reaches the encapsulation point. Agarose samples contain 1.5 x 10^6 $\frac{microdroplets}{mL}$, and the encapsulation process is shown in Figure 20.

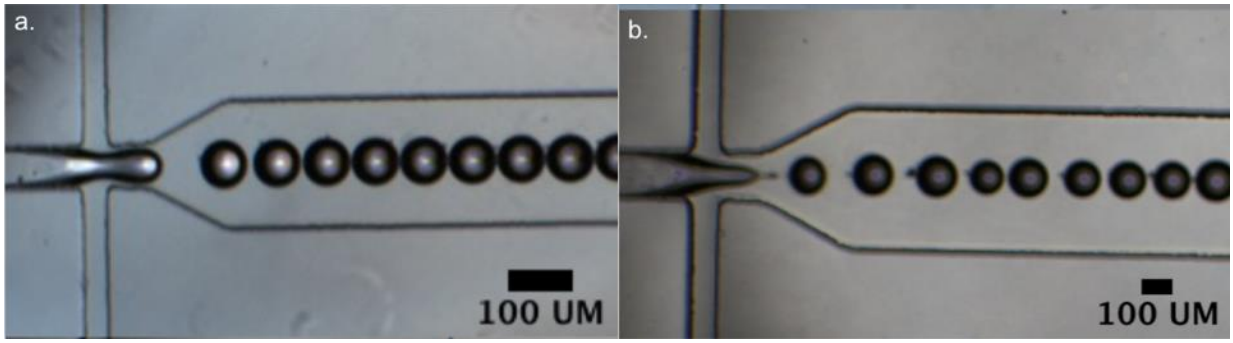

Figure 20. Double emulsion microdroplet formation. 19a depicts single emulsions with polystyrene beads whereas 19b shows double emulsions with cells.

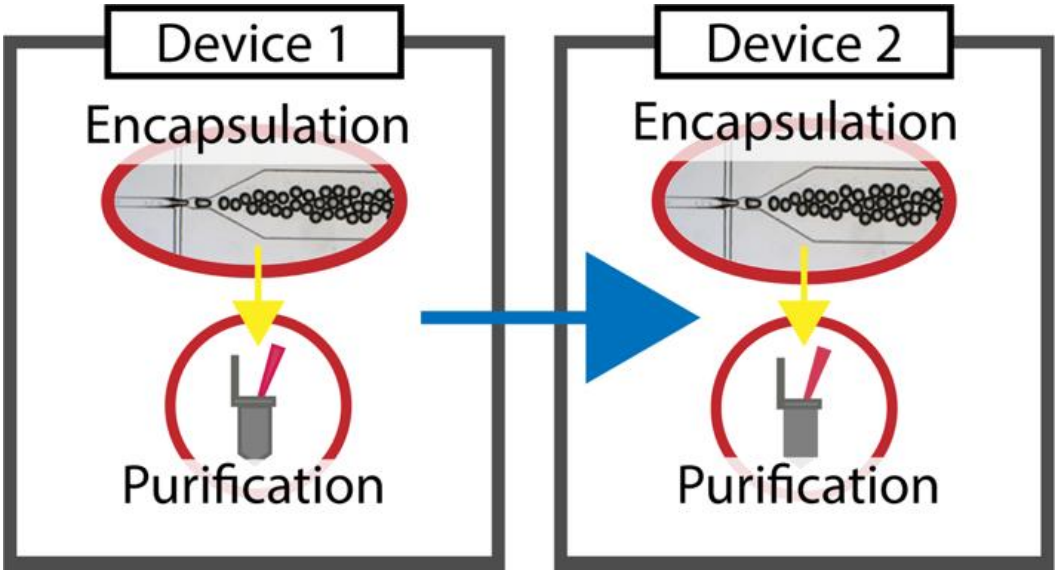

Figure 19. Creating double emulsion microdroplets. Single emulsions are purified and then mixed in with agarose hydrogels prior to being reinserted into a microfluidic cell encapsulation device. Double emulsions are again purified to get the final sample.

Once the double emulsions are created, the sample purification process is identical to that of the single emulsion process.

Poisson Distribution

Theoretically, the number of cells encapsulated within a droplet can be predicted using statistical models. Ideas presented here are based on the review paper by Collins et al. [70]. The Poisson distribution is the probability of events randomly occurring in a fixed time or space under the assumption that the events are random and independent of each other [107]. Therapeutic cells in the agarose hydrogel are suspended heterogeneously and thus arrive at the nozzle in a random order. Furthermore, the arrival of one cell does not impact the arrival of the subsequent cells. While the cells enter the encapsulation point randomly, the sample that contains them and consequently the production of droplets (with or without cells) is continuous. From this, it can be implied that it is impossible to guarantee that all droplets will contain a cell but the number of cell-laden microdroplets can be estimated using the Poisson distribution. In the context of microfluidics, the Poisson distribution equation is described as such

$$p(k,\lambda) = \frac{\lambda^k e^{-\lambda}}{k!}$$

Where λ is the average number of cells per droplet volume and k is the number of particles in an object. To utilize the formula for the Poisson distribution, we must select a cell density, the radius of the droplet and the volume of the droplet. Using the Poisson distribution and an assumption that the cell density used for encapsulation is 7.5 x 10^6 $\frac{cells}{mL}$ for single emulsions and 1.5 x 10^6 $\frac{cocoons}{mL}$ for double emulsions, the average number of cells found in the droplet volume (λ) for different diameters of

microdroplets is shown in Table 2, and the likelihood of a cocoon containing a specific number of cells is shown in Figure 21.

Using the Poisson distribution gives a theoretical number for benchmarking the efficiency of the cocooning platform, however, there is a lot that can alter the actual output. For example, the cells may settle to the bottom of the vial, changing the instantaneous concentration and violating one of the Poisson distribution assumptions. Clumping of cells or microdroplets can lead to occupancy values that are not in line with the Poisson distribution predictions. Actual output values not matching the theoretical values is an issue indeed, however, it does point to factors that might be addressed. For this reason, it is important to keep the Poisson distribution values in mind when analyzing the output from an encapsulation experiment.

Table 2. Average number of cells per droplet. Assuming a cell concentration of 7.5 x 10^6 $\frac{cells}{mL}$ for single emulsions and a cocoon concentration of 1.5 x 10^6 $\frac{cocoons}{mL}$ for double emulsions, the average number of cells expected for a certain diameter is shown in Table 2. The larger the cocoon, the more likely it is that it is occupied, and this holds true for both the single and double emulsions. More so, the larger the cocoon, the higher the likelihood that it is more than one cocoon. The values in bold are the theoretical values of the sizes of microdroplets created for this project, while the other values are present to illustrate the trend.

Expected Occupancy							
Diameter (um)	40	45	50	100	110	120	130
Expected Occupancy (7.5x10^6 cells/mL)	22.22%	30.08%	38.79%	97.31%	95.38%	85.04%	63.62%
Expected Occupancy (10x10^6 cells/mL)	28.47%	37.94%	48.03%	95.35%	83.27%	58.10%	82.20%

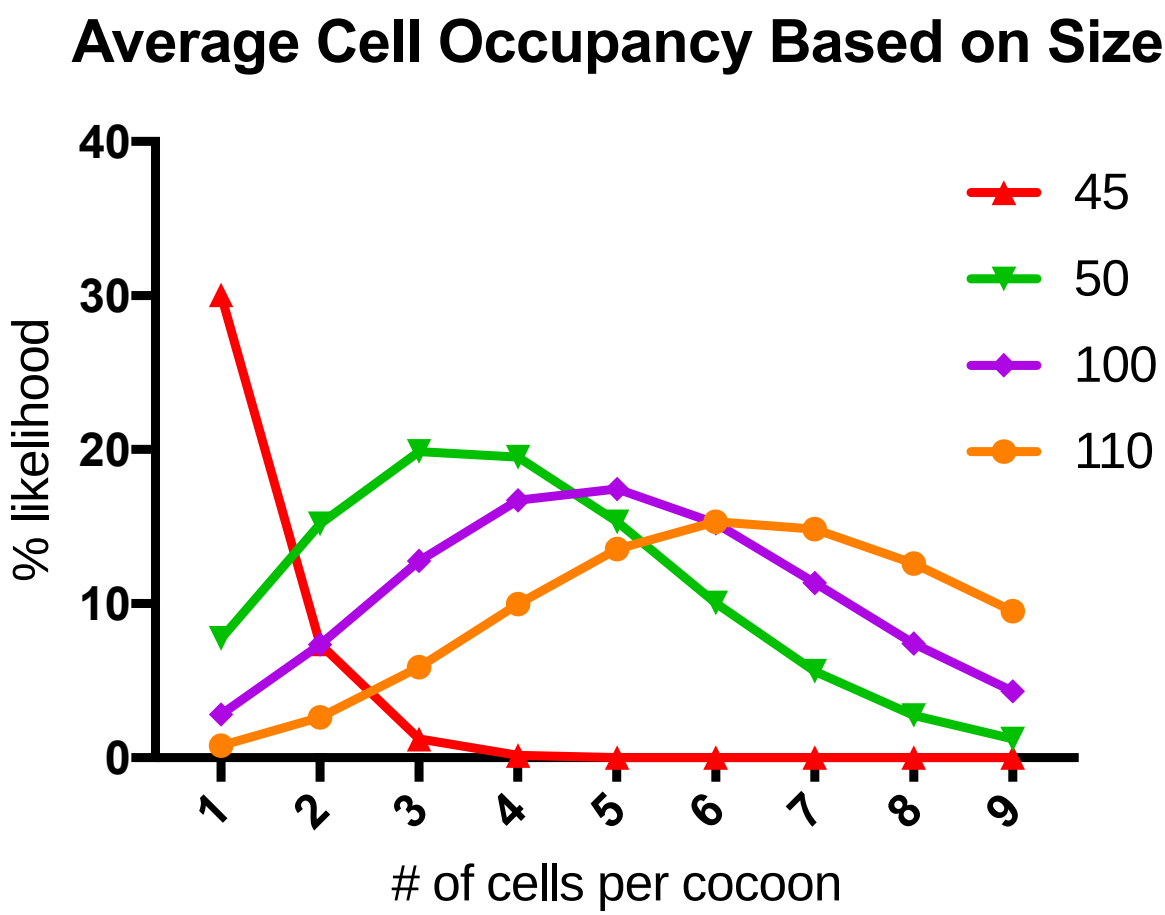

Figure 21. Average cell occupancy based on cocoon diameter. As the size of the cocoons change, so does the probability of finding a certain number of cells within the droplet. The smaller droplets have a higher chance of holding 1-3 cells, while the larger droplets tend to contain more cells. The numbers in the legend list the size of the microdroplet, thus 45 implying 45 μm, and so forth.

Timepoint Imaging

Quantifying cell egress can be done in a few ways, and one such method is time point imaging, which involves samples being seeded into DMEM filled 12 well-plates (22.1 mm diameter) and imaged periodically. For this project, samples are incubated for duration of 48 hours (H) and imaged at time points 0H, 24H and 48H. Time point is a valuable tool because it can be used to gather not only egress data but viability as well. At each time point, information is collected on cell viability via the trypan

blue exclusion method using a 1:0.5 ratio of sample to stain followed by a period of brief incubation. Trypan blue exclusion stains use a negatively charged dye that penetrates compromised cell membranes [108]. Generally, trypan blue requires a mixture of 1:1, however, doing so at a volume of 1 mL leads to poor visibility. The lower volume of stain is compensated through an extended incubation time. Egress data is collected by counting cell occupancy at each time point. For the timepoint experiments, a 12-well plate was used with 1 mL of DMEM and 20,000 microdroplets in each well. To get sufficient statistical powers, 10 images were taken and counted for each time point.

Occupancy, using a timepoint imaging technique, is done similarly for single and double emulsions, with a few key differences. For each image of taken for single emulsion cocoons, empty microdroplets, microdroplets with 1 cell, microdroplets with 2 cells, and microdroplets with >2 cells are counted. Cell-laden microdroplets are considered occupied while microdroplets with no cells are considered empty. Then, occupancy is a measurement of occupied microdroplets divided by empty microdroplets. Measuring occupancy for double emulsion was done similarly, with the difference being that production of double emulsion can lead to a completely empty microdroplet, which is similar to an empty single emulsion, a double emulsion occupied with empty single emulsions, or a double emulsion occupied with cell-laden microdroplet. Two levels of occupancy are calculated for double emulsion. First is regular occupancy, which is the number of cell-laden double emulsion divided by the total number of microdroplets present. The second is the adjusted occupancy, which is the number of cell-laden double emulsion divided by occupied double emulsions.

Egress measurements are treated as a function of the percent change in occupancy over time. Timepoint 0H for all egress is treated as 0% and considered a baseline. Egress at timepoint 24H is calculated by the percentage change between 24H and 0H using the following equation:

$$E_{24H} = \frac{(O_{0H} - O_{24H})}{O_{0H}}$$

Where E is egress and O is occupancy. Similarly, egress at timepoint 48H is calculated using the following equation:

$$E_{48H} = \frac{(O_{0H} - O_{48H})}{O_{0H}}$$

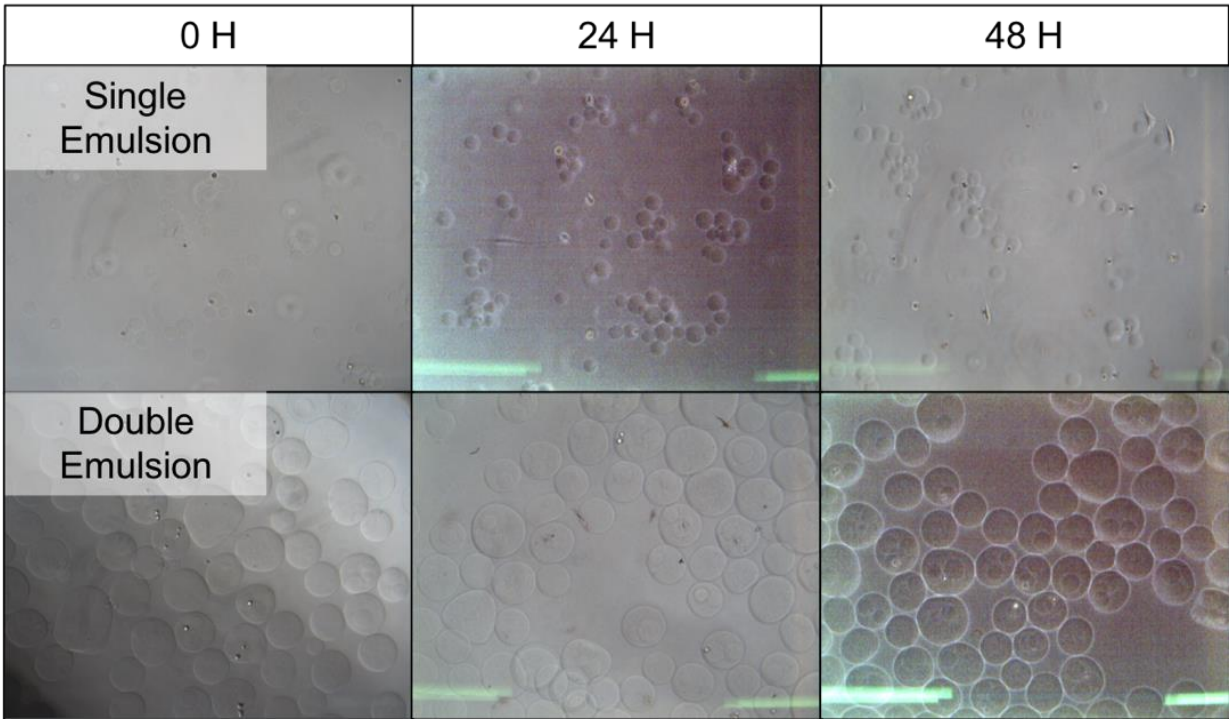

Figure 22. Example of timepoint photography comparing the differences between single emulsions and double emulsions over a 48 hour period. The images are used to measure viability and occupancy. One can observe, qualitatively, that there are more free cells in the single emulsion images than there are for the double emulsion images.

Confocal Microscopy

Brightfield microscopy is a practical, quick and accessible means to image cells for egress and viability, however, there are benefits to using the more advanced confocal microscopy. Firstly, confocal microscopy can use lasers that activate fluorescent dyes such as the Live/Dead kit. Unlike a trypan blue stain, live/dead staining kits identify live cells using a dye that binds to intact cell membranes and another dye to bind to the DNA of dead cells – which is more accurate and

reproducible than the trypan blue stain [108]. An example of the live/dead stain can be seen in Figure 23.

The second advantage of confocal microscopy that brightfield images do not offer is the ability to image in a 3D space. Brightfield images in a timepoint or time lapse experiment provide insight into occupancy, egress and viability, however, they do not reveal the three-dimensional structure of the single and double droplet. Cells within single emulsions are easier to identify using bright field images because cells lack their standard protrusions seen in culture and remain in a spherical morphology. Double emulsions seen through a brightfield microscope on the other-hand show a convincing inner core but leave the outer core in a questionable state. It is challenging to show that the inner core is actually within the outer core and not simply stacked on top of one another. Confocal microscope images are taken using the z-stack method to identify the structure in a three-dimensional configuration.

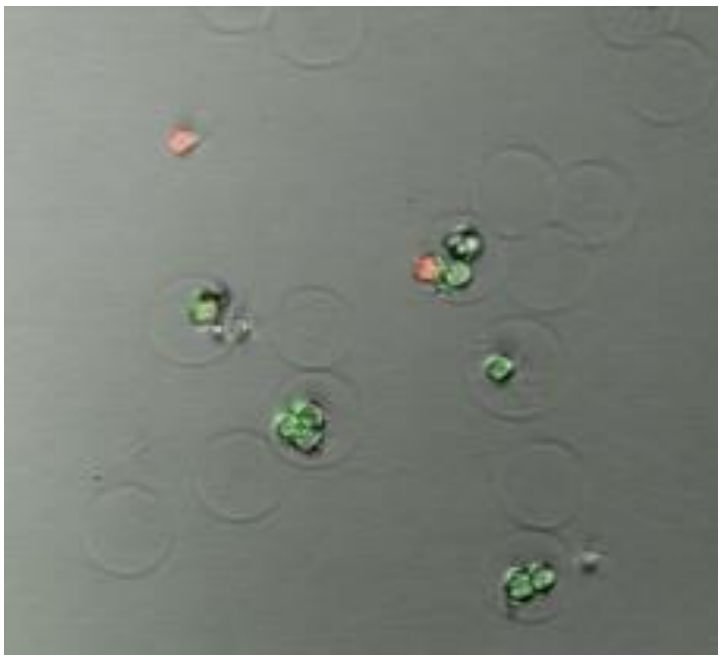

Figure 23. LIVE/DEAD stain of single emulsion cocoons. The image is a composite of a brightfield image, along with lasers illuminating fluorescent dyes taken up by the cells. The green cells indicate live cells while the red indicates dead cells.

RESULTS & DISCUSSION

The goal of this research project is to further the understanding of cell egress. We hypothesize that it is the cells on the edge of microdroplets that leave the sphere [82]. In order to test the hypothesis, a secondary emulsion layer is created to push cells in a droplet towards the center. Given the objective, the goals of this project involve creating hydrogel-in-hydrogel double emulsion microdroplets, confirming their structure, characterizing the creation process of said double emulsions and finally using the double emulsion microdroplet structure to carry out cell egress studies. Firstly, single emulsion and double emulsion microdroplets are created. The process of creating double emulsions is explored and contrasted with the single emulsion counterpart. Device geometries are discussed and compared for the two emulsion configurations. Second, the structure of the double emulsion is confirmed using 3D imaging with a confocal microscope, followed by characterizing some of the parameters required for creating double emulsions and finally, cell studies are carried out to understand the effects of double emulsions on cell egress.

Note: When this document references single emulsions with an agarose concentration, it suggests that the concentration of the whole microdroplet is the stated agarose concentration. For example, "1.5% single emulsion" suggests that the microdroplet is composed of 1.5% agarose solution. In the case of double emulsions, however, the percentage value is only referring to the inner microdroplet of the double emulsion. ***In this study, all double emulsions have an outer agarose concentration of 2%.*** *Therefore, a 1.5% double emulsion implies that the inner spheres are made of 1.5% agarose hydrogel and the outer sphere is 2% agarose. Similarly, a 1.75% agarose double emulsion implies that the inner sphere is made of 1.75% agarose hydrogel while the outer shell is 2%. Finally, a 2% agarose double emulsion implies that both the inner and outer shells are made of 2% agarose hydrogels.*

Creating Double Emulsions

Single emulsion droplets, be it for encapsulating cells or polystyrene beads, were made using a device with the geometry detailed in Figure 24. Work done by Chen *et al* identified that, while it is indeed the capillary number that plays a role in droplet formation, the size of formed droplets within a microchannel can be controlled by the flow rate and width of the channels [109]. The same study found that, given a constant flow rate in the dispersed phase, increasing the flow rate of the continuous phase leads to smaller droplets while decreasing the flow rate leads to larger droplets. More so, the width of the dispersed phase channel was largely responsible for the sizes of droplets a microfluidic device was able to produce, with the most stable sizes being a close approximation to the width of the feature labeled as the 'encapsulation point' [110], [111]. Experimentally, it was observed that the encapsulation process was the most stable, or monodisperse, when the pressurized channels of the

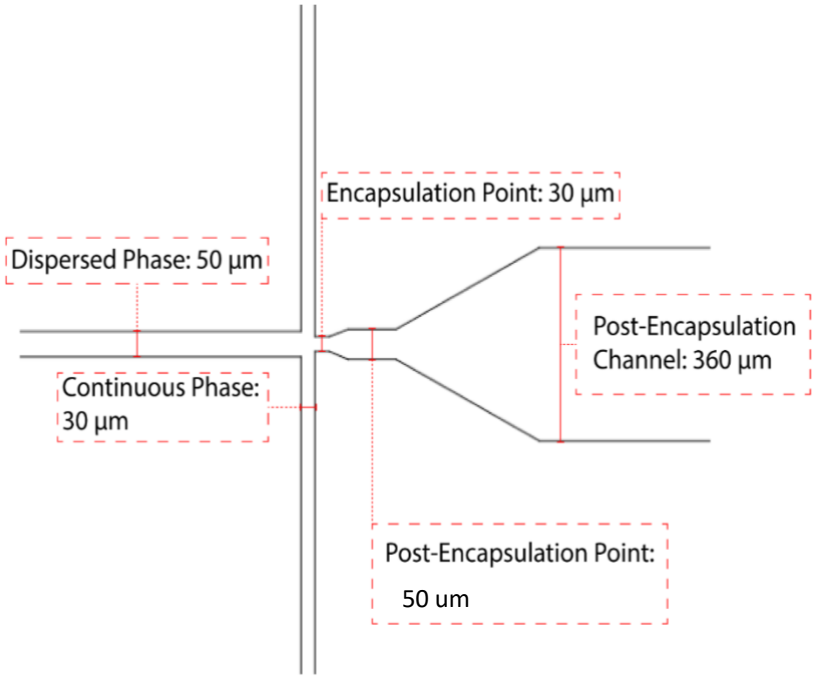

Figure 24. Geometry of a microfluidic device intended to create single emulsions of 40-50 µm.

dispersed and continuous phase were at a ratio of ~1 and although this value would fluctuate a little between experiments, it was used as the standard pressure ratio of operation.

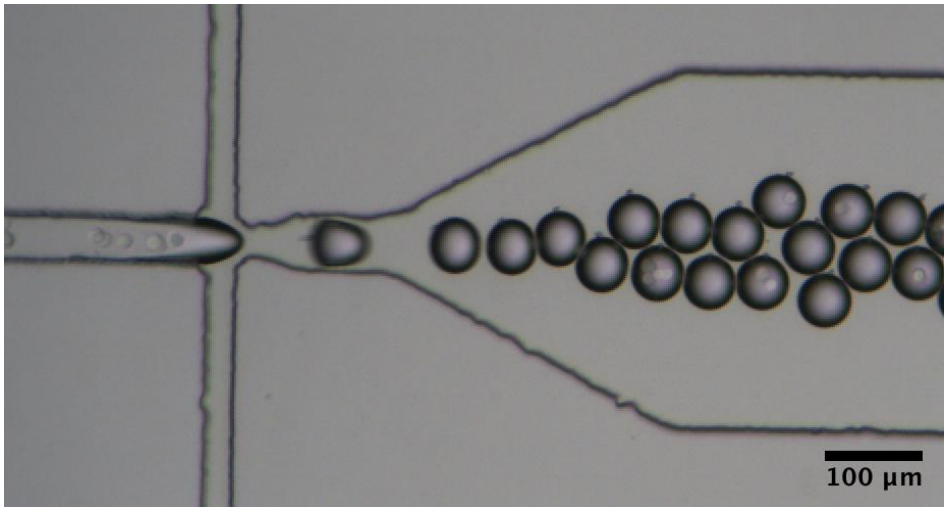

Figure 25. Example of microdroplets being created using a single emulsion microfluidic device. The geometry used is presented in Figure 24. The dispersed phase channel has a width of 50 µm, while the continuous phase channel has width of 30 µm. The encapsulation point width is 30 µm and the post-encapsulation channel is 360 µm.

Using the device in Figure 24, single emulsion droplets of approximately 40-50 µm were achieved. Examples of the microdroplet production are shown in Figure 25, where cell-laden single emulsion microdroplets are created using a geometry with a 50 µm dispersed channel width and 30 µm continuous channel width.

Creating a double emulsion using the same device was troublesome because the dispersed phase channel was 50 µm, while the incoming cocoons meant to be re-encapsulated moving through the channel were ~45 µm. The small size of the channel often led to clogging. Apart from clogging was the issue of microdroplet size. As previously mentioned, the width of the channel determines the average size of the microdroplets. Using the same single emulsion device to create the double emulsions proved difficult – the average size of double emulsion droplets would not exceed 90 µm,

and the ones that did exceed 90 μm came about rather uncontrollably, shown in Figure 26. For this reason, it was decided that a new device must be made with a larger dispersed phase channel width.

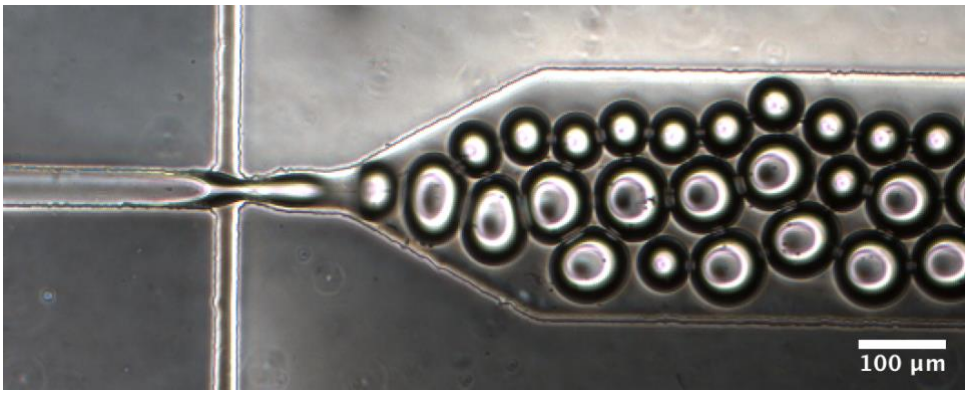

Figure 26. Double emulsion microdroplets created using the device intended to create single emulsions. While double emulsions are created, there was little control over the sizes (the double emulsion microdroplets averaged a size of ~90 μm, while intended size was between 100 μm and 120 μm.

To accommodate more than one single emulsion droplet flowing through the dispersed phase channel, the width of the dispersed phase channel was set to 130 μm, while the width of the post encapsulation point was set to 110 μm, the middle point between the intended droplet size of 100 μm – 120 μm. A marked-up drawing can be seen in Figure 28. While this device was an improvement and led to monodisperse droplets, as seen in Figure 27*,* the ratio of the pressures was imbalanced due to the continuous phase channel being so much smaller than the dispersed phase channel. In order to control the dispersed channel at a low flow rate, the aqueous channel would have to be set much higher. Doing so impacts the reaction of the droplet production device to incoming conglomerated droplets, where the flow rate of the oil is unable to 'cleave' the dispersed phase into proper microdroplets – leading to a long, gelled droplet similar in shape to a jetting regime.

A larger oil channel was thus incorporated into the microfluidic device intended to create double emulsions, of which the dimensions can be seen in Figure 30. Using the new geometries, a

monodisperse sample was attained while having the flexibility to encapsulate at higher pressures, and consequently higher flow rates, shown in Figure 29.

Creating double emulsions has been done using oil-in-water-in-oil (O/W/O) or water-in-oil-in-oil (O/W/O) configurations [112], [113]. While the oil component of double emulsions is always an oil, or oil and surfactant mixture, the aqueous portion can be any type of liquid such as a buffer with dissolved drugs or hydrogels [114]. Using the protocol presented in this work, a means of removing the oil layer and creating hydrogel-in-hydrogel (H/H) double emulsions.

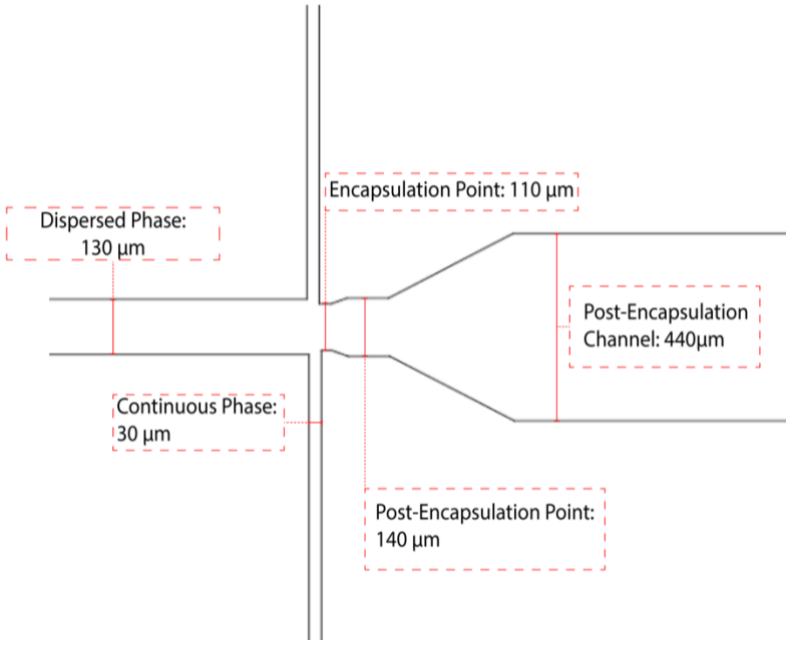

Figure 27. First iteration of a microfluidic encapsulation device intended to create double emulsion microdroplets.

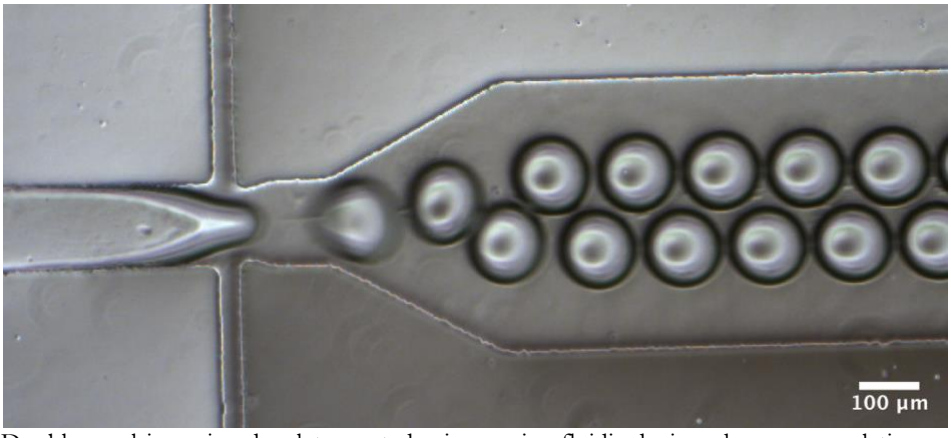

Figure 28. Double emulsion microdroplets created using a microfluidic device whose encapsulation point is set 110 µm as opposed to the 30 µm for the single emulsion devices. Here, the droplets created are within the intended size

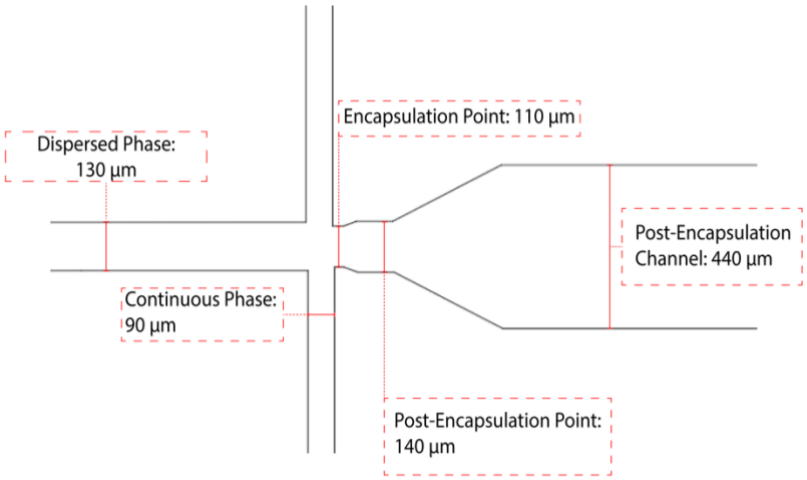

Figure 30. Second iteration of a microfluidic encapsulation device intended to create double emulsion microdroplets.

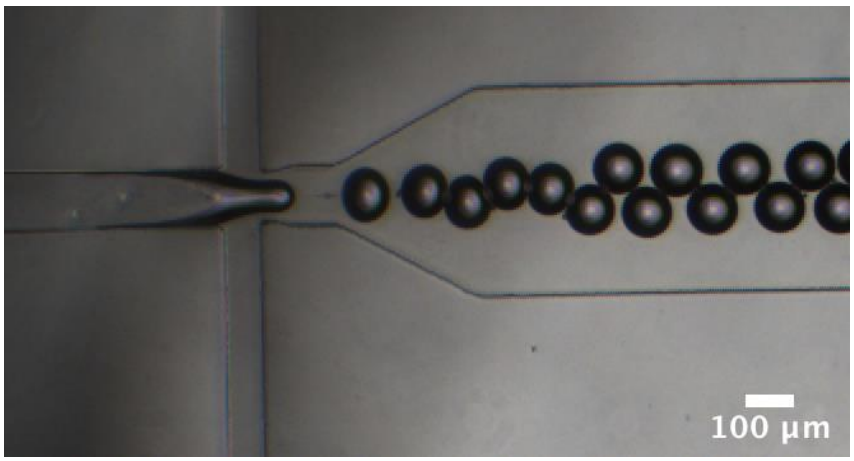

Figure 29. Double emulsion microdroplets created using a microfluidic device whose encapsulation point is set to 110 µm and continuous phase channel width set to 90 µm. The benefit of this device is in addition to being able to produce microdroplets in the intended size range, it can be operated at a higher pressure range than the previous

Size

Single emulsion microdroplets containing polystyrene beads were more monodisperse than their double emulsion counterparts as shown in Figure 31a. The same trend was observed with microdroplets containing cells, shown in Figure 31b. Both results are numerically presented in *table 1*. A higher level of polydispersity is present in larger microdroplets independently of their content (polystyrene beads vs cells) as illustrated through the control microdroplet - a larger single emulsion

intended to be similar in size to the double emulsion. It can be concluded that the polydispersity of microdroplets created using a microfluidic platform increases with the size of the microdroplets. Surface tension increases with the size of the droplet and thus the larger droplets are more likely to fluctuate in size [115].

Microdroplets were created with agarose hydrogel samples mixed with two different cell concentration amounts, 7.5 x 10^6 $\frac{cells}{mL}$ and 10 x 10^6 $\frac{cells}{mL}$, suggesting that the concentration of cells in the agarose hydrogel sample being encapsulated through the device was at either of the stated values, however, microdroplets containing the higher cell concentrations of 10 x 10^6 $\frac{cells}{mL}$ were only tested at an agarose concentration of 1.5% and 2%. It has been demonstrated that too low of an agarose concentration, around 1% agarose, leads to immediate release of free cells reducing occupancy, while a concentration of 3% agarose prevents cell egress entirely [82]. Microdroplets of 1.75% agarose concentration were excluded from the higher concentration to observe the trends in extreme cases. The average size of microdroplets containing different concentrations of cells are shown in Figure 31c and Figure 31d for single and double emulsions respectively. Trends in the monodispersity do not

seem to change based on the concentration of cells. Single emulsions are more monodisperse than their double emulsion counterparts.

Data shows that the size of microdroplets become harder to control as the microdroplet becomes larger, and under similar conditions, encapsulating polystyrene beads or cells does not affect the level of polydispersity. Two levels of cell concentration (7.5 x 10^6 $\frac{cells}{mL}$ vs 10 x 10^6 $\frac{cells}{mL}$) also had negligible effect on the level of polydispersity. Microdroplets used for this project are indeed in the intended range of 40-50 μm for single emulsions and 110-130 μm for double emulsions.

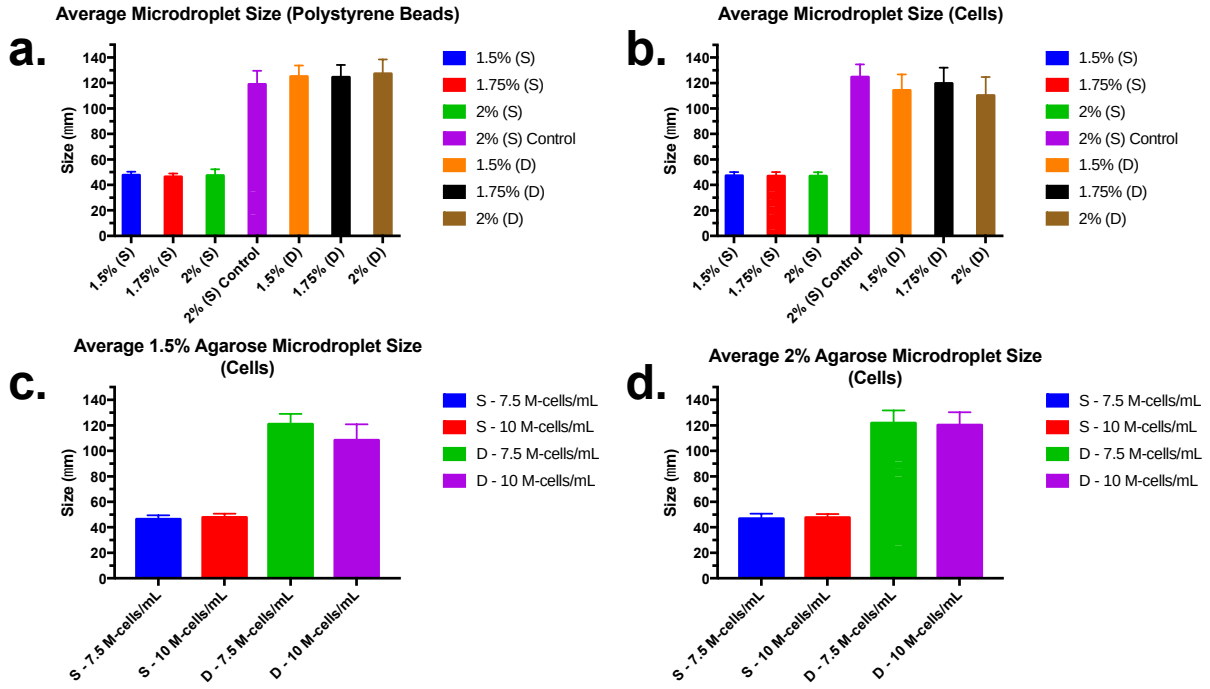

Figure 31. Average size of microdroplets containing polystyrene beads and cells, where (S) refers to single emulsions and (D) refers to double emulsions. 31a. Average microdroplet size for emulsions containing polystyrene beads. Single emulsions exhibit more monodispersity than their double emulsion counterparts and the control microdroplet. 31b. Average microdroplet size containing cells. Smaller single emulsions exhibit more monodispersity than their double emulsion counterparts and the control microdroplet. 31c. Average size for microdroplets composed of 1.5% agarose. There is no apparent difference between single or double emulsion microdroplets containing 7.5 x 10^6 $\frac{cells}{mL}$ versus 10 x 10^6 $\frac{cells}{mL}$. 31d. Average microdroplet size for microdroplets composed of 2% agarose. There is no difference between single or double emulsion microdroplets containing 7.5 x 10^6 $\frac{cells}{mL}$ and 10 x 10^6 $\frac{cells}{mL}$.

Size of cells, along with hydrogel porosity have been shown to impact cell egress and in order to ensure that the egress being compared in later sections was fairly assessed, it was vital for the droplets to be as monodisperse as possible [112], [116][10,11]. While larger microdroplets are indeed harder to control in terms of monodispersity, studies on single emulsion of show that droplets various sizes between 30 to 60 microns can be produced, using microfluidic systems, with a coefficient of variation of 5% - which translates to control with a range of 1.5 to 3 microns[117][14]. Coefficient of variation is computed by dividing the standard deviation of the microdroplet size and dividing it by the mean of the size and provides a unitless percentage value for which samples can be compared [118][15]. Table 3, below, shows the standard deviation for the different types of droplets produced for which the single emulsion variation is comparable to what is presented in literature. Double emulsions showed a high coefficient of variation, further confirming their polydispersity single emulsions in this thesis project as well as to the literature.

An automated, or computer based, method of measuring the droplet sizes may provide a more accurate size distribution as opposed to measuring each droplet by hand – which can change results based on user movement. A script that can measure the diameter of the droplets can provide a more accurate and consistent method of measurement. Outside of refining measurement techniques, investigating alternative pressure ratios and channel geometries to control surface tension effects should be done for creating less polydisperse double emulsions.

Concentration of Inner Agarose	Polystyrene Beads (μm)	Cells (μm)
1.5% (S)	48 ± 3	48 ± 3
1.75% (S)	47 ± 3	47 ± 4
2% (S)	47 ± 5	47 ± 3
1.5% (D)	130 ± 10	110 ± 10
1.75% (D)	130 ± 10	120 ± 10
2% (D)	130 ± 10	110 ± 20
2% - (S,Control)	120 ± 10	130 ± 10

Table 3. Average size and coefficient of variation of agarose microdroplet sizes containing polystyrene beads and cells. (S) denotes single emulsion microdroplets, whereas (D) denotes double emulsion microdroplets. While figure 1 visually demonstrates the level of monodispersity, this table provides numerical values.

Throughput

Throughput of the cell encapsulation process is described as the number of droplets generated per second by the encapsulation device and is measured in hertz (Hz). Information on the throughput of the device helps to determine how long to run the experiment for. Creating double emulsions require a minimal amount of single emulsion microdroplets. More so, both single emulsion and double emulsion microdroplets have to be seeded using a certain amount in order to be measured for viability and egress in a consistent manner. For this reason, the throughput was tracked for each encapsulation run.

Experiments show that the throughput for this project was highly variable. Amongst the entirety of microdroplets created for this research project, including single and double emulsions, the range of throughput was from 40 Hz to 143 Hz, with a mean of 85 Hz for microdroplets created with polystyrene beads and a mean of 79 Hz for samples containing cells, as shown in Figure 32.

Single emulsion microdroplets did show, on average, a higher throughput than double emulsion microdroplets. This is expected as double emulsion microdroplets consume more agarose per droplet and consequently, the same volume of agarose samples will yield lower number of double emulsions. Given the variable nature of throughput, these findings set a precedent of the time it takes to finish an encapsulation session for each experiment. For single emulsions, timepoint imaging requires a total of 60,000 microdroplets per experiment and another 300,000 microdroplets to introduce into the subsequent double emulsion encapsulation process. For a 12 well microplate, supplied with 1 mL of DMEM, 20,000 cells in each well plate provided a window filled with droplets. In creating double emulsions, a concentration of 300,000 microdroplets per sample was chosen because qualitative trials led to clogs with higher number of droplets. In total, 360,000 microdroplets are needed and thus single emulsion encapsulation sessions are carried out for at least 2.5 hours to ensure that sufficient

microdroplets are captured. Double emulsions only require 60,000 total droplets, so it is collected for at least 1 hour. Increasing the throughput would help in reducing the time that cells spend outside of an incubator or within an in-vivo sample. Number of droplets for double emulsions also comes about from supplying each time point microwell in a 12-well plate with 20,000 cells per time point, in order to fill the field of view without overcrowding.

An immediate solution to increase device throughput is to run multiple devices in parallel, however, it is still important to investigate device parameters in order to get a less variable, and consequently, more predictable throughput rate. Future experiments on the duration of the encapsulation time on cell viability could also be of interest because it would provide insight into the importance of throughput. Should a three-hour long experiment have no negative impact on cell viability, a device with poor throughput can still be an acceptable solution for creating encapsulated cells without compromising sample quality. If the results do indeed show that a prolonged experiment reduces cell viability, changes need to be made to the encapsulation protocol.

Results collected for throughput were not as expected. For both single and double emulsions, the continuous phase was always between 0.12 – 0.15 MPa and therefore the expected throughput should have been 100 to 200 Hz which was not achieved in this project [119]. Device geometry was not identical for single and double emulsions, as shown in section 1 of the results. The channels are wider for the double emulsion devices compared to the single emulsion devices (encapsulation nozzle width of 110 μm vs 30 μm respectively). Larger channels using the same pressures have a higher flow rate, however, the volume of a 120 μm microdroplet, 7.2×10^6 μm^3, has a volume thirteen times as much as the volume of a 50 μm microdroplet, which has a volume of 5.3×10^5 μm^3. The agarose consumed by one 120 μm microdroplet is thus more than the agarose consumed by a 50 μm microdroplet, and it makes sense that over the same unit time, the 120 μm microdroplets have a lower throughput. Still,

there needs to be further experimentation to determine the cause of the variable throughput in order to have a more predictable system over all experiments and encapsulations. Changes in pressures directly affect the size, as the flow rates are controlled via the pressure gradient, and a fluctuation in pressure may cause a poor throughput by changing the sizes intermittently between droplet production. Experiments can be done to investigate this by creating droplets using pressure generated from a pressure regulator and droplets created using a syringe pump. Syringe pump driven flow in microfluidic systems are characterized with fluctuating flow rates, while pressure driven flow in microfluidic systems is commonly used due to its smooth and stable pressure properties [120]. A comparison between the peristaltic-like pressure system compared to a smooth continuous pressure flow should be done to ensure that there are no detrimental effects from fluctuations in pressures that come from a variable throughput.

Another source of variation may arise in the sample-counting step. Microdroplets are counted using a hemocytometer and the throughput is calculated by dividing the total number of droplets collected after an encapsulation run by experiment duration. In order to load the samples onto the glass counting contraption, one must use a 10 μL pipette with a very narrow tip. It might be so that microdroplets get caught in the tip. Pipette tips for 10 μL micropipettes have an estimate diameter of 350 μm, which works out to be less than ~3 double emulsions wide, or ~7 single emulsions [121]. The narrow dimension of the pipette tip paired with the sticky nature of agarose could lead to samples being stuck along the interior of the pipette tip. Alternatives to microdroplet counting might be worth exploring to treat this issue. Using videos of the encapsulation method and counting frame-by-frame may be a more accurate, albeit more tedious, alternative to using a hemocytometer. This method, unfortunately, requires a camera with a high frame rate, which is expensive. Perhaps, the hemocytometer method can be tested to ensure that the results indeed align with the theoretical count. An approach for calibrating throughput could be slowing down the live encapsulation rate to below

the frame rate of the camera so the live rate can be measured. The encapsulation can be run for a set period of time then the hemocytometer values can be compared to what should be expected. While this may seem similar to the previous suggestion, this method would slow down the potential of throughput and thus reduce the number of microdroplets collected. For example, the camera used for this project has a framerate of 60 Hz. If we set the encapsulation process flow rate using pressure control to the point where it is 50 droplets per second, we can run it for a set period of time – 1 hour for example, we can expect 180,000 droplets at the end of the encapsulation run. Using a hemocytometer, we can confirm if the hemocytometer underestimates, overestimates or shows the accurate results.

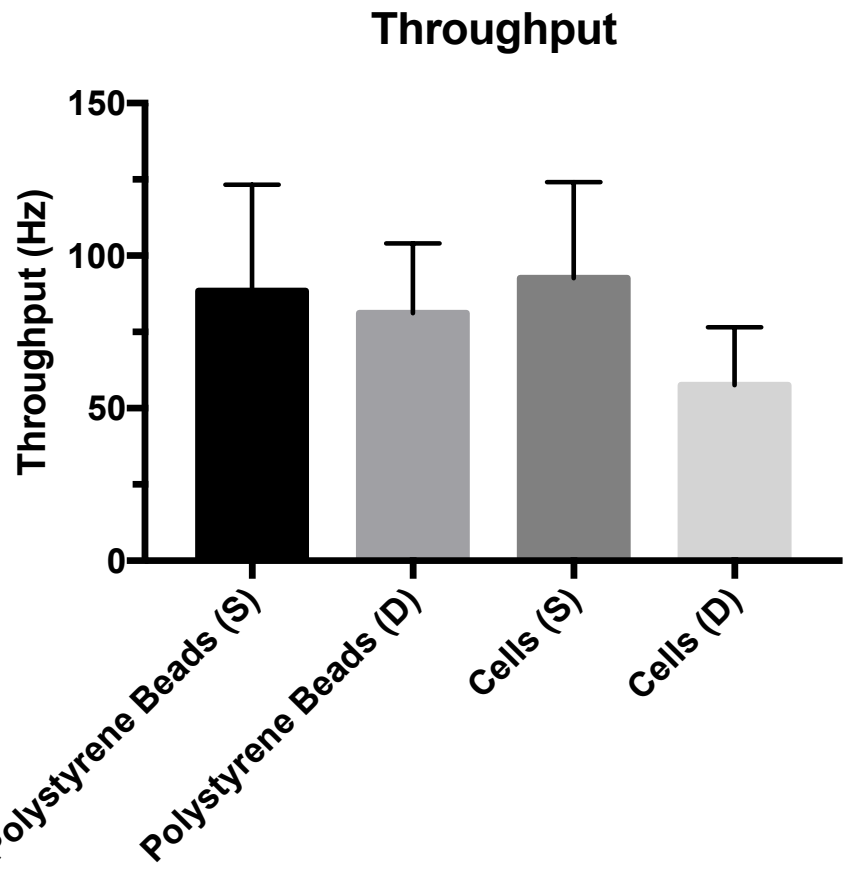

Figure 32. Throughput between single (S) and double (D) emulsion microdroplets. Discriminating between single emulsion and double emulsion microdroplets did little to provide a different trend in throughput.

Viability

Cell viability is a critical metric to ensure sample quality. Using timepoint experiments to track the viability of cells ensures that the single and double emulsion microdroplets are not negatively effecting stem cells. Agarose microdroplets are intended to act as the carrier for sensitive therapeutic cells and although a benefit of agarose is biocompatibility, it is a unique environment and must be tested to ensure it is not to the detriment of cell viability.

Figure 33a and Figure 33b show the viability of single and double emulsion microdroplets with a cell concentration of 10 x 10^6 $\frac{cells}{mL}$. For 1.5% agarose microdroplets, there was no significant difference ($p > .05$) between the microdroplets over time either between or within samples. That is to say that the viability remained unchanged over a 48H period of time on average for single emulsions and double emulsions, and there was no difference between the viability of single emulsion and double emulsions. Viability data for 2% agarose single and double emulsion microdroplets did not show a significant difference ($p > .05$) between the samples. There was, however, a difference ($p = .007$) between the 0H and 48H time point within the 2% single emulsion samples, with a 6% decrease. While the change in viability for the 2% single emulsion microdroplets is less than ideal, the 48H time point between single and double emulsion droplets have no significant difference between them. For this reason, the samples were used to collect cell egress data.

Initial experiments showed rather poor viability, as seen in Figure 34. Three concentrations of agarose were tested for single and double emulsions with a cell concentration of 7.5 x 10^6 $\frac{cells}{mL}$, however, during these experiments, the viability decreased from timepoint 0H to 48H. Here, it is imperative to note that viability was in no way effected by the concentration of cells. The first batch of experiments utilized a lower amount of cell concentration as it is easier to encapsulate lower concentrations due to less frequent clogging within the devices and clumping of the cells. Increase in

concentration was in order to increase the double emulsion occupancy, which was less than desirable in the initial experiments. Poor cell viability can lead to skewed egress results and thus it is vital that cells remain alive over the experiment. Should there be a change in cell viability, results might be skewed to show a higher occupancy, indicating a lower amount of cell egress as the dead cells cannot escape microdroplets, adding false-positive data points to the experiments.

From the initial experiments, it was learned that handling samples played a large role in cell viability. For all experiments carried out, the microfluidic encapsulation device setup was identical as were the devices used. There was no difference between the tools, and therefore the only difference came about from the culturing and handling of the cells. Future experimenters working in cell encapsulation may benefit from a more stringent usage criteria for cells. By and large, future experiments should use a narrower range of cell passages. Experiments done in this body of work used cells from passages as low as 6 and as high as 26 – future experiments may benefit from using cells between a stricter passage number in order to avoid genetic drift [122]. Most importantly, the poor viability results justify tracking viability over a period of time rather than just at time point 0H. Each sample from the initial experiments, outside of one (1.5% double emulsion) had a reasonable initial viability levels and it was at time points 24H and 48H that the values began to decrease, in the most extreme cases as much as 44%.

It is preferable for stem cells to stay viable for as long as possible. In fact, certain neurological stem cell treatments track the cells for up to 14 days after in-vivo implantation, while stroke treatments with stem cell therapies are tracked for up to 4 weeks [123], [124]. To ensure that both single and

double emulsion microdroplets do not impact the stem cells over a long period of time, the viability data collected should be tracked for a longer duration.

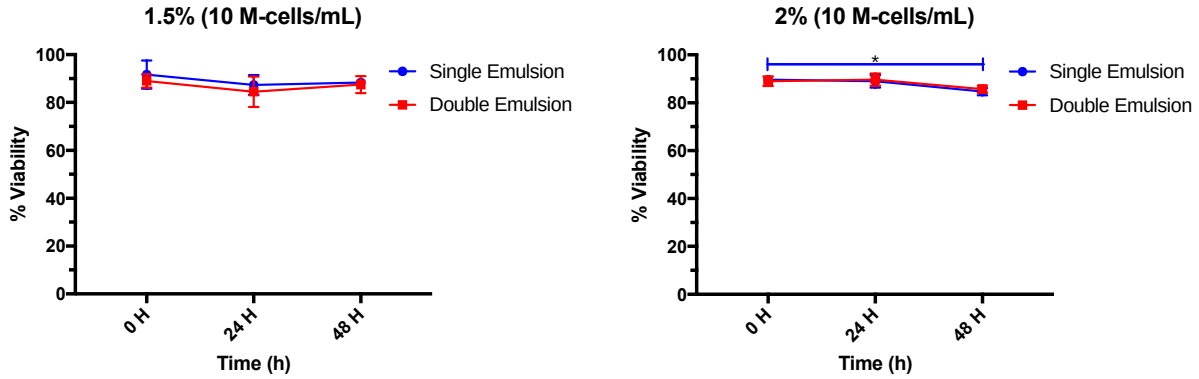

Figure 34. Viability of cells over 48H. 33a. Viability of 1.5% single and double emulsion microdroplets over 48H. There is no significant difference between the single and double emulsion samples at any of the time points, nor is there a significant difference within each type of microdroplet at any of the timepoints. 33b. Viability of 2% single and double emulsions over 48H. There is no significant difference between the single and double emulsion samples at any of the time points and the double emulsion samples do not show a significant difference within the samples at any time points. A difference does arise in the 2% single emulsion between 0H and 48H ($p = .007$). There is no significant difference between 0H - 24H or 24H – 48H, however, over the duration of the experiment, the viability drops a statistically significant amount.

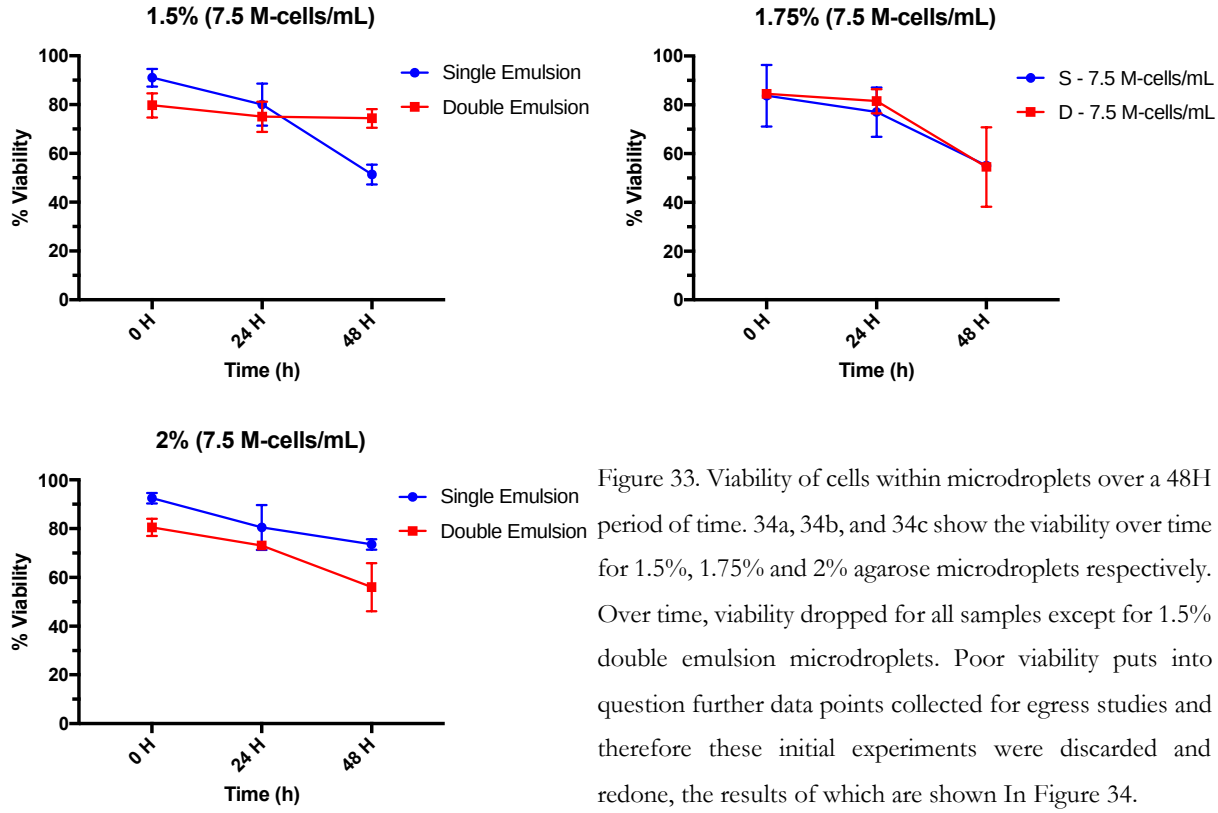

Figure 33. Viability of cells within microdroplets over a 48H period of time. 34a, 34b, and 34c show the viability over time for 1.5%, 1.75% and 2% agarose microdroplets respectively. Over time, viability dropped for all samples except for 1.5% double emulsion microdroplets. Poor viability puts into question further data points collected for egress studies and therefore these initial experiments were discarded and redone, the results of which are shown In Figure 34.

Microdroplet Structure

Z-stack imaging from a confocal microscope is used to gather information on double emulsion microdroplets in a 3D orientation. One might make the argument that 2D images showing single and double emulsions in any sort of configuration, with or without cells, are actually images of objects stacked on top of each other and kept in place by the pressure of a glass cover slip. To ensure that the microdroplets are indeed in the configuration we state that they are in – 3D images are provided to exemplify the structures.

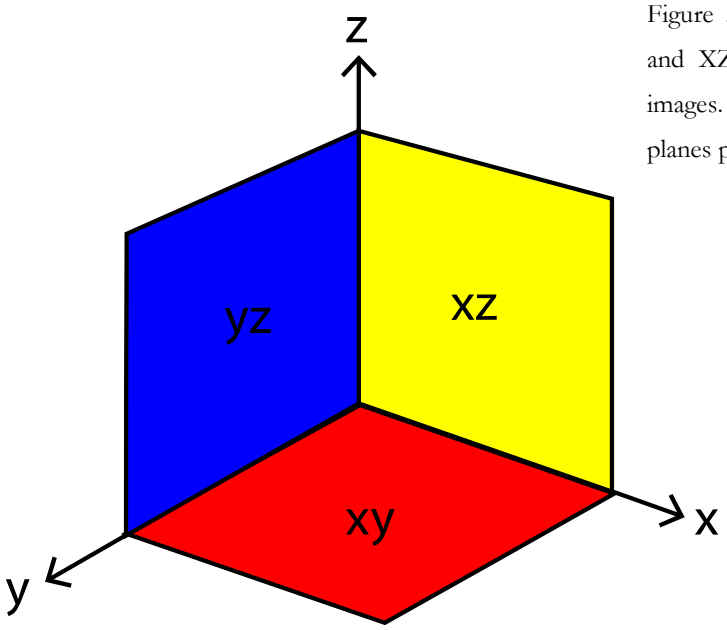

Figure 35. Representation of the XY, ZY and XZ planes shown in the orthogonal images. This figure aims to help visualize the planes presented in the orthogonal views.

3D images from z-stack imaging are best done with a glass bottom well plate, which was not accessible during this research project. Using the standard thick plastic well plates for imaging led to sub-optimal quality images. However, given the LIVE/DEAD kit stain, the cells were still distinguishable from the surrounding microdroplet emulsion. Future work done to visualize the

double emulsion structures would greatly benefit from a multi dye setup which stains the inner shells, outer shells and the cells a different colour without relying on the bright field component.

Orthogonal images are presented as three planes, the XY, YZ and XZ planes, shown in Figure 35. Analyzing the images requires imagining the structure in 3D space.

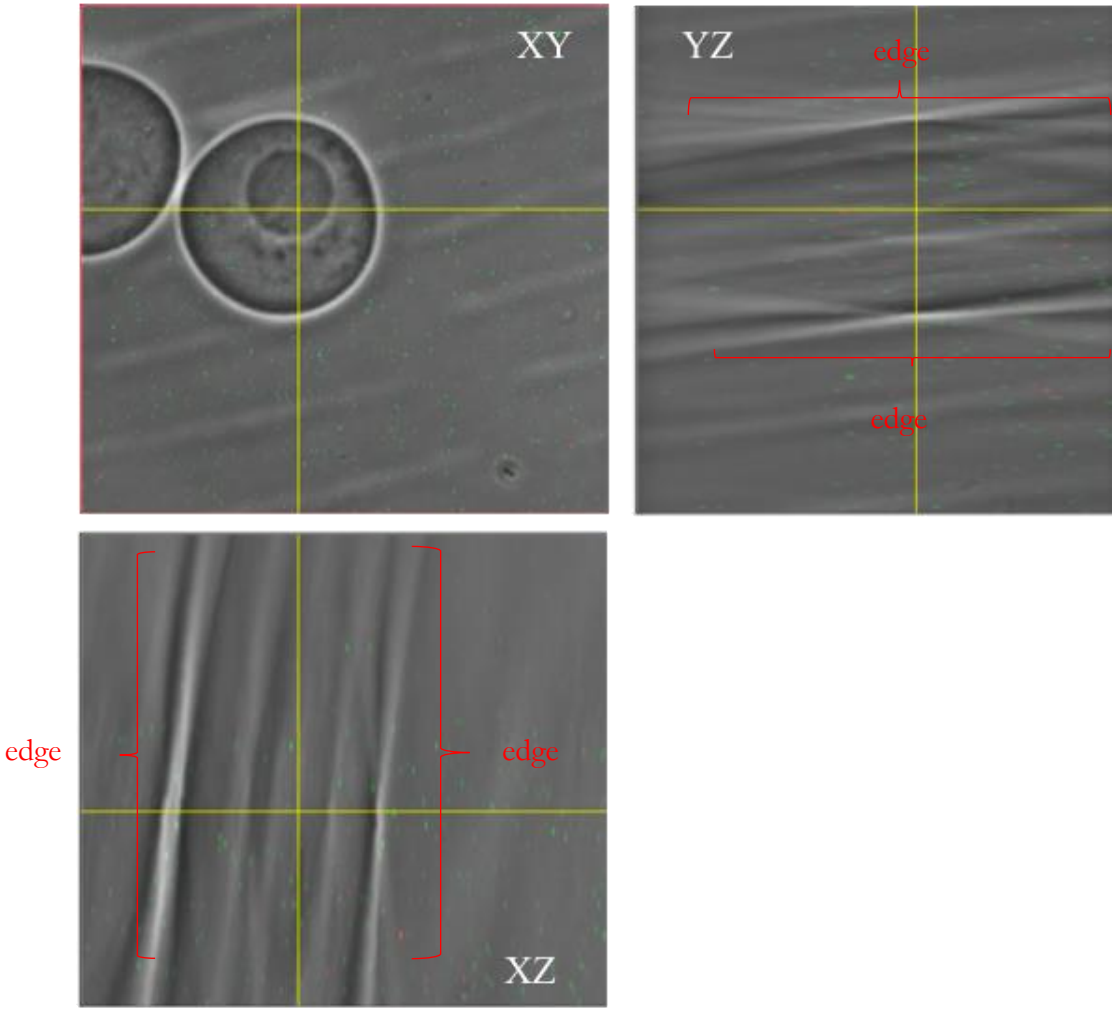

Figure 36. Orthogonal view of a 2% double emulsion microdroplet. Images of the three planes helps to visualize the microdroplets in 3D space and identify their structure.

To serve as a guide and an example of how to interpret the images presented in this section, a brief explanation is provided. Figure 36 depicts an orthogonal view of 2% double emulsion microdroplet, with an empty inner microdroplet. All three images are marked with the plane that they represent. Each image is marked with two yellow lines that relates the position of the intercepting

point to the other two planes. In Figure 36 the intersection of the yellow lines is within the smaller microdroplet positioned either within or above the larger microdroplet. Following the cross section from the XY plane to the right shows YZ plane, and to the bottom the XZ plane. The XY plane represents the standard 2D plane one sees under normal microscopy. To identify the placement of the smaller sphere in relation to the larger sphere, one first follows the yellow line down to the XZ plane. To the left and right of the yellow line intersections are two bright white lines, marked with *"*edge*"*. At points marked "edge", white lines that mark the diffraction of light caused by the brightfield image bending at the edges of the agarose microdroplet can be seen. The diffracted lines align with the edges of the larger microdroplet. The smaller microdroplet's diffraction is not as bright likely due to the fact that it is positioned in between the scanning area. Similarly, the diffraction lines can also be seen in the YZ plane, and in they too hold the smaller microdroplet within the larger microdroplet. Combining the data extracted from each plane, one can reasonably assume that the smaller microdroplet is within the larger microdroplet, confirming the successful creation of a double emulsion.

To then confirm the structure of a single emulsion of cells, one turns to Figure 37, which depicts the orthogonal view of a cell-laden single emulsion microdroplet. In the XY plane, the microdroplet of focus can be identified as the cell-laden microdroplet containing a green-stained cell. The green dye indicates that the cell is alive, but in this case – the dye is used to identify the cell's placement within the microdroplet. Similarly to the previous image, Figure 36, the bending of light from the brightfield component of this confocal image creates a crossing of sorts. In the YZ plane, the cross is a little blurred towards the top due to the directly adjacent microdroplet, while in the XZ plane, the left and right edges can be seen with the two white crosses.

Taking information from the three planes, it can be inferred that the cell is positioned in the center of the Z plane, but close to the edge in the X direction. It is this type of cell that we hypothesize is

likely to leave, as it is located so close to the edge. The porous nature of agarose paired with the cell's proximity to the edge provides the cell a direction out. The blue boxes relate the microdroplets in each plane, showing that in all planes, the cell is within the emulsion.

Finally, Figure 38 shows a double emulsion containing a cell. In this image, the cell is most likely in poor condition as it has begun to take up the red stain which indicates cell death. Regardless, it is a good example of cell positioning and thus presented to display a cell within a presumed double emulsion created using our microfluidic platform. Due to the fact that the inner emulsion is 1.5% agarose, it appears a bit faint in the brightfield image, but the outline can still be made out. The outer droplet can be seen again using the diffracted light, and the XZ plane shows a fairly bright light diffraction for the inner emulsion as well. From this, it can be implied that the cell is nested within the single emulsion which is then nested with a double emulsion.

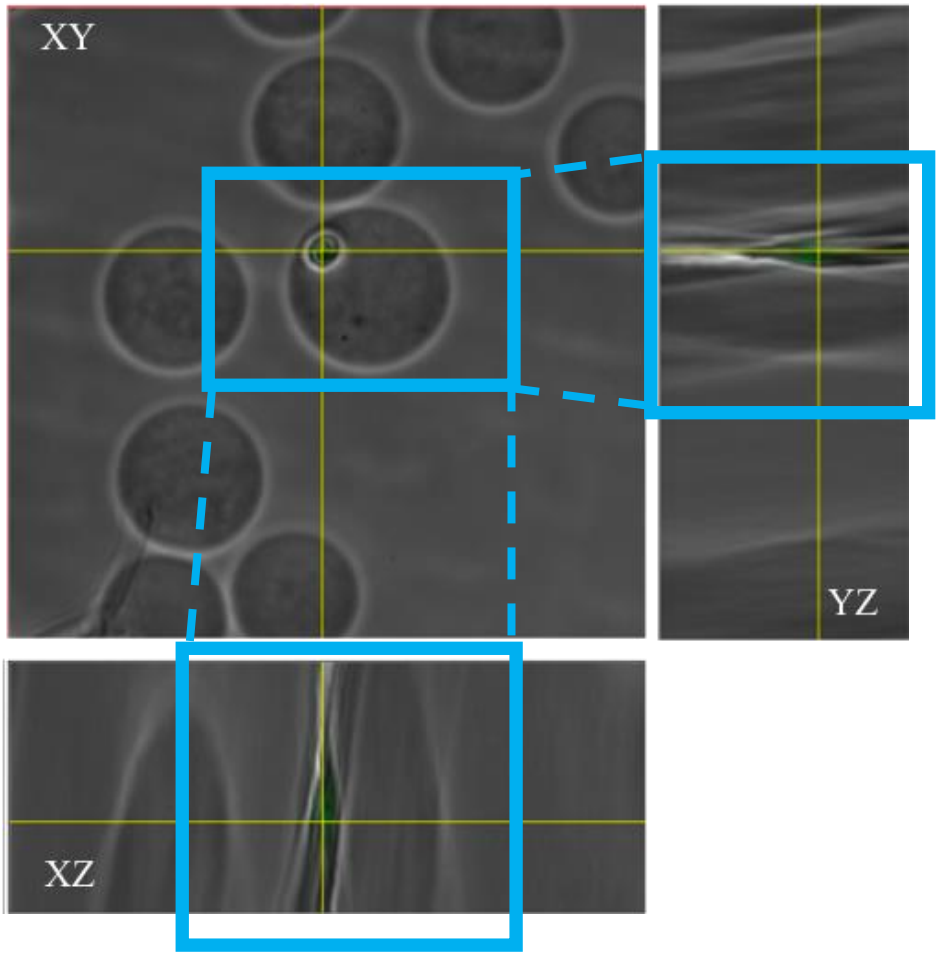

Figure 37. Orthogonal view of a cell-laden 2% single emulsion microdroplet.

Using a confocal microscope to take z-stack images provided proof of concept data of the structure of single and double emulsions. Cell-laden single emulsions, double emulsions with an empty inner droplet and a cell-laden double emulsion droplet are shown. While three images is not enough to provide a dataset to make a claim about double emulsion structures as a whole, experience in creating encapsulations has done little to point towards cells simply being stacked on top or under microdroplets and held in place by the microscope cover slip. When imaging double emulsions, especially with 1.5% inner agarose microdroplets – multiple images must be taken at different points in the z-direction to ensure that there is in fact an inner capsule. This is done because the inner droplets can be difficult to see, however, in doing so, it was also observed that the cells are only in focus in between the points where the inner emulsion is in focus – further supporting the claim that the cells appearing with the double emulsion structure are indeed inside. These claims are, still, anecdotal and based on personal experience and do not provide empirical data. For this reason, future experiments collecting 3D images would be of interest. Using fluorescent agarose, ideally of two different colours to create droplets that fluoresce would be a more clear way to see the structure of the droplets. Two differently dyed agarose hydrogels could also give insight into the distribution of agarose concentrations within the structure when different concentrations are used. For example, if the inner shell is 1.5% agarose and the outer shell is 2% agarose, does the gel form a gradient for any reason? Does the more aqueous components of the lower agarose concentration bleed into the outer shell as a gradient? Such a gradient would imply that at the interface of the inner and outer droplets, the hydrogels are not at either of the expected concentrations. More than just identifying the structural geometry of the microdroplets, the proposed experiments could be used to investigate the general positioning of the microdroplets. It would be interesting to find a correlation between the average number of cells that are close to the edge in a double emulsion and the rate of egress. This would

further support our proposed hypothesis of cells on the edge of microdroplets being the ones that egress out.

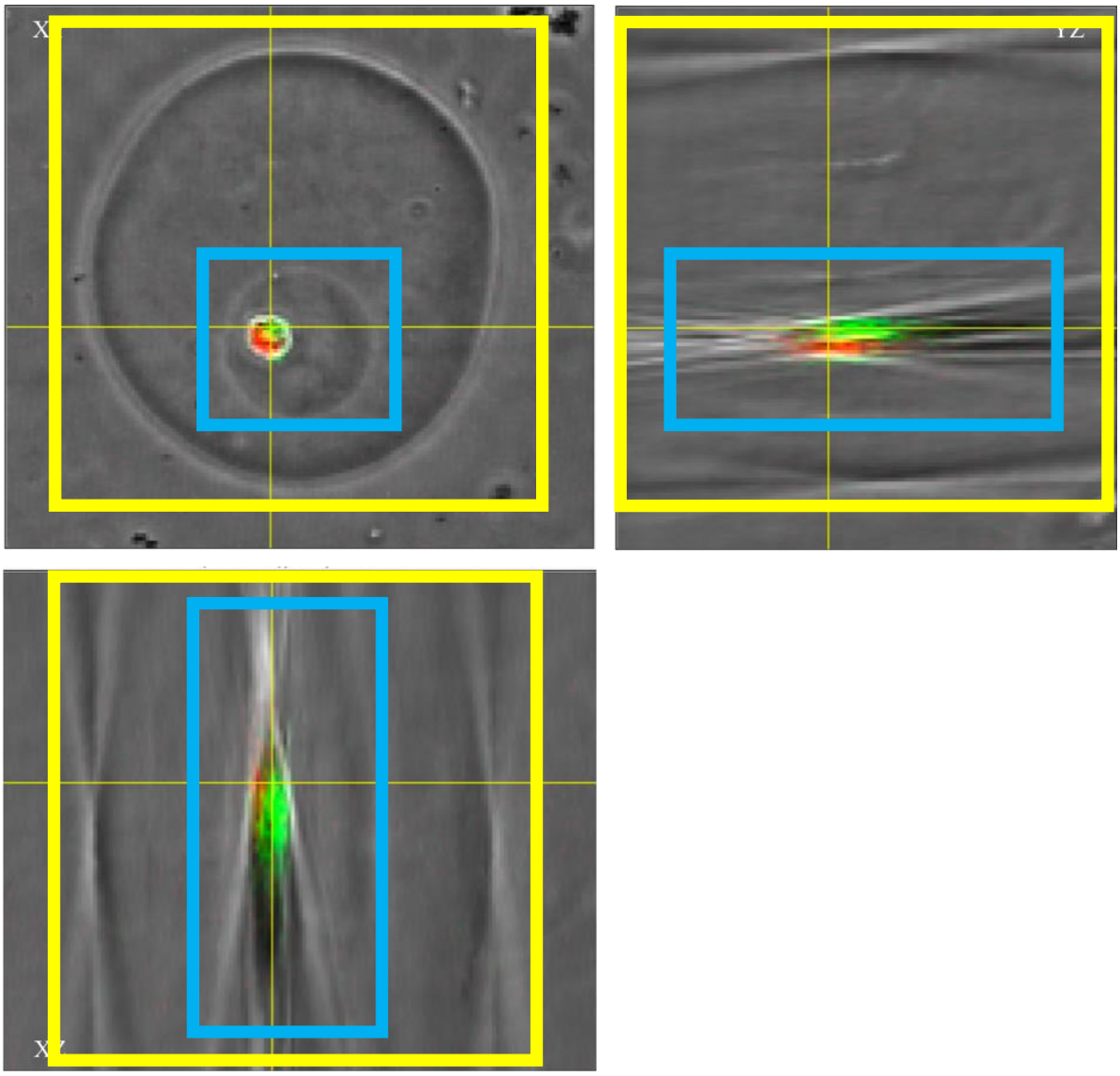

Figure 38. Double emulsion microdroplet with an inner cell-laden 1.5% microdroplet that has taken up both the red and green stain from the LIVE/DEAD kit, implying an inviable cell. However, due to the brightness of the sample, it illustrates the cell position clearly. Objects within the blue box indicates it belongs to the 1.5% inner microdroplet, while the yellow boxes all indicate an outer emulsion.

Egress

Cell egress is a measurement of the percentage of cells that leave the microdroplets after encapsulation over a period of time and is calculated as a function of the change in occupancy. Fundamentally, it is the measurement used to support or disprove our hypothesis.

Firstly, egress of single emulsions is shown in Figure 39. Egress for single emulsions was calculated by using time point imaging. For each time point, 10 random images were taken of a 12-well plate containing 1 mL of DMEM and 20,000 total microdroplets. From the 10 random images, the number of empty microdroplets and the number of cell-laden (or occupied) microdroplets are counted. Occupancy is the total number of cell-laden microdroplets divided by the total number of microdroplets present in all 10 images. As time point images are taken at hours 0H, 24H and 48H – egress at timepoint 0H is considered 0%. Egress at 24H is the percentage change of occupancy from 0H to 24H, and egress at timepoint 48H is the percentage change from 0H to 48H.

Single emulsion microdroplets made of 1.5% agarose and 2% agarose containing 10 x 10^6 $\frac{cells}{mL}$. showed similar egress profiles over a 48H time-point, with 2% agarose microdroplets showing a higher average egress at each time point. At time point 24H, 2% agarose microdroplets had an average egress of 49%, while the 1.5% agarose microdroplets had an average egress of 38%. At time point 48H, 2% agarose microdroplets still had a higher egress, with 66% while 1.5% agarose microdroplets had an egress of 50%. Despite the differences in the average egress, there was no statistical difference ($p > .05$) between the samples at the 24H and 48H time point.

It has been shown that egress is higher for agarose with relatively lower concentrations, for example, 1.5% agarose microdroplets should have higher egress compared to 2% agarose microdroplets [82]. Due to the discrepancy, more experiments need to be done testing single emulsion cell egress to compare with the published data. It is more likely that droplets with a lower

concentration have a higher egress because the microdroplets are structurally more porous and give cells more pathways out [82]. We cannot, therefore, draw an appropriate conclusion from the average egress values between the two agarose concentrations – but only a magnitude of egress. In this case, single emulsions have an egress rate of about 40% - 60% over 48H, if the agarose concentration is in between 1.5% and 2%. Future work should aim to conclude if a pattern exists between the two agarose concentrations, as seen in the literature.

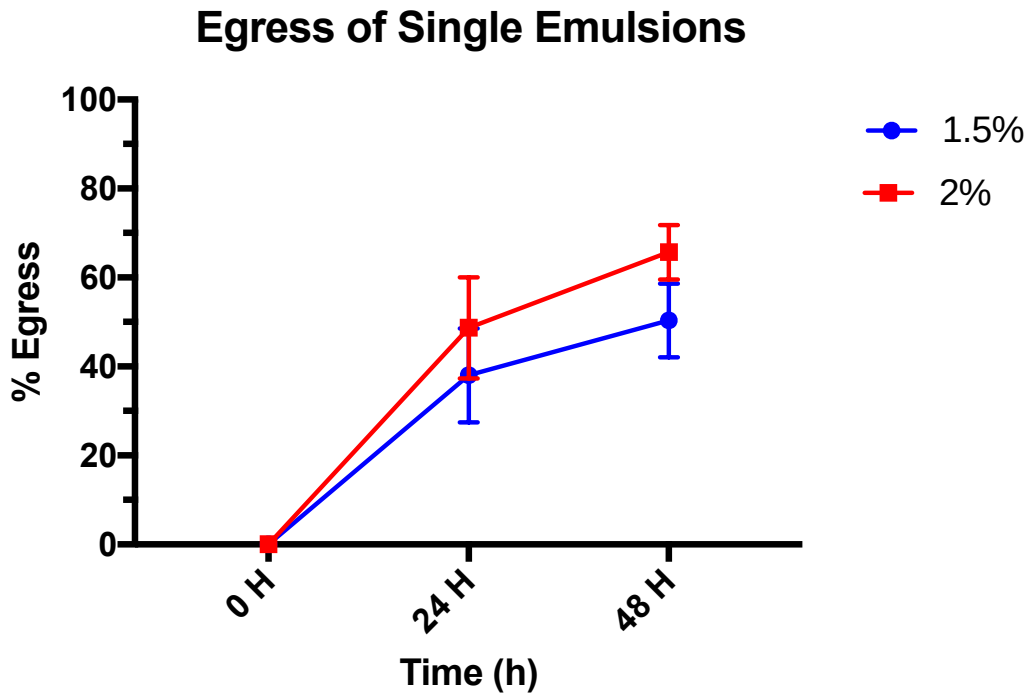

Figure 39. Cell egress from single emulsion microdroplets at 1.5% agarose and 2% agarose concentrations, with a cell concentration of 10 x 10^6 $\frac{cells}{mL}$. Samples did not show a significant difference from one another, with (p=.3 at 24H) and (p=.07 at 48H), there was a continuous trend of cells egressing more for 2% agarose microdroplets compared to 1.5% agarose microdroplets. These results do not line up with published findings and therefore must be further investigated.

Cell egress from double emulsion microdroplets was quantified in two ways, using unadjusted and adjusted egress. Unadjusted egress is calculated using the total number of microdroplets present per

time point, while adjusted egress is counted using only microdroplet-laden emulsions. Details on the methods of counting are provided below.

One must recall that not all double emulsion microdroplets will be occupied with an inner sphere, and because the occupancy of the inner microdroplet is not 100%, the double emulsion samples will have even less cell-laden samples. The three states of existence for a double emulsion is then empty (which is one large empty microdroplet), occupied with single emulsions that have no cells, and occupied with a microdroplet that contains one or more cells. This is different from single emulsions where microdroplets can only exist with or without cells. Adjusted occupancy corrects the double emulsion counts from three potential states of existence to two, which more closely resembles the counting done for single emulsions. To allow for a meaningful comparison, egress from single emulsions was compared to egress from double emulsions as defined using the adjusted counting method.

Unadjusted and adjusted egress counts are compared in Figure 40. Through the comparison, benefits of using the adjusted egress values are seen as the unadjusted counterpart is influenced by fluctuations in how many empty double emulsion microdroplets (meaning no cell-laden or empty single emulsion within the droplet) there are. There is no significant difference between the adjusted and unadjusted egress values for 1.5% double emulsions, shown in Figure 40a. Figure 40b illustrates egress for 2% double emulsions, and like the previous comparison, there is no significant difference between the two measurement methods at any of the three timepoints. Despite the lack of statistical difference between the two measurement types, there is a disparity in the trends demonstrated. Unadjusted values, in both cases, show the 24H time point having higher egress than the 48H time point. 1.5% double emulsion egress goes from 22.5% to 9.5% egress between time points 24H and 48H. Similarly, for 2% double emulsion egress, the egress changes from 19% to 18% between time points 24H and 48H. It is very improbable that the cells re-enter the droplets once they leave, and the

findings are more than likely an error brought on by the counting metric. Unadjusted occupancy is influenced by images that randomly contain more empty emulsions. The data of interest for double emulsion tests is to measure how many cells exit from a double emulsion structure. Large droplets with a cell and no inner droplets have not been observed thus far, and so empty emulsions do little to provide any insight into the egress process. Their presence does, however, dampen the effects of cell egress between occupied double emulsions and cell-laden droplets. In fact, these discrepancies disappear when using the adjusted counting method, which removes the convolution with the droplet occupancy of the double emulsion – perhaps an indication that during some stages of the counting process, there were was an influential amount of totally empty large droplets created during the double emulsion process. Adjusted values show a more sensible pattern, as the egress slightly increases from 24H to 48H for both samples, with 1.5% egress recorded as 15% to 15.3% from 24H to 48H and 2% egress recorded as 8.6% to 9.3% from 24H to 48H. It is far more realistic that there is very little or no change in egress than there is a re-entering of cells. Due to the fact that there is no significant difference between the two types of measurement, it can be implied that the impact of the empty large droplets produced in the double emulsion is effecting the trend. Both types of measurements imply a lower amount of egress compared to the single emulsion droplet type. Therefore, due to the fact that the unadjusted egress repeatedly shows an unlikely trend and the difference between the adjusted and unadjusted values are not significantly different, comparison of single emulsions and double emulsions will be done using the adjusted values of the double emulsion microdroplets.

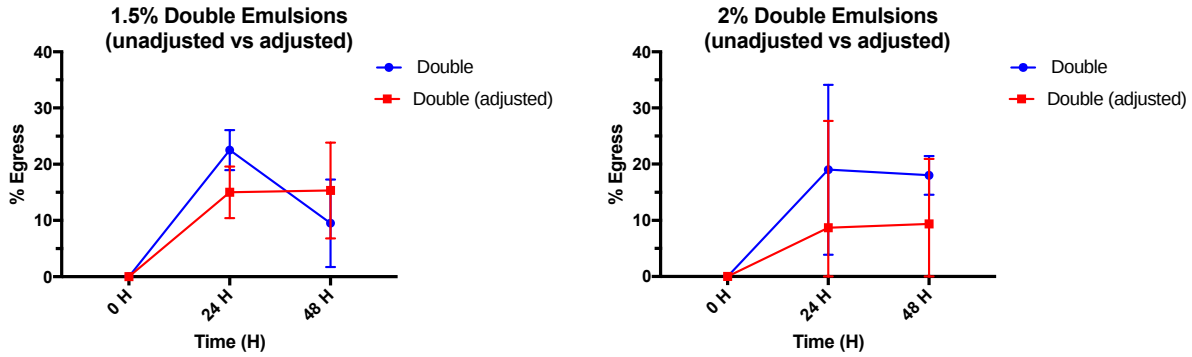

Figure 40. Egress of cells from double emulsion microdroplets using the adjusted and unadjusted methods. 40a. demonstrates egress of 1.5% double emulsions. There is no significant difference between the two methods (p=.14 at 24H) and (p=.50 at 48H). 40b. demonstrates egress of 2% double emulsions. There is no significant difference between the two methods (p=.97 at 24H) and (p=.32 at 48H). As there is no difference between the two methods of measurements, we can conclude that the data Is not altered using the adjusted egress counting method.

Adjusted egress between the two double emulsion samples of 1.5% and 2%, depicted in Figure 41, also showed no significant difference at each time point, however, on average, the egress within double emulsions containing 2% microdroplets with cells was lower than the egress of cells containing 1.5% microdroplets. This seems consistent with the fact that agarose at higher concentrations is stiffer than it is at lower concentrations and thus makes it harder for cells to egress [82]. When comparing the difference between single and double emulsions, it must be noted that each concentration showed similar egress. In other words, 1.5% and 2% single emulsions showed similar egress that was not significantly different from one another, and 1.5% and 2% double emulsions showed egress that was also not significantly different from one another as well. From the data presented in Figure 41, it seems that the inner emulsion concentration is impacting the egress values, however, still lower than the average egress amounts for single emulsions. Experiments presented in this manuscript hold the outer emulsion concentration constant while varying the inner microdroplet concentrations, however, experiments varying the outer emulsion concentration while holding the inner concentration constant might give interesting insight into the impact of the outer shell. With the current data, we cannot determine if the egress is impacted by the concentration of the outer or inner shells. Additionally, the

trends observed here are opposite to the trends observed for the single emulsions. As mentioned previously, it is expected that lower concentration agarose droplets should have a higher cell egress which is what was observed for double emulsions but not single emulsions. These findings give more reason to investigate what may have caused the errors in single emulsions.

Perhaps the egress observed in the double emulsion microdroplets is still only due to cells on the edge of the microdroplet. Cells situated in a double emulsion configuration that contains the inner microdroplet close to the edge may still be produced. While there is no way of knowing, given the current data, if that is indeed the reason for this egress, it may be a reasonable explanation given that there is little egress that takes place between 24H and 48H. All the cells situated close to the edge end up leaving within the first 24H, and those who are not by the edge remain within the capsule. Such an idea can be explored using confocal microscopy to take 3D images and time-lapse imaging to track cells over time.

Finally, egress between single and double emulsions is compared. Double emulsions consistently had a lower egress value than single emulsions at each timepoint. Figure 42a shows the egress of 1.5% agarose single emulsions, with a diameter of 40 – 50 μm and double emulsions, with a diameter of 100-120 μm. At timepoints 24H and 48H, the single emulsion microdroplets had a significantly higher amount of egress than the larger double emulsion. Furthermore, between 24H and 48H, the egress in 1.5% agarose single emulsions continued to increase while it plateaued for double emulsions. Figure 42b shows an identical pattern of higher cell egress for 2% single emulsions with respect to 2% double emulsions. Much like the previous samples, the egress values were significantly different between the two concentrations at each time point. At time points 24H and 48H, 1.5% single and double emulsions had significantly different egress values from each other. Similarly, 2% single and double emulsions had significantly different egress values from each other 24H and 48H. For both cases, single emulsions had a higher egress than the double emulsion counterpart. Additionally, there was a

noticeable plateau in egress for the double emulsion microdroplets for both concentrations between timepoint 24 H and 48 H, while the single emulsion continued to egress between the 24H and 48H point.

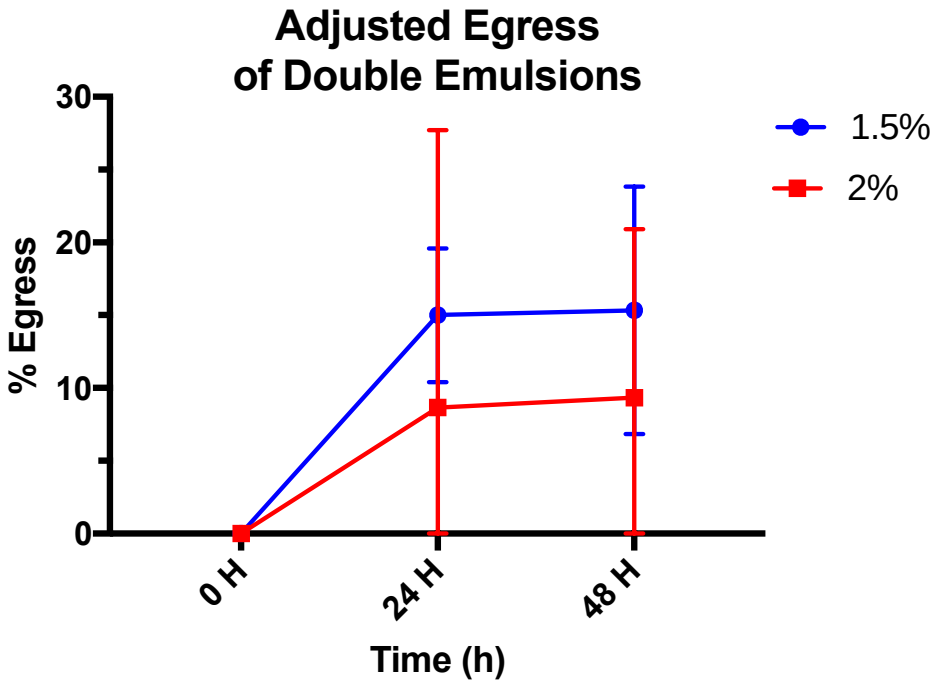

Figure 42. A comparison of cell egress out of double emulsion microdroplets of 1.5% and 2% inner shell concentration using the adjusted egress method. There is no significant difference in cell egress at 24H (p=0.75) and at 48H (p=0.51).

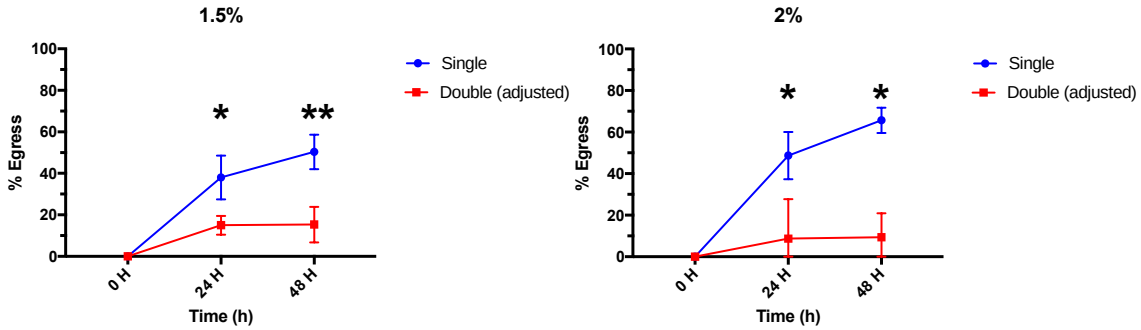

Figure 41. Comparison of egress between single emulsions and double emulsions at two different inner microdroplet concentrations. 42a. depicts egress between 1.5% single and double emulsions. There is a significant difference between the samples at both timepoints 24H (p= .04) and 48H (p=.01). 42b. depicts egress between 2% single and double emulsions. There is a significant difference between samples at both timepoints 24H (p=.01) and 48H (p=.005).

Extending size of a microdroplet by creating a secondary emulsion does indeed lesson the amount of egress – however, there is not enough evidence to explain why. It was hypothesized that it was the cells on the edge of the microdroplets that leave and in order to push the cells towards the center of the microdroplet, the secondary layer would be created. Unfortunately, the double emulsion microdroplet production method used in this thesis did not always center the cells. While the width and height of the double emulsion device are 110 μm and 160 μm respectively, the single emulsion droplets introduced into the device are between 40 – 50 μm. This leaves plenty of space for the droplets to move around. Literature exists on centering samples in a microfluidic encapsulation device, and perhaps the inclusion of such channel features can help in centering the position of the inner droplet – leading to certainty that cells are not close to the edge of the device [116]. Assuming the cells are centered, any amount of egress could contest the hypothesis.

Cell encapsulation work has been done in order to reduce in-culture cell egress and found that the cells remain in capsules for longer [125]. The same study found that untreated encapsulated cells had a tendency to leave within three days. While the purpose of this project is to keep them at the target location for a longer period of time in the context of cell-based therapy, it still investigates a similar phenomenon.

As mentioned previously, there is a need to do more egress experiments in order to explore why 1.5% single emulsions have a lower average egress than 2% single emulsions. This trend is not supported by literature [82]. The double emulsions on the other hand, do show a higher amount of egress when the inner droplets are 1.5% compared to when the inner droplets are 2%. This is certainly a reasonable finding based on the concentrations of the inner droplets, however, impact of the constant 2% agarose concentration of the outer emulsion, which is by volume a much larger component of the entire microdroplet, is unclear from the data.

Finally, regardless of the significant difference, the egress values have a rather large standard deviation. Doing more replicates of this experimental protocol would either a more clear trend with less variance or attribute the egress process variable to microfluidic devices – and perhaps for a more fine-tuned control, one might have to start investigating in controlling cell behavior through other channels.

CONCLUSION

For this research project, two objectives were accomplished. First, a process to create a hydrogel-in-hydrogel double emulsion microdroplet with no intermediate oil layer was developed and characterized. Secondly, double emulsion microdroplets produced using the developed process were applied to cell studies in order to understand the mechanism of cell egress from a microdroplet.

A flow focusing microfluidic device geometry was used to create single and double emulsion microdroplets in the desired size ranges. Single emulsions were intended to be 40 – 50 μm in size, whereas double emulsions were intended to be 110 – 130 μm in size. Coefficient of variation (CV) values were used to measure monodispersity, with a higher CV implying lower monodispersity. Single emulsion microdroplets exhibited a range of CV from 6% - 11%, while the double emulsion microdroplets had a higher CV range from 7% - 14%. Although the droplets were created in the intended range, literature reports that microdroplets can be formed using microfluidic platforms with a CV as low as 1% - 3%, thus aspects of droplet production used in this body of work can indeed be improved upon [67].

Throughput, or the amount of droplets created by the microfluidic device per a unit time, was highly variable, but the variability effected all samples measured with no clear trend. On average, double emulsions had a lower throughput than single emulsions as expected. Double emulsions are larger in size and have a greater volume. For all encapsulation sessions, the same volume of agarose (150 μL) is inserted for both single and double emulsions, therefore, there will be less microdroplets produced. Past work has indicated that the throughput of microfluidic production devices, at least for single emulsions, can be as high as 100 - 200 Hz, compared to the average 85 Hz and 79 Hz (for samples with polystyrene beads and cells respectively) observed in this body of work [119].

Cell viability was maintained throughout this experiment for both single and double emulsion microdroplets, with the highest overall change in viability over 48H being -6%. From our findings, it can be concluded that cells can remain viable in-vitro for 48H after encapsulation for both single and double emulsions alike. It is, however, important to ensure that cells are handled properly as their viability can be negatively impacted by mishandling samples.

Confocal microscopy is used to confirm the structure of the single and double emulsion microdroplet. Using an orthogonal view, we confirm that cells we identify as cell-laden are in-fact cells within agarose droplets. A LIVE/DEAD stain shows both viable and inviable cells in a microdroplet in an orthogonal view. While there was not enough data collected on the 3D structure and positioning of cells within double emulsions to draw a proper conclusion on cell positioning, proof of concept work shown in this project and experience from working with cells gives a level of certainty that the double emulsions seen under standard brightfield microscopy is indeed a double emulsion.

Finally, egress between single and double emulsions is compared. Between single and double emulsions for both tested concentrations, 1.5% and 2% agarose, there was a significant difference in cell egress. Single emulsions show a significantly higher amount of egress at timepoints 24H and 48H. Furthermore, double emulsion microdroplets show the greatest amount of egress within the first 24H with little to no egress between 24H and 48H. Single emulsions on the other hand also showed the largest amount of egress between 0H and 24H but continued to show cell egress between 24H and 48H. Given the results, we claim that viable cells are significantly more likely to egress out if they are closer to the edge of a microdroplets.

Double emulsion microdroplets were used to study the model cell line, *NIH 3T3*, in order to gain insight into cell behavior in terms of viability and egress. It was hypothesized that cells egress when they are at the edge of a microdroplet, and by creating a secondary layer, the position of the cells could be pushed closer towards the center and thus reduce the amount of cells that exit. Creating the double

emulsion did indeed reduce the amount of egress observed while providing an environment in which the cells remain viable thereby supporting our hypothesis that pushing cells further away from the edges will reduce cell egress. While the double emulsions significantly reduced cell egress, it did not completely eliminate egress and for that reason further work needs to be done in order to investigate cell egress mechanisms.

FUTURE WORK

Microfluidic devices used for the encapsulation of stem cells are done so for therapeutic outcomes and therefore must be user-friendly while providing a consistent output. Work done in this project would highly benefit from more investigation into creating a less polydisperse sample. While the 6% coefficient of variation (CV) for single emulsions was close to the 1% - 3% benchmark set by other researchers, the larger droplets in this body of work had a much higher CV and should be better controlled. A possible approach for this is to investigate multiple flow rates, pressures, and surfactant concentrations on the effects of monodispersity of double emulsion microdroplets, as has been done for single emulsions [119]. In a clinical setting, the microfluidic device should perform consistently and therefore the throughput of the device needs to have less variability. Potential approaches to better control throughput may be found in modifying device geometry for better pressure ratio controls.

Cell egress results show that double emulsion microdroplets do not entirely prevent cell egress and this is worth further investigation. While single and double emulsions both have the largest egress amounts between timepoints 0H and 24H, cells continue to egress out of single emulsions between 24H and 48H, while the egress remains almost zero for the same time period in double emulsions. Work must be done to understand why this happens as it opens the door to creating tunable cell release profiles.

One reason that double emulsions may not have shown a total lack of egress might be in that our method of double emulsion production failed to center all the cell-laden microdroplets to ensure that they were away from the edges. Given the data collected, the distribution of cell placement is unclear for both single and double emulsion microdroplets, and understanding such a factor might give more insight into cell egress. Collecting more data using the z-stack capabilities of a confocal microscope to experimentally quantify the number of cells at the edge and comparing that number to cell egress

might paint a more clear picture of the mechanisms of cell egress. Such an experiment might also give insight into additional motivations for cells wanting to exit a microdroplet. If all cells positioned close to the edge of a microdroplet leave within the first 24H, then there might be a secondary mechanism of egress in place that is observed between 24H – 48H, as seen in the single emulsion data.

Double emulsion microdroplets created in this project were always done with an outer layer concentration of 2% agarose. Investigating the effects of changing concentration of the outer emulsion while keeping the inner emulsion concentration constant might prove to be a method for controlling egress over time, as a change in agarose concentration changes the porosity of the hydrogel matrix [82]. Given that there was no significant difference between the two samples of double emulsions tested (1.5% and 2% inner concentrations), cell egress in a double emulsion system may be a function of outer microdroplet concentration. Should the outer layer agarose concentration be the determining factor of cell egress in a double emulsion, a decreased agarose concentration from the 2% used here should yield a higher amount of egress while a higher outer layer agarose concentration should yield a lower amount of egress, assuming a constant inner microdroplet concentration.

The ability to control cell egress can play a crucial role in cell-based therapy, where cell retention may be preferred to having mobile cells that can exist at the target location after an acute therapeutic effect or integrate into the target tissue [82]. Benefits of the sticky nature of agarose hydrogel paired with the reduced level of cell egress provide a cell therapy solution that keeps cells at the desired target location. Of course, before being used in animal trials, effects of double emulsions on the viability of therapeutic cells must be investigated. *NIH 3T3* cells are a model cell line commonly used for their robustness in drug discovery studies and tissue engineering – not for therapeutic applications [126]. While double emulsion configurations did not negatively impact the viability of *NIH 3T3* cell samples, in-vitro tests with the more sensitive therapeutic cell lines such as HUVEC and hMSCS still have to be done in order to ensure that double emulsion microdroplet systems remain safe for cells in terms

of viability. Furthermore, therapeutic cell egress profiles must be studied to ensure the effects of double emulsion microdroplets are similar for all cell lines. Should there be a difference, it may arise due to different egress mechanisms and alternative methods of controlling egress have to be investigated. Perhaps it is a combination of mechanisms such as proximity to the edge and chemical signals from neighboring cells or tissues.

From a technological stand-point, creating a hydrogel-in-hydrogel double emulsion with a microfluidic cell encapsulation platform was an interesting and useful success, however, further work into the creation of double emulsion microdroplets must be done. Current practices involve two sample purification methods to remove oil from the output. At this point, it is possible that there is some sample loss due to manipulation. Frequent manipulation and agitation of the sample in the form of pipetting and centrifugation might also promote cells to prematurely egress out of the microdroplets, altering the occupancy. As seen in the results, the most egress takes place within the first 24H after encapsulation, and the time (generally about an hour) between creating the first emulsion and second emulsion could prove to affect the occupancy of the double emulsion. For this reason, work must be done in order to create a microfluidic platform that removes oil on-chip. On-chip oil removal would eliminate the need to manipulate the sample in-between single and double emulsion encapsulation points, leading to a ready-to-use output.

Hydrogel-in-hydrogel double emulsion droplets provide a function outside of cell egress studies as well. Agarose hydrogel can be modified to alter certain properties by adding fluorescence, loading it with nanoparticles to change the electrical characteristics or by mixing it with chemicals to change how cells interact with the material. Usually, these changes must be carefully considered due to the

potential for cytotoxicity, however, double emulsions allow for the presence of sub environments, so the cells can be kept in a biocompatible and non-cytotoxic setting.

A combination of hydrogels or different materials can also be incorporated into double emulsion systems, with one shell being a different material, or phase from the other. Such a combination also provides users of the microfluidic platform to create more biomimetic environments. An outer shell that acts as the solid surface for cells to attach onto can be augmented with common proteins and molecules found in the native cell environment, while the inner layer, can be supplemented with substances found in the extra cellular matrix.

This project has demonstrated a proof of concept hydrogel-in-hydrogel double emulsion microdroplet, characterized the monodispersity and throughput of the microdroplet. The effects of double emulsions on cell egress is explored in order to better understand cell behavior in the context of stem cell therapy. Moreover, it has identified the current shortcomings of the double emulsion system, potential solutions for how to address the issues, as well as avenues in which interested researchers can explore further.

References

[1] P. Boisseau and B. Loubaton, "Nanomedicine, nanotechnology in medicine," *Comptes Rendus Phys.*, vol. 12, no. 7, pp. 620–636, Sep. 2011.

[2] G. M. Whitesides, "The origins and the future of microfluidics," *Nature*, vol. 442, no. 7101, pp. 368–373, Jul. 2006.

[3] D. Di Carlo, "Inertial microfluidics," *Lab. Chip*, vol. 9, no. 21, p. 3038, 2009.

[4] J. Zhang *et al.*, "Fundamentals and applications of inertial microfluidics: a review," *Lab. Chip*, vol. 16, no. 1, pp. 10–34, 2016.

[5] D. B. Weibel and G. M. Whitesides, "Applications of microfluidics in chemical biology," *Curr. Opin. Chem. Biol.*, vol. 10, no. 6, pp. 584–591, Dec. 2006.

[6] C. D. Ahrberg, A. Manz, and B. G. Chung, "Polymerase chain reaction in microfluidic devices," *Lab. Chip*, vol. 16, no. 20, pp. 3866–3884, Oct. 2016.

[7] H. S. Rho, A. T. Hanke, M. Ottens, and H. Gardeniers, "Mapping of Enzyme Kinetics on a Microfluidic Device," *PLOS ONE*, vol. 11, no. 4, p. e0153437, Apr. 2016.

[8] D. J. Beebe, G. A. Mensing, and G. M. Walker, "Physics and Applications of Microfluidics in Biology," *Annu. Rev. Biomed. Eng.*, vol. 4, no. 1, pp. 261–286, Aug. 2002.

[9] X. Leng, W. Zhang, C. Wang, L. Cui, and C. J. Yang, "Agarose droplet microfluidics for highly parallel and efficient single molecule emulsion PCR," *Lab. Chip*, vol. 10, no. 21, p. 2841, 2010.

[10] F. A. Gomez, *Biological Applications of Microfluidics*. John Wiley & Sons, 2008.

[11] S.-Y. Teh, R. Lin, L.-H. Hung, and A. P. Lee, "Droplet microfluidics," *Lab. Chip*, vol. 8, no. 2, pp. 198–220, Jan. 2008.

[12] X. Sun, K. Tang, R. D. Smith, and R. T. Kelly, "Controlled dispensing and mixing of pico- to nanoliter volumes using on-demand droplet-based microfluidics," *Microfluid. Nanofluidics*, vol. 15, no. 1, pp. 117–126, Jul. 2013.

[13] J.-W. Choi, G.-J. Kim, S. Lee, J. Kim, A. J. deMello, and S.-I. Chang, "A droplet-based fluorescence polarization immunoassay (dFPIA) platform for rapid and quantitative analysis of biomarkers," *Biosens. Bioelectron.*, vol. 67, pp. 497–502, May 2015.

[14] P. Xue, Y. Wu, N. V. Menon, and Y. Kang, "Microfluidic synthesis of monodisperse PEGDA microbeads for sustained release of 5-fluorouracil," *Microfluid. Nanofluidics*, vol. 18, no. 2, pp. 333–342, Feb. 2015.

[15] G. Aubry, M. Zhan, and H. Lu, "Hydrogel-droplet microfluidic platform for high-resolution imaging and sorting of early larval Caenorhabditis elegans," *Lab. Chip*, vol. 15, no. 6, pp. 1424–1431, Mar. 2015.

[16] W.-L. Chou, P.-Y. Lee, C.-L. Yang, W.-Y. Huang, and Y.-S. Lin, "Recent Advances in Applications of Droplet Microfluidics," *Micromachines*, vol. 6, no. 9, pp. 1249–1271, Sep. 2015.

[17] R. R. Nadig, "Stem cell therapy – Hype or hope? A review," *J. Conserv. Dent. JCD*, vol. 12, no. 4, pp. 131–138, 2009.

[18] H. Yin and D. Marshall, "Microfluidics for single cell analysis," *Curr. Opin. Biotechnol.*, vol. 23, no. 1, pp. 110–119, Feb. 2012.

[19] N. Wen *et al.*, "Development of Droplet Microfluidics Enabling High-Throughput Single-Cell Analysis," *Molecules*, vol. 21, no. 7, p. 881, Jul. 2016.

[20] R. K. Shah *et al.*, "Designer emulsions using microfluidics," *Mater. Today*, vol. 11, no. 4, pp. 18–27, Apr. 2008.

[21] W. Wang, M.-J. Zhang, and L.-Y. Chu, "Microfluidic approach for encapsulation via double emulsions," *Curr. Opin. Pharmacol.*, vol. 18, pp. 35–41, Oct. 2014.

[22] J. Yan, W.-A. Bauer, M. Fischlechner, F. Hollfelder, C. Kaminski, and W. Huck, "Monodisperse Water-in-Oil-in-Water (W/O/W) Double Emulsion Droplets as Uniform Compartments for High-Throughput Analysis via Flow Cytometry," *Micromachines*, vol. 4, no. 4, pp. 402–413, Dec. 2013.

[23] "Hierarchical Biomolecular Emulsions Using 3-D Microfluidics with Uniform Surface Chemistry - Biomacromolecules (ACS Publications)." [Online]. Available: https://pubs.acs.org/doi/pdfplus/10.1021/acs.biomac.7b01159?src=recsys. [Accessed: 24-Jan-2019].

[24] P. Garstecki, I. Gitlin, W. DiLuzio, G. M. Whitesides, E. Kumacheva, and H. A. Stone, "Formation of monodisperse bubbles in a microfluidic flow-focusing device," *Appl. Phys. Lett.*, vol. 85, no. 13, pp. 2649–2651, Sep. 2004.

[25] J. D. Tice, H. Song, A. D. Lyon, and R. F. Ismagilov, "Formation of Droplets and Mixing in Multiphase Microfluidics at Low Values of the Reynolds and the Capillary Numbers," *Langmuir*, vol. 19, no. 22, pp. 9127–9133, Oct. 2003.

[26] "Laminar, Transitional or Turbulent Flow." [Online]. Available: https://www.engineeringtoolbox.com/laminar-transitional-turbulent-flow-d_577.html. [Accessed: 24-Jan-2019].

[27] S. B. Pope, *Turbulent flows*, Reprinted with corr.. Cambridge ; New York: Cambridge University Press, 2001.

[28] M. Schobeiri, *Applied fluid mechanics for engineers*. New York: McGraw Hill Education, 2014.

[29] J. P. Brody, P. Yager, R. E. Goldstein, and R. H. Austin, "Biotechnology at low Reynolds numbers," *Biophys. J.*, vol. 71, no. 6, pp. 3430–3441, Dec. 1996.

[30] D. Cheng *et al.*, "Laminar Flow in Microfluidic Channels," p. 14.

[31] B. Lautrup, *Physics of continuous matter: exotic and everyday phenomena in the macroscopic world*, 2nd ed. Boca Raton: Taylor & Francis, 2011.

[32] H. Gu, M. H. G. Duits, and F. Mugele, "Droplets Formation and Merging in Two-Phase Flow Microfluidics," *Int. J. Mol. Sci.*, vol. 12, no. 4, pp. 2572–2597, Apr. 2011.

[33] "Effect of surfactant on emulsification in microchannels - ScienceDirect." [Online]. Available: https://www.sciencedirect.com/science/article/pii/S0009250917306425. [Accessed: 24-Jan-2019].

[34] J. K. Nunes, S. S. H. Tsai, J. Wan, and H. A. Stone, "Dripping and jetting in microfluidic multiphase flows applied to particle and fiber synthesis," *J. Phys. Appl. Phys.*, vol. 46, no. 11, Mar. 2013.

[35] T. M. Tran, S. Cater, and A. R. Abate, "Coaxial flow focusing in poly(dimethylsiloxane) microfluidic devices," *Biomicrofluidics*, vol. 8, no. 1, Feb. 2014.

[36] P. Garstecki, M. J. Fuerstman, H. A. Stone, and G. M. Whitesides, "Formation of droplets and bubbles in a microfluidic T-junction—scaling and mechanism of break-up," *Lab. Chip*, vol. 6, no. 3, pp. 437–446, Feb. 2006.

[37] H. Liu and Y. Zhang, "Droplet formation in a T-shaped microfluidic junction," *J. Appl. Phys.*, vol. 106, no. 3, p. 034906, Aug. 2009.

[38] P. A. Romero and A. R. Abate, "Flow focusing geometry generates droplets through a plug and squeeze mechanism," *Lab. Chip*, vol. 12, no. 24, pp. 5130–5132, Nov. 2012.

[39] X. Chen and C. L. Ren, "Experimental study on droplet generation in flow focusing devices considering a stratified flow with viscosity contrast," *Chem. Eng. Sci.*, vol. 163, pp. 1–10, May 2017.

[40] D. Conchouso, E. Rawashdeh, D. Castro, A. Arevalo, and I. G. Foulds, "Optimized Channel Geometry of a Flow-Focusing Droplet Generator for Parallelization.," p. 6.

[41] M. Nooranidoost, D. Izbassarov, and M. Muradoglu, "Droplet formation in a flow focusing configuration: Effects of viscoelasticity," *Phys. Fluids*, vol. 28, no. 12, p. 123102, Dec. 2016.

[42] J.-C. Baret, "Surfactants in droplet-based microfluidics," *Lab. Chip*, vol. 12, no. 3, pp. 422–433, Jan. 2012.

[43] S. Allazetta and M. P. Lutolf, "Stem cell niche engineering through droplet microfluidics," *Curr. Opin. Biotechnol.*, vol. 35, pp. 86–93, Dec. 2015.

[44] A. Trounson, R. G. Thakar, G. Lomax, and D. Gibbons, "Clinical trials for stem cell therapies," *BMC Med.*, vol. 9, no. 1, Dec. 2011.

[45] B. A. Tompkins *et al.*, "Preclinical Studies of Stem Cell Therapy for Heart Disease," *Circ. Res.*, vol. 122, no. 7, pp. 1006–1020, Mar. 2018.

[46] M. Gnecchi, Z. Zhang, A. Ni, and V. J. Dzau, "Paracrine mechanisms in adult stem cell signaling and therapy," *Circ. Res.*, vol. 103, no. 11, pp. 1204–1219, Nov. 2008.

[47] L. A. Fortier, "Stem Cells: Classifications, Controversies, and Clinical Applications," *Vet. Surg.*, vol. 34, no. 5, pp. 415–423, Sep. 2005.

[48] R. Barker, M. Jain, R. Armstrong, and M. Caldwell, "Stem cells and neurological disease," *J. Neurol. Neurosurg. Psychiatry*, vol. 74, no. 5, pp. 553–557, May 2003.

[49] H. J. Kim and J.-S. Park, "Usage of Human Mesenchymal Stem Cells in Cell-based Therapy: Advantages and Disadvantages," *Dev. Reprod.*, vol. 21, no. 1, pp. 1–10, Mar. 2017.

[50] S. Aggarwal and M. F. Pittenger, "Human mesenchymal stem cells modulate allogeneic immune cell responses," *Blood*, vol. 105, no. 4, pp. 1815–1822, Feb. 2005.

[51] V. Turinetto, E. Vitale, and C. Giachino, "Senescence in Human Mesenchymal Stem Cells: Functional Changes and Implications in Stem Cell-Based Therapy," *Int. J. Mol. Sci.*, vol. 17, no. 7, p. 1164, Jul. 2016.

[52] Y. L. Tang, Y. J. Wang, L. J. Chen, Y. H. Pan, L. Zhang, and N. L. Weintraub, "Cardiac-derived stem cell-based therapy for heart failure: progress and clinical applications," *Exp. Biol. Med.*, vol. 238, no. 3, pp. 294–300, Mar. 2013.

[53] D. Harris, "Stem Cell Banking for Regenerative and Personalized Medicine," *Biomedicines*, vol. 2, no. 1, pp. 50–79, Feb. 2014.

[54] V. F. M. Segers and R. T. Lee, "Stem-cell therapy for cardiac disease," *Nature*, vol. 451, pp. 937–942, Feb. 2008.

[55] R. Champlin, "Selection of Autologous or Allogeneic Transplantation," *Holl.-Frei Cancer Med. 6th Ed.*, 2003.

[56] S. Slavin, "Graft-versus-host disease, the graft-versus-leukemia effect, and mixed chimerism following nonmyeloablative stem cell transplantation," *Int. J. Hematol.*, vol. 78, no. 3, pp. 195–207, Oct. 2003.

[57] S. G. Holtan, M. Pasquini, and D. J. Weisdorf, "Acute graft-versus-host disease: a bench-to-bedside update," *Blood*, vol. 124, no. 3, pp. 363–373, Jul. 2014.

[58] S. Zhao *et al.*, "Bioengineering of injectable encapsulated aggregates of pluripotent stem cells for therapy of myocardial infarction," *Nat. Commun.*, vol. 7, p. 13306, Oct. 2016.

[59] J. Ferrara, "Cellular therapy of the host to prevent GVHD," *Blood*, vol. 124, no. 11, pp. 1703–1704, Sep. 2014.

[60] J. N. Anderl, T. E. Robey, P. S. Stayton, and C. E. Murry, "Retention and biodistribution of microspheres injected into ischemic myocardium," *J. Biomed. Mater. Res. A*, vol. 88A, no. 3, pp. 704–710, Mar. 2009.

[61] K. Shah, "Encapsulated stem cells for cancer therapy," *Biomatter*, vol. 3, no. 1, Jan. 2013.

[62] D. Jing, A. Parikh, and E. S. Tzanakakis, "Cardiac Cell Generation from Encapsulated Embryonic Stem Cells in Static and Scalable Culture Systems," *Cell Transplant.*, vol. 19, no. 11, pp. 1397–1412, Nov. 2010.

[63] M. Hashemi and F. Kalalinia, "Application of encapsulation technology in stem cell therapy," *Life Sci.*, vol. 143, pp. 139–146, Dec. 2015.

[64] "Hydrogel Biomaterials for Stem Cell Microencapsulation.pdf." .

[65] G. J. Lim, S. J. Lee, and A. Atala, "55 - Cell-Based Drug Delivery," in *Principles of Regenerative Medicine*, A. Atala, R. Lanza, J. A. Thomson, and R. M. Nerem, Eds. San Diego: Academic Press, 2008, pp. 954–966.

[66] Z. Jiang, B. Xia, R. McBride, and J. Oakey, "A microfluidic-based cell encapsulation platform to achieve high long-term cell viability in photopolymerized PEGNB hydrogel microspheres," *J. Mater. Chem. B Mater. Biol. Med.*, vol. 5, no. 1, pp. 173–180, Jan. 2017.

[67] D. R. Link, S. L. Anna, D. A. Weitz, and H. A. Stone, "Geometrically Mediated Breakup of Drops in Microfluidic Devices," *Phys. Rev. Lett.*, vol. 92, no. 5, Feb. 2004.

[68] G. Velve-Casquillas, M. Le Berre, M. Piel, and P. T. Tran, "Microfluidic tools for cell biological research," *Nano Today*, vol. 5, no. 1, pp. 28–47, Feb. 2010.

[69] E. Amici, G. Tetradis-Meris, C. P. de Torres, and F. Jousse, "Alginate gelation in microfluidic channels," *Food Hydrocoll.*, vol. 22, no. 1, pp. 97–104, Jan. 2008.

[70] D. J. Collins, A. Neild, A. deMello, A.-Q. Liu, and Y. Ai, "The Poisson distribution and beyond: methods for microfluidic droplet production and single cell encapsulation," *Lab. Chip*, vol. 15, no. 17, pp. 3439–3459, Aug. 2015.

[71] P. Zucca, R. Fernandez-Lafuente, and E. Sanjust, "Agarose and Its Derivatives as Supports for Enzyme Immobilization," *Molecules*, vol. 21, no. 11, p. 1577, Nov. 2016.

[72] A. Ellis and J. C. Jacquier, "Manufacture and characterisation of agarose microparticles," *J. Food Eng.*, vol. 90, no. 2, pp. 141–145, Jan. 2009.

[73] J. E. Kolesar, C. Y. Wang, Y. V. Taguchi, S.-H. Chou, and B. A. Kaufman, "Two-dimensional intact mitochondrial DNA agarose electrophoresis reveals the structural complexity of the mammalian mitochondrial genome," *Nucleic Acids Res.*, vol. 41, no. 4, p. e58, Feb. 2013.

[74] E. Mercey, P. Obeïd, D. Glaise, M.-L. Calvo-Muñoz, C. Guguen-Guillouzo, and B. Fouqué, "The application of 3D micropatterning of agarose substrate for cell culture and in situ comet assays," *Biomaterials*, vol. 31, no. 12, pp. 3156–3165, Apr. 2010.

[75] "A5030-BULK_____SIAL_____.pdf." .

[76] Y. Reissis, E. García-Gareta, M. Korda, G. W. Blunn, and J. Hua, "The effect of temperature on the viability of human mesenchymal stem cells," *Stem Cell Res. Ther.*, vol. 4, no. 6, p. 139, 2013.

[77] T. S. Kaminski, O. Scheler, and P. Garstecki, "Droplet microfluidics for microbiology: techniques, applications and challenges," *Lab. Chip*, vol. 16, no. 12, pp. 2168–2187, 2016.

[78] J. Wan, "Microfluidic-Based Synthesis of Hydrogel Particles for Cell Microencapsulation and Cell-Based Drug Delivery," *Polymers*, vol. 4, no. 2, pp. 1084–1108, Apr. 2012.

[79] S. Swioklo and C. J. Connon, "Keeping cells in their place: the future of stem cell encapsulation," *Expert Opin. Biol. Ther.*, vol. 16, no. 10, pp. 1181–1183, Oct. 2016.

[80] L. Hidalgo San Jose, P. Stephens, B. Song, and D. Barrow, "Microfluidic Encapsulation Supports Stem Cell Viability, Proliferation, and Neuronal Differentiation," *Tissue Eng. Part C Methods*, vol. 24, no. 3, pp. 158–170, Mar. 2018.

[81] A. S. Mao *et al.*, "Deterministic encapsulation of single cells in thin tunable microgels for niche modeling and therapeutic delivery," *Nat. Mater.*, vol. 16, no. 2, pp. 236–243, Feb. 2017.

[82] A. Benavente-Babace, K. Haase, D. J. Stewart, and M. Godin, "Microfluidic Encapsulation to Tune Therapeutic Cell Delivery," *J. Tissue Eng. Regen. Med.*, vol. accepted for publication.

[83] S. Okushima, T. Nisisako, T. Torii, and T. Higuchi, "Controlled Production of Monodisperse Double Emulsions by Two-Step Droplet Breakup in Microfluidic Devices," *Langmuir*, vol. 20, no. 23, pp. 9905–9908, Nov. 2004.

[84] C. J. Martinez *et al.*, "A Microfluidic Approach to Encapsulate Living Cells in Uniform Alginate Hydrogel Microparticles," *Macromol. Biosci.*, vol. 12, no. 7, pp. 946–951, Jul. 2012.

[85] L. Liu *et al.*, "Preparation of monodisperse calcium alginate microcapsules via internal gelation in microfluidic-generated double emulsions," *J. Colloid Interface Sci.*, vol. 404, pp. 85–90, Aug. 2013.

[86] Y. Zhang *et al.*, "A programmable microenvironment for cellular studies via microfluidics-generated double emulsions," *Biomaterials*, vol. 34, no. 19, pp. 4564–4572, Jun. 2013.

[87] B. G. Chung, K.-H. Lee, A. Khademhosseini, and S.-H. Lee, "Microfluidic fabrication of microengineered hydrogels and their application in tissue engineering," *Lab. Chip*, vol. 12, no. 1, pp. 45–59, Dec. 2011.

[88] S. K. Y. Tang and G. M. Whitesides, "Basic Microfluidic and Soft Lithographic Techniques," p. 26.

[89] F. Walther *et al.*, "Stability of the hydrophilic behaviour of oxygen plasma activated SU-8," *J Micromech Microeng*, p. 11.

[90] M. Leester-Schädel, T. Lorenz, F. Jürgens, and C. Richter, "Fabrication of Microfluidic Devices," in *Microsystems for Pharmatechnology*, A. Dietzel, Ed. Cham: Springer International Publishing, 2016, pp. 23–57.

[91] Datasheet, "SU-82000DataSheet2000_5thru2015Ver4.pdf," 2015.

[92] "SU-8 photolithography: Baking - Elveflow." [Online]. Available: https://www.elveflow.com/microfluidic-tutorials/soft-lithography-reviews-and-tutorials/how-to-get-the-best-process/su-8-photolithography-baking/. [Accessed: 25-Jan-2019].

[93] "SU-82000DataSheet2000_5thru2015Ver4.pdf." .

[94] "Silanization of Photoresist Master Protocol.pdf." .

[95] N. R. Glass, R. Tjeung, P. Chan, L. Y. Yeo, and J. R. Friend, "Organosilane deposition for microfluidic applications," *Biomicrofluidics*, vol. 5, no. 3, pp. 036501-036501–7, Aug. 2011.

[96] "Advances in Microfluidic Materials, Functions, Integration, and Applications - Chemical Reviews (ACS Publications)." [Online]. Available: https://pubs.acs.org/doi/pdf/10.1021/cr300337x. [Accessed: 25-Jan-2019].

[97] "Materials for Microfluidic Chip Fabrication." [Online]. Available: https://pubs.acs.org/doi/pdf/10.1021/ar300314s. [Accessed: 25-Jan-2019].

[98] P. Abgrall and A.-M. Gué, "Lab-on-chip technologies: making a microfluidic network and coupling it into a complete microsystem—a review," *J. Micromechanics Microengineering*, vol. 17, no. 5, pp. R15–R49, May 2007.

[99] S. K. Sia and G. M. Whitesides, "Microfluidic devices fabricated in Poly(dimethylsiloxane) for biological studies," *ELECTROPHORESIS*, vol. 24, no. 21, pp. 3563–3576, Nov. 2003.

[100] "Poly(dimethylsiloxane) as a Material for Fabricating Microfluidic Devices - Accounts of Chemical Research (ACS Publications)." [Online]. Available: https://pubs.acs.org/doi/pdf/10.1021/ar010110q. [Accessed: 25-Jan-2019].

[101] S. D. Minteer, Ed., *Microfluidic techniques: reviews and protocols*. Totowa, N.J: Humana Press, 2006.

[102] "*NIH 3T3* Protocol." .

[103] C. Elliott, V. Vijayakumar, W. Zink, and R. Hansen, "National Instruments LabVIEW: A Programming Environment for Laboratory Automation and Measurement," *J. Assoc. Lab. Autom.*, vol. 12, no. 1, pp. 17–24, Feb. 2007.

[104] J. Schindelin *et al.*, "Fiji: an open-source platform for biological-image analysis," *Nat. Methods*, vol. 9, no. 7, pp. 676–682, Jul. 2012.

[105] J. R. Wünsch, *Polystyrene: Synthesis, Production and Applications*. iSmithers Rapra Publishing, 2000.

[106] "microscope counting chamber (hemocytometer)." [Online]. Available: http://www.ruf.rice.edu/~bioslabs/methods/microscopy/cellcounting.html. [Accessed: 26-Jan-2019].

[107] J. Marchini, "Lecture 5 : The Poisson Distribution," p. 9.

[108] S. Johnson, V. Nguyen, and D. Coder, "Assessment of Cell Viability," *Curr. Protoc. Cytom.*, vol. 64, no. 1, pp. 9.2.1-9.2.26, Apr. 2013.

[109] J. M. Chen, M.-C. Kuo, and C.-P. Liu, "Control of Droplet Generation in Flow-Focusing Microfluidic Device with a Converging-Diverging Nozzle-Shaped Section," *Jpn. J. Appl. Phys.*, vol. 50, no. 10, p. 107301, Oct. 2011.

[110] S. L. Anna, N. Bontoux, and H. A. Stone, "Formation of dispersions using 'flow focusing' in microchannels," *Appl. Phys. Lett.*, vol. 82, no. 3, pp. 364–366, Jan. 2003.

[111] A. Gupta, H. S. Matharoo, D. Makkar, and R. Kumar, "Droplet formation via squeezing mechanism in a microfluidic flow-focusing device," *Comput. Fluids*, vol. 100, pp. 218–226, Sep. 2014.

[112] W. Wang, M.-J. Zhang, and L.-Y. Chu, "Microfluidic approach for encapsulation via double emulsions," *Curr. Opin. Pharmacol.*, vol. 18, pp. 35–41, Oct. 2014.

[113] M.-N. Iancu, Y. Chevalie, M. Popa, and T. Hamaide, "Internally gelled W/O and W/O/W double emulsions," *E-Polym.*, vol. 9, no. 1, Jan. 2009.

[114] E. Y. Liu, S. Jung, D. A. Weitz, H. Yi, and C.-H. Choi, "High-throughput double emulsion-based microfluidic production of hydrogel microspheres with tunable chemical functionalities toward biomolecular conjugation," *Lab. Chip*, vol. 18, no. 2, pp. 323–334, Jan. 2018.

[115] R. C. Tolman, "The Effect of Droplet Size on Surface Tension," *J. Chem. Phys.*, vol. 17, no. 3, pp. 333–337, Mar. 1949.

[116] T. Kamperman, S. Henke, C. W. Visser, M. Karperien, and J. Leijten, "Centering Single Cells in Microgels via Delayed Crosslinking Supports Long-Term 3D Culture by Preventing Cell Escape," *Small*, vol. 13, no. 22, p. 1603711, Jun. 2017.

[117] C.-X. Zhao and A. P. J. Middelberg, "Two-phase microfluidic flows," *Chem. Eng. Sci.*, vol. 66, no. 7, pp. 1394–1411, Apr. 2011.

[118] D. J. Pike, R. R. Sokal, and P. J. Rohlf, "The Principles and Practice of Statistics in Biological Research.," *J. Appl. Ecol.*, vol. 19, no. 3, p. 985, Dec. 1982.

[119] N. Monette-Catafard, "HIGH-THROUGHPUT CELL ENCAPSULATION IN MONODISPERSE AGAROSE MICROCAPSULES USING A MICROFLUIDIC DEVICE," p. 86.

[120] W. Zeng, S. Li, and Z. Wang, "Characterization of syringe-pump-driven versus pressure-driven microfluidic flows," in *2015 International Conference on Fluid Power and Mechatronics (FPM)*, Harbin, China, 2015, pp. 711–715.

[121] "Pipette tips epT.I.P.S. Standard 0.1 ul - 10 ul 0030000811 Eppendorf | Lab Unlimited." [Online]. Available: https://www.labunlimited.com/s/ALL/4AJ-9409410/Pipette-tips-epT.I.P.S.-Standard-0.1-ul---10-ul-0030000811-Eppendorf. [Accessed: 26-Jan-2019].

[122] R. J. Geraghty *et al.*, "Guidelines for the use of cell lines in biomedical research," *Br. J. Cancer*, vol. 111, no. 6, pp. 1021–1046, Sep. 2014.

[123] M. Rodriguez-Porcel, "In Vivo Imaging and Monitoring of Transplanted Stem Cells: Clinical Applications," *Curr. Cardiol. Rep.*, vol. 12, no. 1, pp. 51–58, Jan. 2010.

[124] G. V. Goldmacher, R. Nasser, D. Y. Lee, S. Yigit, R. Rosenwasser, and L. Iacovitti, "Tracking Transplanted Bone Marrow Stem Cells and Their Effects in the Rat MCAO Stroke Model," *PLoS ONE*, vol. 8, no. 3, p. e60049, Mar. 2013.

[125] P. S. Lienemann, T. Rossow, A. S. Mao, Q. Vallmajo-Martin, M. Ehrbar, and D. J. Mooney, "Single cell-laden protease-sensitive microniches for long-term culture in 3D," *Lab. Chip*, vol. 17, no. 4, pp. 727–737, Feb. 2017.

[126] X. (James) Li, A. V. Valadez, P. Zuo, and Z. Nie, "Microfluidic 3D cell culture: potential application for tissue-based bioassays," *Bioanalysis*, vol. 4, no. 12, pp. 1509–1525, Jun. 2012.